Journal of Organometallic Chemistry, 467 (1994) 251–281

Cluster chemistry

XC. * Some complexes obtained from reactions between $M_3(CO)_{12}$ (M = Ru or Os) or $Ru_3(\mu\text{-dppm})(CO)_{10}$ and 2-substituted triphenylphosphines and related keto-phosphine ligands

Chris J. Adams, Michael I. Bruce, Paul A. Duckworth, Paul A. Humphrey, Olaf Kühl and Edward R.T. Tiekink

Jordan Laboratories, Department of Chemistry, University of Adelaide, Adelaide, S.A. 5005 (Australia)

William R. Cullen

Department of Chemistry, 2036 Main Mall, University of British Columbia, Vancouver V6T 1Z1 (Canada)

Pierre Braunstein and Silverio Coco Cea

Laboratoire de Chimie de Coordination, associé au CNRS (URA 416), Université Louis Pasteur, 4 rue Blaise Pascal, 67070 Strasbourg (France)

Brian W. Skelton and Allan H. White

Department of Chemistry, University of Western Australia, Nedlands, W.A. 6009 (Australia)

(Received April 15, 1993)

Abstract

Several complexes of the type $M_3L_n\{PR_2(C_6H_4X)\}$ [$M_3L_n = (Ru/Os)_3(CO)_{11}$ or $Ru_3(\mu\text{-dppm})(CO)_9$; X = NH_2, NHCOPh, N=CHPh, CHO or CH=NNHAr, but not all combinations] have been prepared and their reactions studied. Predominant were H-migrations from the aryl substituent X to cluster; less facile were C–C bond cleavage reactions, and P–C bond cleavages were not observed. Under the conditions used, the complexes $Ru_3(CO)_{11}\{PPh_2(C_6H_4X\text{-}2)\}$ were transient intermediates in the formation of $Ru_3(\mu\text{-H})\{\mu\text{-}PPh_2(C_6H_4(X\text{–}H)\text{-}2)\}(CO)_9$; the analogous $Ru_3(\mu\text{-dppm})$ and $Os_3(\mu\text{-dppm})$ complexes were more robust. Similar reactions were found for clusters made by reaction of $Ru_3(CO)_{12}$ and related complexes with $PPh_2\{CH_2C(O)Ph\}$, in which H-migration from the ligand to the cluster results in formation of a phosphino-enolate system. X-ray structures are reported for the complexes $Os_3(CO)_{11}\{PPh_2(C_6H_4X\text{-}2)\}$ [X = NH_2, NHC(O)Ph, CHO, CH=NNHC$_6$H$_3$(NO$_2$)$_2$-2,4], $Ru_3(\mu\text{-dppm})(CO)_9\{PPh_2(C_6H_4X\text{-}2)\}$ [X = NHC(O)Ph, CHO], $Ru_3(\mu\text{-H})\{\mu\text{-}PPh_2(C_6H_4Y\text{-}2)\}(CO)_9$ [Y = NH, NC(Ph)O, N=CPh], $Ru_3(\mu\text{-H})\{\mu\text{-}PPh_2[C_6H_4NC(Ph)O\text{-}2]\}(\mu\text{-dppm})(CO)_7$, $Ru_3(\mu\text{-H})(\mu\text{-dppm})\{\mu\text{-}PPh_2(C_6H_4NH\text{-}2)\}(CO)_7$ and $Os_3(\mu\text{-H})\{\mu\text{-}PPh_2(C_6H_4CO\text{-}2)\}(CO)_9$.

Key words: Ruthenium; Osmium; Carbonyl; Functional phosphines

1. Introduction

A multitude of derivatives of the trinuclear Group 8 cluster carbonyls containing tertiary phosphine and phosphite ligands have been made especially since a variety of methods of activating the parent $M_3(CO)_{12}$ molecules towards substitution became available [1,2]. Prominent among their reactions are C–H and P–C bond-breaking reactions under mild conditions, which have been used, for example, to make complexes containing unstable molecules such as benzyne attached to

Correspondence to: Professor M.I. Bruce.

* For Part LXXXIX, see ref. 38.

0022-328X/94/$7.00
SSDI 0022-328X(93)24001-L

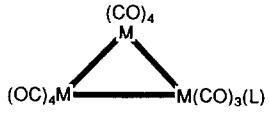

	M	L
1	Ru	CO
2	Os	NCMe
7	Os	$PPh_2(C_6H_4NH_2\text{-}2)$
10	Os	$PPh_2\{C_6H_4NHC(O)Ph\text{-}2\}$
18	Os	$PPh_2(C_6H_4CHO\text{-}2)$
20	Os	$PPh_2\{C_6H_4[CH{=}NNHC_6H_3(NO_2)_2\text{-}2,4]\text{-}2\}$
21	Ru	$PPh_2\{CH_2C(O)Ph\}$

the cluster. However, until recently only a few cluster compounds containing tertiary phosphines bearing functional groups were known. Interest in this aspect has been motivated largely by: (i) the desire to combine the multi-site attachment and possible activation of the functional ligand that can be provided by a cluster with the chemoselectivity expected as a result of the presence of different chemical functions within the same ligand, and (ii) the search for molecular systems that can be anchored on to a surface, such as silica, in order to provide hybrid catalysts [3]. The silylated ligand $PPh_2\{CH_2CH_2Si(OEt)_3\}$ has been used to attach the Ru_3 cluster to silica [4]. The reactions of the hemilabile ligand $PPh_2\{CH_2C(O)R\}$ (R = Ph) with $Ru_3(CO)_{12}$ afforded not only the simple substitution products but also the hydrido cluster $Ru_3(\mu\text{-}H)\{\mu\text{-}PPh_2[CH{\cdots}C(\cdots O)Ph]\}(CO)_9$, which contains an unusual bridging phosphino-enolate ligand formed by hydride migration from the ligand to the cluster [5]. Triruthenium complexes of the phosphinoketone are also degraded readily by halogen (Cl from CH_2Cl_2, or I_2) to give halide-bridged diruthenium complexes containing chelating phosphino-enolate ligands [6]. In contrast, reactions of this ligand with $Fe_3(CO)_{12}$ result in the ready formation of mononuclear complexes [7].

In an attempt to obtain the simple substitution complexes of several related ligands, we have studied their chemistry in more detail; we report below the synthesis of several examples of such complexes together with their X-ray structural characterisation and hydrogen-migration reactions. The studies reported here were carried out with $Ru_3(CO)_{12}$ (**1**), $Os_3(CO)_{11}$(NCMe) (**2**) and $Ru_3(\mu\text{-dppm})(CO)_{10}$ (**3**), and we concentrated mainly on 2-substituted derivatives of triphenylphosphine containing NH_2, NC(O)Ph, N=CHPh, CHO and $CH{=}NNHC_6H_3(NO_2)_2$-2,4 as functional

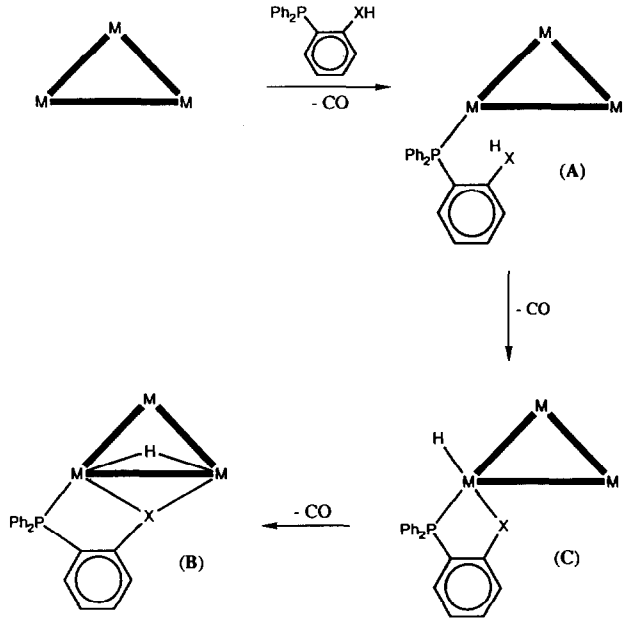

Scheme 1.

groups. Some further reactions of $Ru_3(CO)_{12}$ and related complexes with the phosphino-ketone $PPh_2\{CH_2C(O)Ph\}$ are also reported. The reactions generally proceed *via* the formation of simple CO-substitution products (A) to give complexes (B), in which a hydrogen atom has migrated from the functional group to the cluster, with concomitant formation of a bridging ligand (Scheme 1). Reactions of amines with $M_3(CO)_{12}$ have been long known, the products containing ligands formed by combination of the amine with a cluster-bound CO [8]. In the case of reactions with aldehydes and imines, the earlier work by the groups of Kaesz [9], Deeming [10] and of Lewis and Johnson [11] has been summarised in a recent paper from Vahrenkamp's group [12].

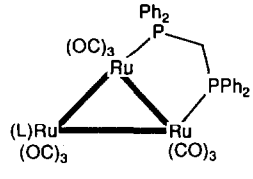

	L
3	CO
5	$PPh_2(C_6H_4NH_2\text{-}2)$
8	$PPh_2\{C_6H_4NHC(O)Ph\text{-}2\}$
12	$PPh_2(C_6H_4N{=}CHPh\text{-}2)$
15	$PPh_2(C_6H_4CHO\text{-}2)$

2. Results and discussion

2.1. Reactions of $PPh_2(C_6H_4NH_2$-2)

The reaction of this ligand with $Ru_3(CO)_{12}$ initially afforded a red complex, probably $Ru_3(CO)_{11}\{PPh_2(C_6H_4NH_2$-2)}, which could not be isolated, but was converted into $Ru_3(\mu$-H)$\{\mu$-$PPh_2(C_6H_4NH$-2)}$(CO)_9$ (**4**) on heating or attempted isolation. This complex was identified by a combination of spectroscopic and X-ray methods. The ^{1}H NMR spectrum contained a high-field signal at $\delta = -13.54$, showing coupling to the ^{31}P nucleus, while the FAB mass spectrum contained a molecular ion at m/z 834 and ions formed by loss of up to nine CO ligands. The structural study (see below) is consistent with migration of a hydrogen atom from the ligand to the cluster.

The reaction between equimolar amounts of **3** and the ligand at room temperature overnight afforded red $Ru_3(\mu$-dppm)$(CO)_9\{PPh_2(C_6H_4NH_2$-2)} (**5**) in high yield. At 30°C, a mixture of **5** (35%) and the hydride-migration product $Ru_3(\mu$-H)$\{\mu$-$PPh_2(C_6H_4NH$-2)}-$(\mu$-dppm)$(CO)_7$ (**6**) (37%) was obtained; pure **6** was formed by heating **5** in refluxing THF for 45 min. These complexes were identified by standard methods, **5** and **6** being distinguished by the presence of the appropriate molecular ions at m/z 1218 and 1162 respectively, in the FAB mass spectra, and the signal at $\delta = -13.27$ for the hydride ligand in **6**. The NH_2 protons were found at $\delta = 3.77$ for **5**, while the CH_2 protons of the unchanged dppm ligands in **5** and **6** were found at $\delta = 4.17$ and $\delta = 4.43$ respectively; in the latter, a complex multiplet could not be resolved to confirm the expected ABXX′ pattern. In the ^{13}C NMR spectrum of **5**, all the CO groups give a singlet at $\delta = 212$ as a result of their fluxional behaviour; for **6**, seven signals were found between $\delta = 189$ and 223. The carbon *ipso* to the N atom resonates at $\delta = 147.7$ in **5** and at $\delta = 173.3$ in **6**, the difference being attributed to dehydrogenation of the amino group and the formation of the Ru–N bonds.

Of interest here is the configuration about the N atom. Single-crystal molecular structure determinations carried out on **4** and **6** showed that in both cases the formation of the five-membered RuPCCN chelate ring results in the H atom bonded to N(12) being directed above and away from the Ru_3 plane. In a related osmium system, $Os_3(\mu$-NHPh)$(\mu$-Cl)$(CO)_{10}$, two isomers were crystallographically characterised as containing either the H atom or the Ph group above the Os_3 plane [13]. These were termed *exo* and *endo* respectively, and could also be distinguished on the basis of their ^{1}H NMR spectra, which contained the NH resonances at $\delta = 3.64$ and $\delta = 5.17$ respectively. The NH resonance of **4** was found at $\delta = 6.08$, while the spectrum of **6** contained two signals, at $\delta = 4.95$ and $\delta = 5.34$, with approximate relative intensities 2:3. These signals may arise from two isomers similar to those found for the osmium complex, but we note that in the *endo* conformation, the C_6H_4 group would experience considerable steric interaction with one of the Ph groups of the dppm ligand were the latter to retain the configuration found in the crystallographically studied complex, which has the *exo* configuration (see below).

Reaction between 2-diphenylphosphino-aniline and **2** afforded the yellow-orange $Os_3(CO)_{11}\{PPh_2(C_6H_4$-$NH_2$-2)} (**7**) in high yield, together with a minor product which was not identified conclusively, but may have been the Os analogue of **4**. Identification of **7** was straightforward, the expected features being present in the ^{1}H and ^{13}C NMR spectra, and the FAB mass spectrum containing M^+ at m/z 1156 together with ions formed by loss of up to 11 CO groups. The molecular structure of **7** is described below. We did not examine the thermolysis of **7**, so are unable to comment on the relative stabilities of **5** and **7**; it is evident, however, that **7** is considerably more robust than the Ru analogue.

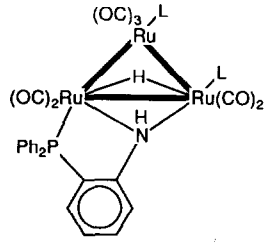

	LL
4	$(CO)_2$
6	dppm

2.2. Reactions of $PPh_2\{C_6H_4NHC(O)Ph$-2}

The reaction of the acylated aminophosphine with **3** in CH_2Cl_2 at room temperature gave the simple CO-substitution product $Ru_3(\mu$-dppm)$(CO)_9\{PPh_2(C_6H_4$-$NHC(O)Ph$-2)} (**8**) in moderate yield as dark red crystals which were suitable for a single-crystal X-ray study (below). Its identification followed from the FAB mass spectrum, which contained a molecular ion at m/z 1322 and showed loss of up to nine CO groups. The ^{13}C NMR spectrum contained a singlet at $\delta = 211.5$ for the fluxional CO groups together with a resonance for the amide CO group at $\delta = 165.2$.

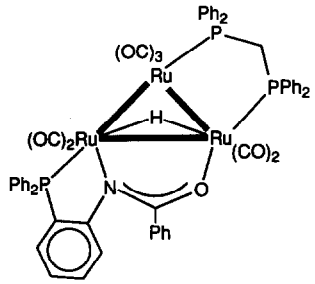

(9)

Pyrolysis of **8** in refluxing cyclohexane for 1 h gave the hydrido cluster $Ru_3(\mu\text{-H})\{\mu\text{-PPh}_2[C_6H_4NC(O)\text{-Ph-2}]\}(\mu\text{-dppm})(CO)_7$ (**9**), initially characterised from the molecular ion at m/z 1247 in the FAB mass spectrum, an IR ν(CO) spectrum similar to that of **6** and a high-field resonance at $\delta = -11.3$. A single-crystal X-ray structure determination (see below) revealed that the deprotonated ligand bridges an Ru–Ru vector through bonds from the O and N atoms to the Ru atoms, once again showing the tendency of acyl groups to be involved in bridging groups on clusters. However, the bridging amido group is unusual in that most previously characterised examples of this type of ligand adopt a $\mu\text{-}\eta^2(O,C)\text{-O=CNR}_2$ mode of bonding. The only previous example of the system present in **9** that we are aware of is provided by the major product formed by insertion of (tol)NCO into an Os–H bond of $Os_3(\mu\text{-H})(CO)_{10}$, namely $Os_3(\mu\text{-H})\{\mu\text{-}\eta^2(O,N)\text{-OCHN(tol)}\}(CO)_{10}$ [14]. In this complex, the amido ligand occupies two coordination positions perpendicular to the Os_3 plane (di-axial coordination) as found for **9**.

The osmium cluster carbonyl complex **10** was prepared from **2** in 67% yield as yellow needles, of which the IR and FAB mass spectra contained no unusual features. The molecular structure of **10** is described below.

2.3. Reactions of $PPh_2(C_6H_4N{=}CHPh\text{-}2)$

The sodium benzophenone ketyl-catalysed reaction between $Ru_3(CO)_{12}$ and the imino-phosphine afforded initially the simple CO-substitution product $Ru_3(CO)_{11}\{PPh_2(C_6H_4N{=}CHPh\text{-}2)\}$; as in the case of the reaction of $PPh_2(C_6H_4NH_2\text{-}2)$, this compound could not be isolated, but was readily converted into the hydrido cluster $Ru_3(\mu\text{-H})\{\mu\text{-PPh}_2(C_6H_4N{=}CPh\text{-}2)\}(CO)_9$ (**11**), which was obtained as red crystals in 90% yield. This compound was characterised from its ^{1}H NMR spectrum, which contained an Ru–H signal at $\delta = -13.95$, its FAB mass spectrum, which contained a molecular ion at m/z 922 and fragment ions formed by loss of up to nine CO groups, and by a single-crystal X-ray structure determination (see below).

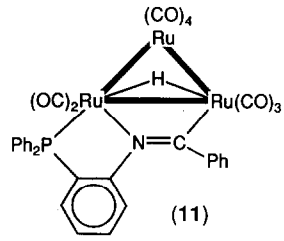

(11)

Stirring equimolar amounts of **3** and the imino-phosphine in dichloromethane at room temperature overnight afforded $Ru_3(\mu\text{-dppm})(CO)_9\{PPh_2(C_6H_4N{=}CHPh)\text{-}2\}$ (**12**) as orange crystals in 60% yield. The complex was characterised spectroscopically. The FAB mass spectrum contained a molecular ion at m/z 1306, from which there was loss of up to nine CO groups. The ^{1}H NMR spectrum contained resonances at $\delta = 4.16$ and $\delta = 8.10$, assigned to the CH_2 and CH protons respectively. The ^{13}C NMR spectrum contained one signal, at $\delta = 212.35$, for the fluxional carbonyl groups and a resonance caused by the CH group at $\delta = 159.13$.

No hydrogen migration occurred at room temperature, but heating of **12** in refluxing THF for 6.5 h or in refluxing cyclohexane for 1 h afforded $Ru_3(\mu\text{-H})\{\mu_3\text{-PPh}_2(C_6H_4N{=}CPh)\text{-}2\}(\mu\text{-dppm})(CO)_6$ (**13**). This complex was characterised earlier with the aid of a single-crystal X-ray study [15]; in contrast to the situation found with other complexes described above, the imino function bridges all three Ru atoms. The cluster-bonded proton was not located in the X-ray study, nor was there any resonance in the high-field region of the ^{1}H NMR spectrum. A parent ion was present in the FAB mass spectrum at m/z 1221, and it underwent fragmentation by the loss of up to six CO groups and two phenyl groups.

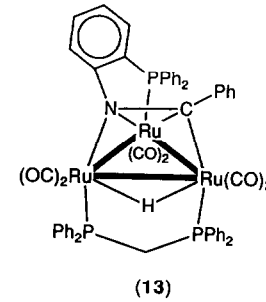

(13)

2.4. Reactions of $PPh_2(C_6H_4CHO\text{-}2)$

The reaction of $Ru_3(CO)_{11}(NCMe)$ with the phosphino-aldehyde in dichloromethane gave the orange compound $Ru_3(\mu\text{-H})\{\mu\text{-PPh}_2(C_6H_4CO\text{-}2)\}(CO)_9$ (**14**)

in 39% yield. The IR ν(CO) spectrum is virtually identical with that observed for **11**. The FAB mass spectrum contained $[M-CO]^+$ as the highest mass ion, suggesting that ready decarbonylation of this complex occurs under FAB conditions. Ions at m/z 819–567 are formed by further loss of up to nine CO groups. A second decomposition pattern (m/z 718–530), growing in intensity toward lower mass numbers, is consistent with the loss of two phenyl groups becoming increasingly competitive with loss of CO. The ^{1}H NMR spectrum contained two high-field resonances for cluster-bound hydrides, indicating the presence of two isomeric complexes; the signal at $\delta = -6.00$ ppm is consistent with the presence of a terminal hydride in one (**14a**), while that at $\delta = -13.30$ is characteristic of a bridging hydride in the other (**14b**). The two isomers are present in nearly equal amounts in the product isolated by preparative t.l.c. from the original reaction mixture. Repeated attempts to separate the two isomers by further preparative t.l.c. were unsuccessful, **14a** being completely transformed into **14b** during this process. The IR ν(CO) spectra for both isomers were identical. The ^{13}C NMR spectrum contained eight Ru–CO resonances between $\delta = 184.6$ and $\delta = 210.6$, together with a signal for the acyl carbonyl at $\delta = 249$. The ^{31}P NMR signal for **14a** was observed at $\delta = 66.40$ and that for **14b** at $\delta = 62.92$.

Stirring equimolar amounts of **3** with $PPh_2(C_6H_4$-CHO-2) in dichloromethane overnight at room temperature afforded $Ru_3(\mu$-dppm$)(CO)_9\{PPh_2(C_6H_4CHO$-2$)\}$ (**15**) as red crystals. The red compound $Ru_3(\mu$-H$)\{\mu$-$PPh_2(C_6H_4CO$-2$)\}(\mu$-dppm$)(CO)_7$ (**16**) was formed as a minor product. Complex **15** was characterised from its IR ν(CO), FAB mass and NMR spectra, elemental analysis, and X-ray crystallography (see below). The FAB mass spectrum contained an M^+ ion at m/z 1230 along with fragment ions at m/z 1202–874, indicating the loss of up to ten CO groups (nine from the cluster and one from the phosphine ligand) as well as of one phenyl group. The ^{1}H NMR spectrum contained the C*H*O signal at $\delta = 10.0$ as well as two signals for the CH_2 group, at $\delta = 4.20$ and $\delta = 4.11$ respectively. The ^{13}C NMR spectrum contained one signal, at $\delta = 211.6$, for the fluxional cluster-bound CO groups, and the aldehydic signal was at $\delta = 189.9$ ppm.

Heating **15** in refluxing cyclohexane resulted in H-migration to give the red hydrido complex $Ru_3(\mu$-H$)\{\mu$-$PPh_2(C_6H_4CO$-2$)\}(\mu$-dppm$)(CO)_7$ (**16**) in 66% yield. The highest mass ion in the FAB mass spectrum was at m/z 1147, corresponding to loss of two CO groups, and ions between m/z 1119–876 formed by loss of up to eight CO groups (seven from the cluster and the acyl carbonyl group) and of a phenyl group. The ^{1}H NMR spectrum contained two signals for the CH_2 group, at $\delta = 4.78$ and $\delta = 4.25$, together with two doublets of doublets at high field for the Ru–H atoms, indicating the presence of two isomers. The ^{13}C NMR spectrum contained signals for the carbonyl groups between $\delta = 190.1$ and $\delta = 218.2$, as well as the signal for the acyl carbonyl at $\delta = 286.4$ ppm. The ^{31}P NMR spectrum contained signals at $\delta = 14.2$ and $\delta = 9.6$ for the dppm ligand, and a singlet at $\delta = 61.5$ for the μ-$PPh_2(C_6H_4CO$-2$)$ ligand. The position of the signal at $\delta = 61.5$ is similar to that in the spectrum of **8**. The two phosphorus nuclei of the dppm ligand do not couple with that in the μ-$PPh_2(C_6H_4CO$-2$)$ group, but do couple with each other.

The ready loss of the acyl CO group evident from the FAB mass spectra of these complexes suggested that CO elimination might also proceed thermally, to generate a complex containing a metallated PPh_3 ligand, or (with a concomitant P–C bond cleavage reaction) another benzyne-cluster complex. In the event, heating **16** in refluxing toluene for 10 min resulted in a lightening of the colour of the solution, from which orange crystals of $Ru_3(\mu$-H$)\{\mu_3$-$PPh_2(C_6H_4CO)\}(\mu$-dppm$)(CO)_6$ (**17**) were obtained in 50% yield.

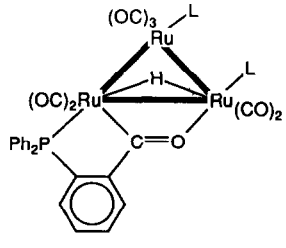

	M	LL
14	Ru	$(CO)_2$
16	Ru	dppm
19	Os	$(CO)_2$

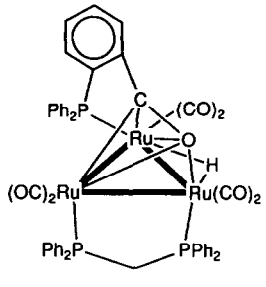

(17)

Prolonged heating (30 min) resulted in decomposition. Complex **17** was characterised by IR ν(CO), FAB

mass, and NMR spectroscopy. The IR ν(CO) (cyclohexane) spectrum showed six bands. The FAB mass spectrum was virtually identical to that of **16**, containing a highest mass ion at m/z 1147. A high-field signal for a cluster-bound hydride was observed in the ^{1}H NMR spectrum at $\delta = -14.95$. A single-crystal X-ray study, reported elsewhere [15], showed that the complex contained an unusual μ_3-acyl ligand.

Stirring equimolar amounts of **2** and the phosphino-aldehyde in dichloromethane for 3 h afforded $Os_3(CO)_{11}\{PPh_2(C_6H_4CHO\text{-}2)\}$ (**18**) as yellow diamond-shaped plates in 91% yield. The complex was characterised from its IR ν(CO), FAB mass and NMR spectra, as well as by elemental analysis and X-ray crystallography. (There were two phases; for one of them seemingly a CH_2Cl_2 hemi-solvate, the structure was less precisely determined; see below.) The FAB mass spectrum contained a molecular ion at m/z 1168. Further signals clearly showed loss of up to 12 CO groups (11 from the cluster and one from the phosphine ligand) as well as one phenyl group.

The presence of the aldehyde group was confirmed by the ^{1}H and ^{13}C NMR signals at $\delta = 10.13$ and $\delta = 189.46$ respectively; three signals for the fluxional carbonyl groups were observed. Complex **18** is stable for at least 30 min in refluxing toluene, and is only transformed slowly in refluxing xylene (140°C) to $Os_3(\mu\text{-}H)\{\mu\text{-}PPh_2(C_6H_4CO\text{-}2)\}(CO)_9$ (**19**). An alternative route to **19**, which afforded the complex in moderate yield under milder thermal conditions, was the reaction of **18** with Me_3NO in dichloromethane/acetonitrile solution. Complex **19** was characterised by its IR ν(CO), FAB mass and NMR spectra, and a single-crystal X-ray study (see below). The FAB mass spectrum contained signals for $[M\text{-}n CO]^+$ ($n = 1\text{–}10$) and an ion formed by the loss of C_6H_4 from the CO-free ion. A high-field resonance at $\delta = -13.4$ ppm in the ^{1}H NMR spectrum shows that a cluster-bound hydride is present in **19**. The nine carbonyl groups were observed in the ^{13}C NMR spectrum as separate signals between $\delta = 162.4$ and $\delta = 191.7$, together with a signal for the metal-bonded acyl carbonyl group at $\delta = 271.7$. The ^{31}P NMR spectrum contained a single resonance at $\delta = 35.7$. FAB mass spectrometry indicated that one of the minor products from the pyrolysis was an Os_4 cluster, although complete characterisation of this species has not yet been achieved.

Conversion of $PPh_2(C_6H_4CHO\text{-}2)$ into its 2,4-dinitrophenylhydrazone was readily achieved by standard procedures. Reaction of the modified ligand with $Os_3(CO)_{11}(NCMe)$ gave orange crystals of the expected MeCN-substitution product $Os_3(CO)_{11}\{PPh_2[C_6H_4(CH{=}NNHC_6H_3(NO_2)_2\text{-}2,4\text{-}2]\}$ (**20**) in high yield. This product was characterised from its IR ν(CO) spectrum and by a single-crystal X-ray study (see below). On heating in refluxing EtOH, it was hydrolysed in high yield to the parent phosphino-aldehyde complex **18**.

2.5. Reactions of $PPh_2\{CH_2C(O)Ph\}$

We have briefly described the preparation of $Ru_3(CO)_{11}\{PPh_2[CH_2C(O)Ph]\}$ (**21**) and its conversion into the hydrido cluster $Ru_3(\mu\text{-}H)\{\mu\text{-}PPh_2[CH{\equiv}C(\equiv O)Ph]\}(CO)_9$ (**22**) which contains a phosphino-enolate ligand [5]. This conversion proceeds easily in refluxing THF and can be reversed by carbonylation (20°C, 1 bar, 2 h). The hydrido complex can also be prepared directly from the reaction of $Ru_3(CO)_{12}$, $PPh_2\{CH_2C(O)Ph\}$ and [PPN][OAc], the latter reagent activating the first CO towards substitution and the second to generate a vacant coordination site to accommodate the bridging enolate ligand. In this regard, the reaction is similar to those described above for the Os_3 clusters.

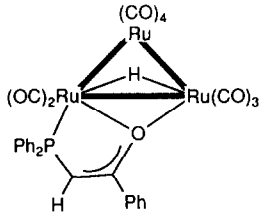

(22)

Protonation of **22** afforded the cationic cluster $[Ru_3(\mu\text{-}H)(CO)_{10}\{\mu\text{-}PPh_2[CH_2C(O)Ph]\}][BF_4]$ (**23**), readily characterised by the presence of the Ru–H resonance at $\delta = -15.2$ and the CH_2 protons of the keto-phosphine as the AB part of an ABX system at $\delta = 4.89$ and $\delta = 5.27$. The protonation could be reversed by addition of ethanolic NaOH, whereupon the orange-yellow **23** changed immediately to the yellow **22**. Addition of $PPh_2\{CH_2C(O)Ph\}$ to **22**, followed by Me_3NO and HBF_4, afforded the disubstituted cationic cluster $[Ru_3(\mu\text{-}H)(CO)_8\{PPh_2[CH_2C(O)Ph]\}_2][BF_4]$ (**24**) as red crystals. This complex was identified from its ^{1}H NMR spectrum, which contained a high-field triplet resonance at $\delta = -11.75$ and the characteristic signals of the PCH_2R ligands at $\delta = 3.01$ and $\delta = 4.74$. The single ^{31}P resonance at $\delta = 42.2$ confirmed the equivalence of the two phosphine ligands.

Thermolysis of the di- and tri-substituted clusters $Ru_3(CO)_{12-n}\{PPh_2[CH_2C(O)Ph]\}_n$ ($n = 2, 3$) gave only $Ru_3(\mu\text{-}H)\{\mu\text{-}PPh_2[CH{\equiv}C(\equiv O)Ph]\}(CO)_9$ and $Ru_3(CO)_{10}\{PPh_2[CH_2C(O)Ph]\}_2$ respectively.

An Me_3NO-instigated reaction between $Ru_3(\mu\text{-}H)(\mu_3\text{-}C_2{}^tBu)(CO)_9$ and $PPh_2\{CH_2C(O)Ph\}$ gave the mono-substituted complex $Ru_3(\mu\text{-}H)(\mu_3\text{-}C_2{}^tBu)(CO)_8\{PPh_2[CH_2C(O)Ph]\}$ (**25**), conclusively identified from

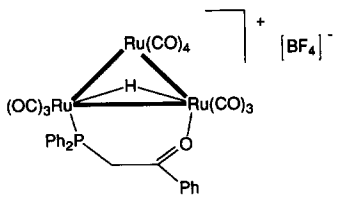

23

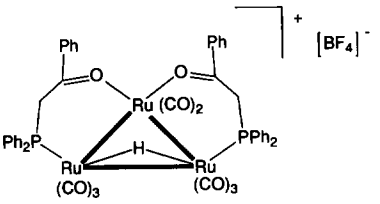

24

its ^{1}H NMR spectrum, which in addition to the high-field doublet at $\delta = -21.1$, contained resonances from the ^{t}Bu group at $\delta = 1.24$ and the phosphine CH_2 group at $\delta = 4.01$. A second ligand was introduced by treating a mixture of **25** and the phosphino-ketone with Me_3NO to give $Ru_3(\mu\text{-}H)(\mu_3\text{-}C_2{}^t\text{Bu})(CO)_7\{PPh_2[CH_2C(O)Ph]\}_2$ (**26**). In this case, the ^{1}H NMR spectrum contained a high-field doublet at room temperature, which at -63°C was replaced by two doublets, suggesting that **26** exists in solution as a mixture of interconverting isomers. At -23°C, the ^{31}P NMR spectrum contained four signals between $\delta = 23$–46.

Deprotonation of **25** with ethanolic NaOH, followed by addition of $AuCl(PPh_3)$, afforded a yellow complex characterised as $AuRu_3(\mu_3\text{-}C_2{}^t\text{Bu})(CO)_8\{PPh_2[CH_2C(O)Ph]\}(PPh_3)$ (**27**) by elemental microanalysis and specifically from its FAB mass spectrum, which contained a molecular ion at m/z 1373. The ^{1}H NMR spectrum contained resonances from the ^{t}Bu and PCH_2 groups ($\delta = 1.37$ and $\delta = 4.25$ respectively), while the ^{31}P NMR spectrum contained two resonances at $\delta =$ 44.3 and $\delta = 60.15$, assigned to the keto-phosphine and PPh_3 ligands respectively.

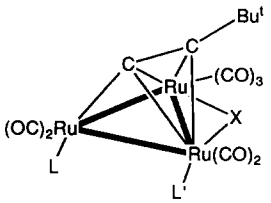

	X	L	L'
25	H	$PPh_2\{CH_2C(O)Ph\}$	CO
26	H	$PPh_2\{CH_2C(O)Ph\}$	$PPh_2\{CH_2C(O)Ph\}$
27	$Au(PPh_3)$	$PPh_2\{CH_2C(O)Ph\}$	CO

3. Molecular structures

In the course of this work, several of the complexes were characterised with the aid of single-crystal X-ray studies. However, because of the gross similarities between the structures, only the notable features will be discussed in detail. For complexes $M_3(CO)_{11}(PR_3)$, there has already been an extensive study of the effects of coordinating tertiary phosphines and phosphites to the M_3 systems, and the present results do not differ significantly from the general conclusions arrived at previously [16].

3.1. $Os_3(CO)_{11}\{PPh_2(C_6H_4X\text{-}2)\}$ [X = NH_2 (7), NHC(O)Ph (10), CHO (18) and $CH{=}NNHC_6H_3(NO_2)_2$-2,4 (20)]

The structures of the four molecules are shown in Figs. 1–4 and selected bond distances and angles are listed in Table 1. These molecules contain a bonded Os_3 triangle with two shorter bonds [Os–Os 2.875(2)–2.883(1) Å] and one longer bond [2.898(1)–2.927(1) Å], the latter being adjacent to the functional phosphine ligand; the separations are within the normal range. The tertiary phosphine ligands occupy equatorial sites, with Os–P separations between 2.353(3) Å and 2.377(3) Å. The substituent groups on the phosphines do not interact with the metal atoms. The steric effects of the phosphines result in P(1)–Os(1)–C(13) and P(1)–Os(1)–Os(2) angles of between 96.8(4)° and 100.5(4)°, and 103.2(1)° and 108.05(7)° respectively. While the precision of the Os–CO bond lengths does not permit detailed comments, the Os–C(13) separations [1.85(1)–

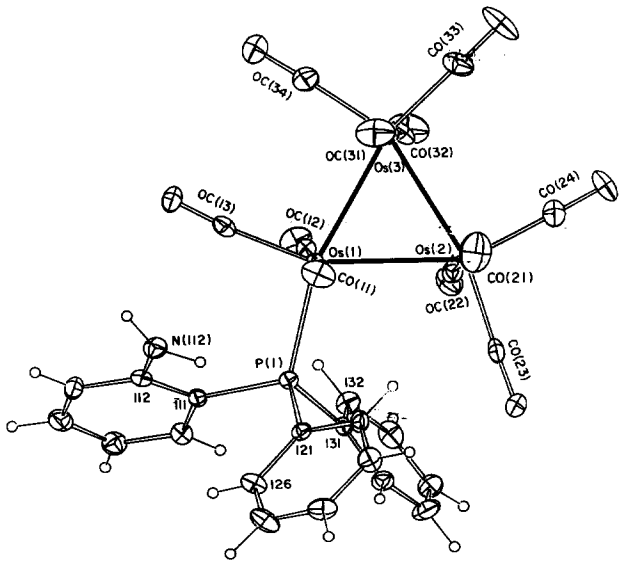

Fig. 1. Plot of a molecule of $Os_3(CO)_{11}\{PPh_2(C_6H_4NH_2\text{-}2)\}$ (7).

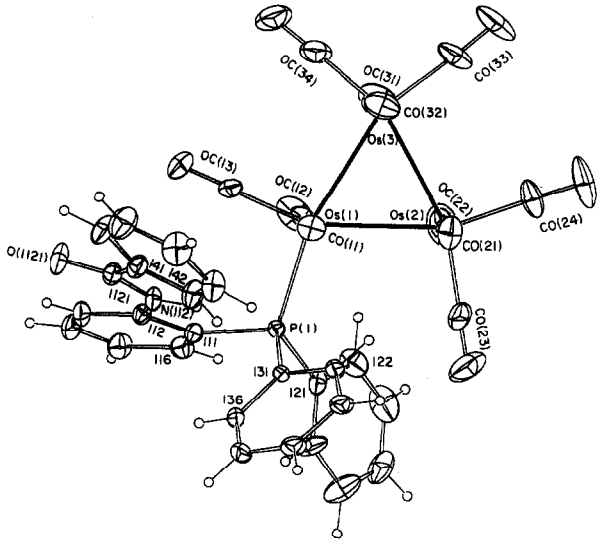

Fig. 2. Plot of a molecule of $Os_3(CO)_{11}\{PPh_2[C_6H_4NHC(O)Ph\text{-}2]\}$ (**10**).

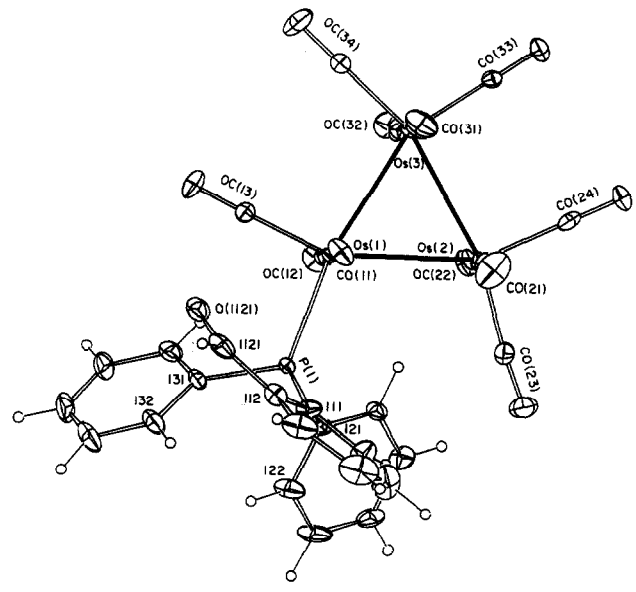

Fig. 3. Plot of a molecule of $Os_3(CO)_{11}\{PPh_2(C_6H_4CHO\text{-}2)\}$ (**18**).

1.88(2) Å] are generally shorter as a result of increased back-bonding of electron density from the phosphine ligand. The axial CO groups are generally further away from the metal atoms than the remaining equatorial CO groups. All these features are similar to the results reported earlier [16].

TABLE 1. Some bond parameters for complexes $Os_3(CO)_{11}\{PPh_2(C_6H_4X\text{-}2)\}$

X	NH_2 (**7**)	NHCOPh (**10**)	CHO (**18**)	CH=NNH(dnp) [a] (**20**)
Bond lengths (Å)				
Os(1)–Os(2)	2.898(1)	2.901(2)	2.927(1)	2.903(1)
Os(1)–Os(3)	2.877(1)	2.875(1)	2.876(1)	2.876(1)
Os(2)–Os(3).	2.877(2)	2.875(2)	2.883(1)	2.879(1)
Os(1)–P(1)	2.377(3)	2.353(3)	2.357(3)	2.345(3)
Os–CO(ax)	1.91–1.96	1.88–1.92	1.92–1.95	1.86–1.92
Os–CO(eq)	1.88–1.92	1.86–1.91	1.85–1.92	1.86–1.94
C(112)–X	1.40(2) (N)	1.38(1) (N)	1.44(2) (C)	1.49(2) (C)
Bond angles (°)				
Os(2)–Os(1)–P(1)	103.17(9)	105.42(6)	108.05(7)	101.39(9)
Os(3)–Os(1)–C(11)	92.2(3)	89.7(3)	86.1(4)	84.0(4)
Os(3)–Os(1)–C(12)	85.4(3)	88.6(4)	93.2(4)	93.2(4)
Os(3)–Os(1)–C(13)	96.9(3)	97.3(4)	95.4(4)	100.6(4)
P(1)–Os(1)–C(11)	90.9(4)	92.1(3)	90.8(4)	90.0(4)
P(1)–Os(1)–C(12)	92.4(4)	90.3(4)	89.6(4)	92.9(4)
P(1)–Os(1)–C(13)	100.5(4)	97.7(4)	96.8(4)	98.2(4)
C(111)–P(1)–C(121)	103.5(5)	104.1(4)	101.6(5)	105.3(7)
C(111)–P(1)–C(131)	105.6(6)	105.3(4)	108.6(6)	104.6(7)
C(121)–P(1)–C(131)	102.1(6)	99.6(5)	97.3(6)	95.9(6)
Atom deviations from Os_3 plane (Å)				
δP(1)	0.189(4)	0.099(3)	0.095(4)	0.260(4)
δC(13)	−0.21(2)	−0.10(2)	0.10(3)	−0.02(2)
δC(23)	−0.13(2)	0.08(2)	−0.06(2)	−0.09(2)
δC(24)	0.25(2)	−0.11(2)	−0.05(2)	0.17(2)
δC(33)	−0.19(2)	0.07(2)	−0.14(1)	−0.25(2)
δC(34)	0.16(2)	0.06(2)	0.13(2)	0.27(2)

[a] dnp = $C_6H_3(NO_2)_2$-2,4

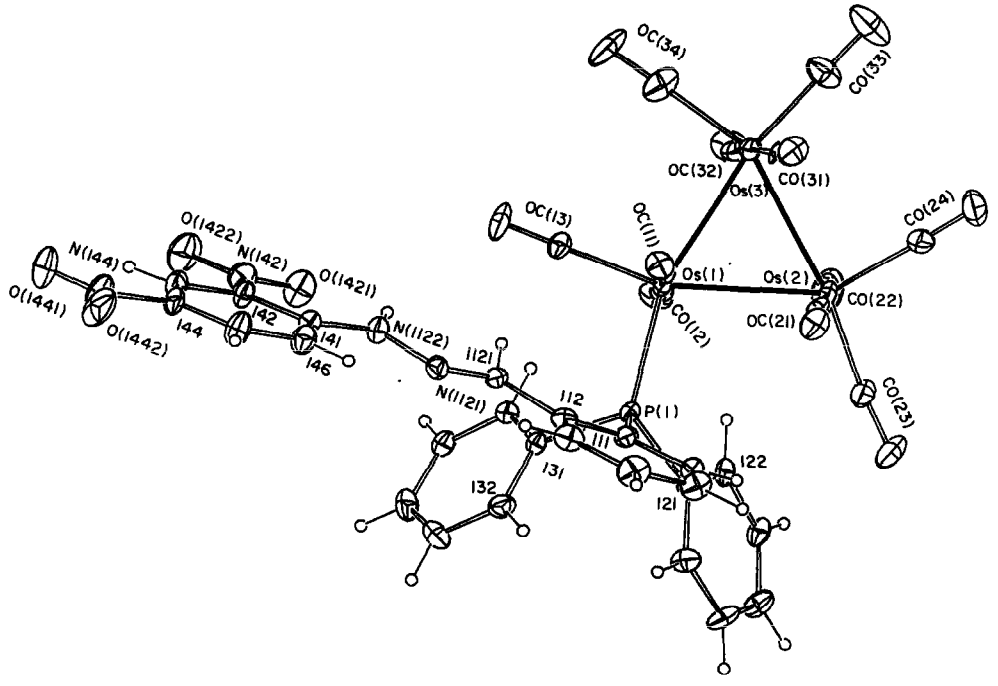

Fig. 4. Plot of a molecule of $Os_3(CO)_{11}\{PPh_2[C_6H_4CH{=}NNHC_6H_3(NO_2)_2\text{-}2,4]\text{-}2\}$ (**20**).

3.2. *$Ru_3(\mu\text{-dppm})(CO)_9\{PPh_2(C_6H_4X\text{-}2)\}$ [X = NHC(O)Ph (8) and CHO (15)]*

The structures of these two molecules are shown in Figs. 5 and 6, and selected bond parameters are given in Table 2. These appear to be the first determinations of molecular structures of phosphine-substituted derivatives of **3**. Like the parent complex, the dppm ligand occupies equatorial positions, as does the PR_3 ligand. The bonded Ru_3 triangle has two shorter Ru–Ru bonds [2.827(2)–2.8541(9) Å] and one longer [2.9272(9), 2.899(1) Å for **8** and **15** respectively], the latter being adjacent to the monodentate phosphine. In **8**, the dppm-bridged Ru–Ru bond is 2.842(1) Å, while the other two Ru–Ru vectors are 2.827(1) Å and 2.927(1) Å; the lengthening in the present case is probably the result of the steric size of the functional phosphine ligand, as found for other trisubstituted $Ru_3(CO)_9(PR_3)_3$ complexes. The Ru–P distances fall in the range 2.316(2)–2.359(2) Å, the functional phosphine ligand being *trans* to P(1) of the dppm ligand. Within the Ru_2PCP cycle, the angles Ru–Ru–P fall

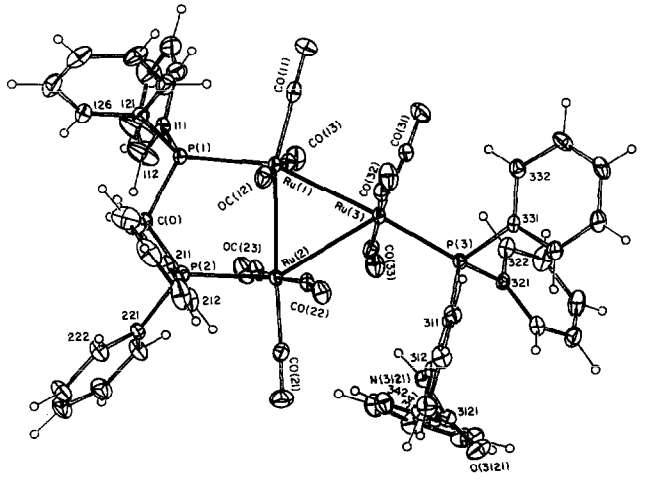

Fig. 5. Plot of a molecule of $Ru_3(\mu\text{-dppm})(CO)_9\{PPh_2[C_6H_4\text{-}NHC(O)Ph\text{-}2]\}$ (**8**).

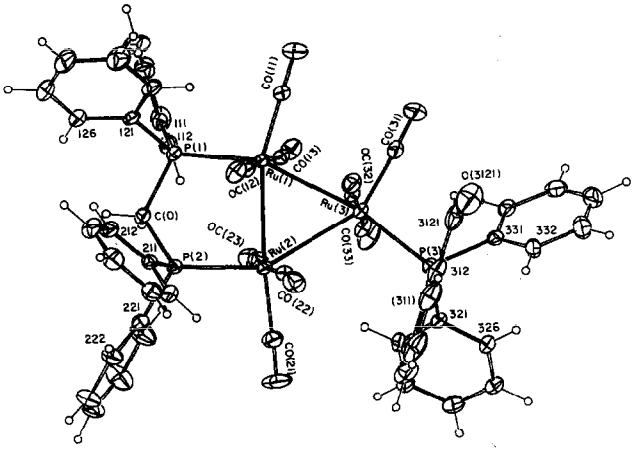

Fig. 6. Plot of a molecule of $Ru_3(\mu\text{-dppm})(CO)_9\{PPh_2(C_6H_4CHO\text{-}2)\}$ (**15**).

TABLE 2. Some bond parameters for $Ru_3(\mu\text{-dppm})(CO)_9\{PPh_2(C_6H_4X\text{-}2)\}$

X	NHCOPh (8)	CHO (15)
Bond lengths (Å)		
Ru(1)–Ru(2)	2.8421(9)	2.8343(9)
Ru(1)–Ru(3)	2.827(2)	2.8541(9)
Ru(2)–Ru(3)	2.9272(9)	2.899(1)
Ru(1)–P(1)	2.316(2)	2.316(2)
Ru(2)–P(2)	2.336(2)	2.327(2)
Ru(3)–P(3)	2.340(2)	2.359(2)
Ru–CO(ax)	1.897–1.924(7)	1.903–1.921(6)
Ru–CO(eq)	1.864–1.870(6)	1.861–1.889(6)
Bond angles (°)		
Ru(1)–Ru(2)–P(2)	86.76(5)	87.84(5)
Ru(2)–Ru(1)–P(1)	95.97(5)	96.17(5)
Ru(3)–Ru(2)–C(21)	118.0(3)	114.7(2)
Ru(2)–Ru(3)–P(3)	117.28(5)	108.61(4)
P(3)–Ru(3)–C(31)	101.3(3)	101.0(2)
P(1)–Ru(1)–C(11)	100.1(3)	101.6(2)
P(2)–Ru(2)–C(21)	97.8(3)	98.2(2)
Atom deviations from Ru_3 plane (Å)		
δP(1)	−0.309(3)	−0.496(2)
δP(2)	0.612(3)	0.275(2)
δP(3)	0.479(3)	0.415(3)
δC(11)	0.187(9)	0.138(6)
δC(21)	−0.194(8)	1.878(6) − 0.192(7)
δC(31)	−0.731(8)	−1.852(6) − 0.300(7)

between 86.76(5)° and 96.17(5)°, while the P(3)–Ru(3)–Ru(2) angle is 117.28(5)° for **8** and 108.61(4)° for **15**. These values are similar to those found for **3** [17]. Again the equatorial CO groups are closer to the respective Ru atoms than are the axial CO groups; the mean difference is *ca* 0.04 Å. Compared with **3**, however, the average values are considerably smaller, values of 1.90_4 Å and 1.94_5 Å being found in **8** for the equatorial and axial Ru–C bonds respectively. This effect is the result of having a third strongly electron-donating ligand on the cluster, leading to more back-bonding into the Ru–CO anti-bonding orbitals and hence shortening of the Ru–CO bonds. The N(3121)–C(3121) and C(3121)–O(3121) bonds are 1.349(8) Å and 1.23(1) Å, respectively; both are significantly shorter than single bonds, perhaps a result of some delocalisation of electron density in the NHCO system.

3.3. $Ru_3(\mu\text{-}H)\{\mu\text{-}PPh_2(C_6H_4NH\text{-}2)\}(LL)(CO)_7$ [LL = $(CO)_2$ (4), μ-dppm (6)]

Figures 7 and 8 show the molecular structures of **4** and **6**; some bond distances and angles are presented in Table 3. In these molecules, the functional phosphine has been dehydrogenated to give an edge-bridging amido ligand; the P atom is also attached to one of these two Ru atoms [Ru–P 2.310(2), 2.289(9)–2.299(8) Å in **4** and **6** respectively], so that a bicyclic 5/3

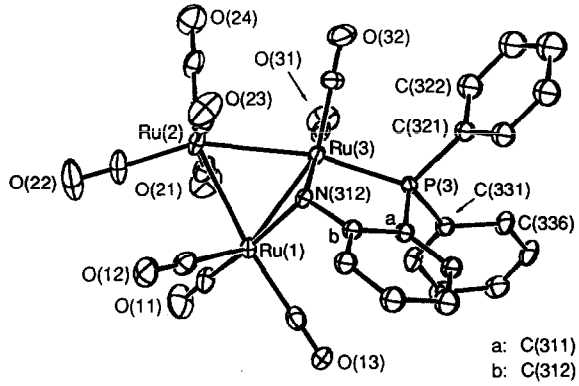

Fig. 7. Plot of a molecule of $Ru_3(\mu\text{-}H)\{\mu\text{-}PPh_2(C_6H_4NH\text{-}2)\}(CO)_9$ (**4**).

$RuPC_2N/Ru_2N$ system is formed. In both complexes the N atom bridges an Ru–Ru vector [Ru–N 2.146(6), 2.115(5); 2.10, 2.20(2) Å]. The geometry about the N atom in the two complexes requires the associated hydrogen atom to lie above the Ru_3 core, that is, in the *exo* position, as also suggested by its chemical shift (δ = 4.95). The four atoms Ru(1), Ru(3), N(312) and C(312) lie −0.001(1), −0.001(1), 0.463(6) and −0.367(7) Å out of the least-squares plane through these atoms.

Coordination of the bridging ligand splays out the Ru–P and Ru–CO ligands [angles P–Ru–Ru 105.4(1)° and 102.7(2)–105.7(2)°; C–Ru–Ru 120.1(3)° and 114.8(9)–117(1)° for **4** and **6** respectively]. The "axial" CO groups are generally nearer to the respective Ru atoms than are the "equatorial" CO groups, but the

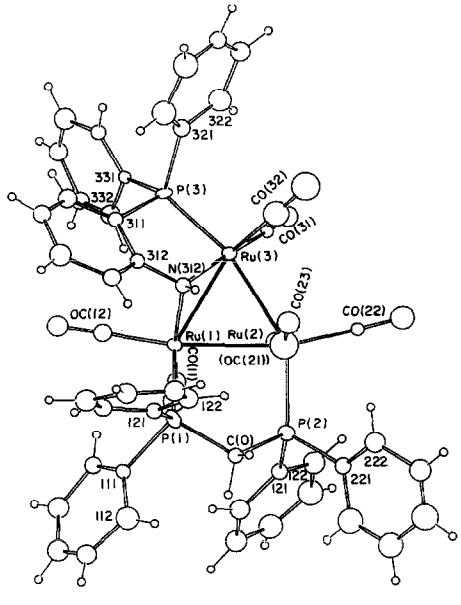

Fig. 8. Plot of a molecule of $Ru_3(\mu\text{-}H)\{\mu\text{-}PPh_2(C_6H_4NH\text{-}2)\}(\mu\text{-dppm})(CO)_7$ (**6**).

TABLE 3. Some bond parameters for $Ru_3(\mu\text{-H})\{\mu\text{-PPh}_2C_6H_4NH\text{-}2\}(LL)(CO)_7$

LL	$(CO)_2$ (4)	μ-dppm (6) [a]
Bond lengths (Å)		
Ru(1)–Ru(2)	2.835(1)	2.845(3)–2.859(4)
Ru(1)–Ru(3)	2.768(1)	2.763(4)–2.781(4)
Ru(2)–Ru(3)	2.827(1)	2.801(4)–2.813(4)
Ru(1)–P(1)	–	2.297(9)–2.321(9)
Ru(1)–P(3)	2.310(2)	–
Ru(2)–P(2)	–	2.299(9)–2.316(9)
Ru(3)–P(3)	–	2.289(9)–2.312(8)
Ru(1)–N(312)	2.146(6)	2.17(2)–2.24(2)
Ru(3)–N(312)	2.115(5)	2.07(2)–2.11(2)
Ru(1)–CO(11)	1.891(9)	1.66(3)–1.91(3)
Ru(1)–CO(12)	1.910(9)	1.80(3)–1.92(3)
Ru(1)–CO(13)	1.97(1)	–
Ru(2)–CO(21,23)	1.946(11), 1.927(9)	1.60(5)–1.96(2)
Ru(2)–CO(22)	1.907(9)	1.77(4)–1.93(3)
Ru(2)–CO(24)	1.95(1)	–
Ru(3)–CO(31)	1.869(9)	1.62(3)–1.86(4)
Ru(3)–CO(32)	1.887(8)	1.80(3)–1.96(4)
P(3)–C(311)	1.817(6)	1.79(3)–1.88(3)
P(3)–C(321,331)	1.825(5), 1.829(4)	1.72(3)–2.00(3)
Bond angles (°)		
Ru(1)–Ru(3)–P(3)	105.4(1)	102.7(2)–105.7(2)
Ru(2)–Ru(3)–P(3)	165.8(1)	164.0(2)–167.3(3)
Ru(3)–P(3)–C(311)	101.5(2)	102(1)–104(1)
Ru(1)–N(312)–Ru(3)	81.0(2)	79.5(7)–81.2(9)
Ru(1)–N(312)–C(312)	116.0(4)	114(2)–126(2)
Ru(3)–N(312)–C(312)	119.1(4)	119(2)–122(2)
Ru(1)–Ru(3)–C(31)	118.9(3)	117.1(1)–121.6(8)
Ru(3)–Ru(1)–C(11)	120.1(3)	114.8(9)–117(1)
Ru(3)–Ru(1)–C(12)	132.8(3)	–
Ru(3)–Ru(1)–P(1)		136.2(3)–137.6(2)
Ru(1)–P(1)–C(0)		115(1)–116.7(9)
Ru(2)–P(2)–C(0)		108.4(9)–113(1)

[a] Range of values for three molecules. Values for displacement of P atoms from Ru_3 plane: δP(1) 1.24(1), 1.239(10), 1.32(1); δP(2) 0.19(1), 0.25(1), 0.29(1); δP(3) 0.03(1), 0.05(1), 0.04(1).

differences are not so marked as in the other complexes described above.

In the Ru_3 triangles, the non-bridged Ru–Ru separations are remarkably similar, with average values of *ca.* 2.81 Å; the N-bridged Ru–Ru lengths are 2.768(1), 2.763(4)–2.781(4) Å. The location of the bridging H atom in the two complexes is a matter of some conjecture as neither were located in the X-ray studies. Normally, the presence of this ligand is revealed by a lengthening of the M–M vector over similar non-bridged systems. However, in the present cases, we are inclined to think that the H atom bridges the N-bridged Ru–Ru vector in both complexes, as suggested by the disposition of the CO ligands about this vector.

In **6**, the dppm ligand occupies equatorial sites on the associated ruthenium atoms [Ru–P 2.289(9)–2.321(9) Å], although P(1) lies considerably above the Ru_3 plane (see Table 3). This distortion is associated with the bending of Ru(1)–CO(11) [Ru(3)–Ru(1)–C(11) 114.8(9)–117(1)°]; a larger displacement of C(31) is found [Ru(1)–Ru(3)–C(31) 117.1(1)–121.6(8)°]. Both of these are presumably the result of the μ-H ligand spanning the Ru(1)–Ru(3) vector. There is a close approach of H(316) to the centre of the Ph(12) group of the dppm ligand [H(316) $\cdots$ C(321, 326) (est.) 2.8, 3.0 Å]. This interaction may assist in stabilising the observed structure and results from a twist of Ru(1) coordination sites (with respect to the Ru_3 plane) upon coordination of N(312); both CO(31) and CO(11) are approximately *trans* to N(312) [N(312)–Ru(1)–C(11) 163(1), N(312)–Ru(3)–C(31) 173(1)° (av.)] which results in P(1) being lifted above the Ru_3 plane on the same side as N(312).

Both complexes are unusual in that the dehydrogenated ligand is found bridging a vector which includes the Ru atom to which the P atom is attached. In other examples, such as those formed by the well-known cyclometallation reactions [18], the functional group bridges the other two Ru atoms. Here, the observed stereochemistry suggests that the formation of a five-membered $RuPC_2N$ ring is preferred over that of the six-membered $RuPC_2NRu$ system which would be formed if the latter course were followed.

TABLE 4. Some bond parameters for $Ru_3(\mu\text{-H})\{\mu\text{-PPh}_2[C_6H_4NC(Ph)O\text{-}2]\}(\mu\text{-dppm})(CO)_7$ (9)

Bond lengths (Å)			
Ru(1)–Ru(2)	2.854(2)	Ru(1)–CO(11,12)	1.916, 1.902(6)
Ru(1)–Ru(3)	2.863(2)	Ru(1)–CO(13)	1.88(1)
Ru(2)–Ru(3)	2.899(1)	Ru(2)–CO(21)	1.821(6)
Ru(1)–P(1)	2.319(2)	Ru(2)–CO(22)	1.895(8)
Ru(2)–P(2)	2.332(2)	Ru(3)–CO(31)	1.893(9)
Ru(3)–P(3)	2.330(3)	Ru(3)–CO(32)	1.847(5)
Ru(2)–O(3121)	2.157(4)	C(3121)–N(3121)	1.30(1)
Ru(3)–N(3121)	2.160(4)	C(3121)–O(3121)	1.27(1)
Bond angles (°)			
Ru(1)–Ru(3)–P(3)	166.83(4)	Ru(3)–N(3121)–C(3121)	125.4(5)
Ru(2)–Ru(3)–P(3)	123.28(7)	N(3121)–C(3121)–O(3121)	123.5(5)
Ru(3)–P(3)–C(311)	97.7(2)	Ru(2)–O(3121)–C(3121)	126.9(4)

3.4. $Ru_3(\mu\text{-}H)(\mu\text{-}dppm)\{\mu\text{-}PPh_2[C_6H_4NC(Ph)O\text{-}2]\}(CO)_7$ (9)

A molecule of **9** is depicted in Fig. 9, and selected bond parameters are listed in Table 4. As noted above, the functional group of the tertiary phosphine has been deprotonated to give a three-atom edge-bridging group which is attached to the cluster by the N and O atoms [Ru(2)–O(3121) 2.157(4) Å, Ru(3)–N(3121) 2.160(4) Å]; the central carbon of the carboxamide ligand does not interact with the cluster. Electron delocalisation within the carboxamide function is indicated by the N(3121)–C(3121) [1.30(1) Å] and C(3121)–O(3121) [1.27(1) Å] bond lengths; internal angles at atoms N, C, O(3121) are 125.4(5), 123.5(5) and 126.9(4)° respectively. The metal-bonded hydrogen was located and refined in the X-ray study, and bridges Ru(2)–Ru(3) [2.899(1) Å], while the dppm-bridged Ru(1)–Ru(2) [2.854(2) Å] and non-bridged Ru(1)–Ru(3) vectors [2.863(2) Å] are within the expected ranges. The dppm ligand occupies equatorial coordination sites [Ru(1)–P(1) 2.319(2), Ru(2)–P(2) 2.332(2) Å].

3.5. $Ru_3(\mu\text{-}H)\{\mu\text{-}PPh_2(C_6H_4N{=}CPh\text{-}2)\}(CO)_9$ (11)

A molecule of **11** is depicted in Fig. 10, and selected bond parameters are listed in Table 5. Again, we find that the tertiary phosphine has been dehydrogenated at the functional group to give an edge-bridging ligand: in **11**, the N=C unit bridges the Ru(1)–Ru(2) vector [Ru(1)–C(40) 2.088(5) Å, Ru(2)–N(12) 2.114(4) Å]. We note that bridging by the C=N group increases this separation to 2.920(1) Å from the values found in **4** and **6** (above). The atoms of the $CNRu_2$ cycle are almost

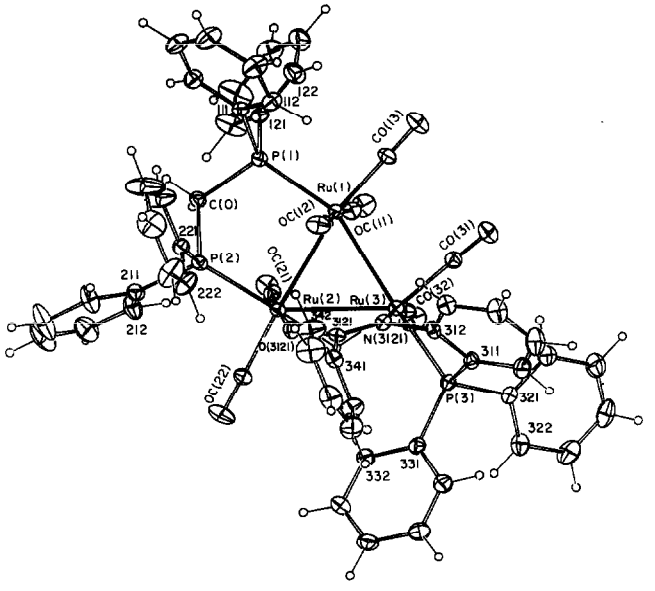

Fig. 9. Plot of a molecule of $Ru_3(\mu\text{-}H)\{\mu\text{-}PPh_2[C_6H_4NC(Ph)O\text{-}2]\}(\mu\text{-}dppm)(CO)_7$ (**9**).

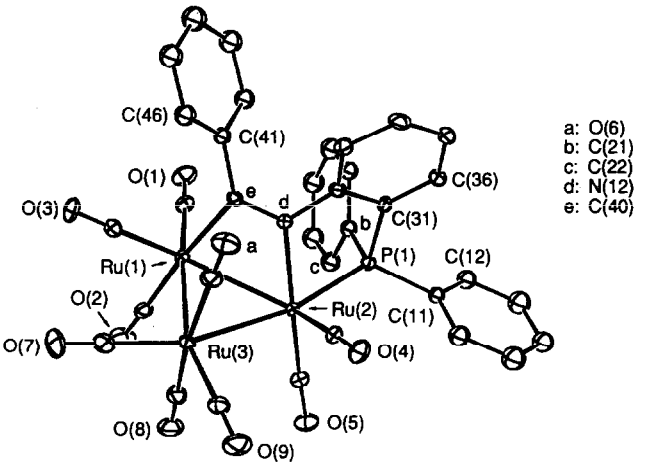

Fig. 10. Plot of a molecule of $Ru_3(\mu\text{-}H)\{\mu\text{-}PPh_2(C_6H_4N{=}CPh\text{-}2)\}(CO)_9$ (**11**).

coplanar, the maximum deviation being 0.020(6) Å for C(40), with internal angles at N(12) and C(40) of 112.0(1)° and 116.9(2)° respectively; the C–N bond length is 1.292(6) Å. The hydride ligand was not located in the X-ray study, but similar considerations to those presented for **4** and **6** suggest that the H atom bridges the Ru(1)–Ru(2) vector.

3.6. $Os_3(\mu\text{-}H)\{\mu\text{-}PPh_2(C_6H_4CO\text{-}2)\}(CO)_9$ (19)

The structure of a molecule of **19** is shown in Fig. 11 and selected bond parameters are listed in Table 6. The triangular Os_3 core has Os–Os separations between 2.833(2)–2.918(1) Å. The deprotonated acyl ligand bridges Os(1)–Os(2), O(1121) being attached to Os(2) [2.13(1) Å] and both the acyl carbon and the phosphorus atom chelating Os(1) [Os(1)–P(1) 2.319(5)

TABLE 5. Some bond parameters for $Ru_3(\mu\text{-}H)\{\mu\text{-}PPh_2(C_6H_4N{=}CPh\text{-}2)\}(CO)_9$ (**11**)

Bond lengths (Å)		Bond angles (°)	
Ru(1)–Ru(2)	2.920(1)	Ru(1)–Ru(2)–P(1)	112.0(1)
Ru(1)–Ru(3)	2.850(1)	Ru(3)–Ru(2)–P(1)	167.4(1)
Ru(2)–Ru(3)	2.833(1)	Ru(2)–P(1)–C(31)	100.4(2)
Ru(2)–P(1)	2.333(1)	Ru(2)–N(12)–C(32)	118.0(3)
Ru(2)–N(12)	2.114(4)	Ru(2)–N(12)–C(40)	113.6(3)
Ru(1)–C(40)	2.088(5)	Ru(1)–C(40)–N(12)	112.0(3)
Ru(2)–CO(5)	1.867(6)		
Ru(2)–CO(4)	1.880(6)		
Ru(1)–CO(3)	1.914(6)		
Ru(1)–CO(2)	1.948(6)		
Ru(1)–CO(1)	1.929(6)		
Ru(3)–CO(7,9)	1.935(8), 1.909(6)		
Ru(3)–CO(8,6)	1.951(8), 1.960(8)		
P(1)–C(31)	1.829(5)		
P(1)–C(11,21)	1.823(4), 1.812(4)		
N(12)–C(40)	1.292(6)		

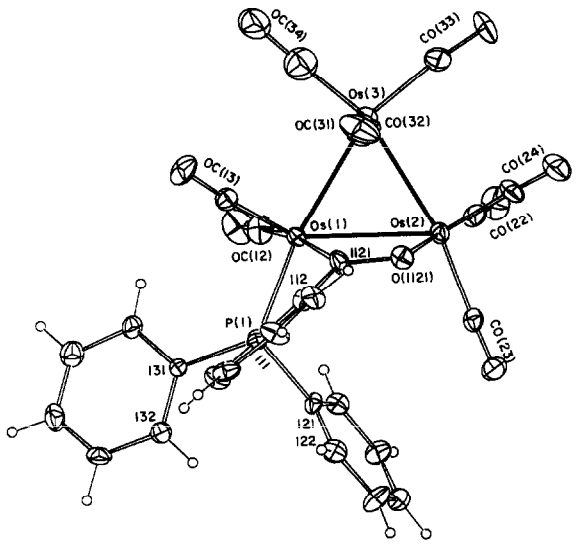

Fig. 11. Plot of a molecule of $Os_3(\mu\text{-H})\{\mu\text{-PPh}_2(C_6H_4CO\text{-}2)\}(CO)_9$ (**19**).

Å, Os(1)–C(1121) 2.05(2) Å]. In the μ-acyl group the C–O distance [1.29(2) Å] may be somewhat longer than that found in the immediate precursor **18**, with a similar C_6H_4–CO bond [1.46(3) Å]. As in **18**, P(1) occupies an equatorial site, although bent up from the Os_3 plane by the geometrical requirements of the bicyclic $OsPC_3/Os_2C_2$ system. Again, axial Os–CO distances are approximately 0.04 Å longer than the equatorial Os–CO distances. The hydrogen atom, not located in the X-ray study, but clearly shown to be present by the ^1H NMR spectrum ($\delta = -13.39$), probably bridges Os(1)–Os(2), as revealed both by the lengthening of this separation and by the characteristic splaying of the CO groups attached to the two Os atoms [Os(1)Os(2)C(22) 112.6(8)°, Os(2)Os(1)C(12) 116.6(7)°].

Most of these complexes contain an edge-bridging ligand formed by the H-migration reactions. Comparison of their molecular structures shows that the dihedral between the M_3 and $M_2(\mu\text{-X})$ planes varies as follows: 111.8(5) and 68.54(5), 70.59(5), 66.15(5)° [for X = NH in **4** and **6** (three molecules)], 72.5(4)° (X = N=CPh in **11**) and 74.30(4)° (X = CO in **19**).

4. Discussion

This work has examined the reactions of some tertiary phosphines bearing functional groups with ruthenium and osmium cluster carbonyls. With $Ru_3(CO)_{12}$, the presumed first-formed complexes of type $Ru_3(CO)_{11}\{PPh_2(C_6H_4XH\text{-}2)\}$ are readily converted to the hydrido clusters $Ru_3(\mu\text{-H})\{\mu\text{-PPh}_2(C_6H_4X\text{-}2)\}(CO)_9$ either thermally or by the isolation procedure. In contrast, but not unexpectedly [2c], the corresponding complexes derived from $Os_3(CO)_{12}$ are kinetically stable, and examples with X = NH_2, NHCOPh, CHO and $CH{=}NNHC_6H_3(NO_2)_2\text{-}2,4$ have been isolated and fully characterised. On heating, the ruthenium complexes undergo hydride migration from the ligand to the cluster with concomitant formation of a bridging phosphine ligand. The behaviour of derivatives of the substituted cluster $Ru_3(\mu\text{-dppm})(CO)_{10}$ is similar, but the rearrangements take place more readily. Thus, in refluxing cyclohexane, the phosphino-aldehyde complex **15** rearranges to **16** in 45 min (66%); in toluene after 10 min, further transformation by cluster decarbonylation and formation of a μ_3-acyl ligand occurs to give **17**. In contrast, the Os_3 complex **18** required heating in refluxing xylene for 7 h to give **19** in 84% yield; no evidence was obtained for the formation of a μ_3-acyl complex analogous to **17**.

TABLE 6. Some bond parameters for $Os_3(\mu\text{-H})\{\mu\text{-PPh}_2(C_6H_4CO\text{-}2)\}(CO)_9$ (**19**)

Bond lengths (Å)			
Os(1)–Os(2)	2.918(1)	Os(2)–CO(23)	1.95(2)
Os(1)–Os(3)	2.857(1)	Os(2)–CO(24)	1.90(2)
Os(2)–Os(3)	2.833(2)	Os(3)–CO(31,32)	1.83, 1.94(2)
Os(1)–P(1)	2.319(5)	Os(3)–CO(33,34)	1.87, 1.77(4)
Os(2)–O(1121)	2.13(1)	P(1)–C(111)	1.81(1)
Os(1)–C(1121)	2.05(2)	P(1)–C(121,131)	1.83, 1.81(2)
Os(1)–CO(12)	1.98(2)	C(112)–C(1121)	1.46(3)
Os(1)–CO(13)	1.82(2)	C(1121)–O(1121)	1.29(2)
Os(2)–CO(22)	1.87(2)		
Bond angles (°)			
Os(2)–Os(1)–P(1)	111.1(1)	Os(1)–C(1121)–O(1121)	120(1)
Os(3)–Os(1)–P(1)	165.6(1)	Os(2)–O(1121)–C(1121)	106(1)
Os(1)–P(1)–C(111)	102.6(6)	Os(1)–Os(2)–C(22)	112.6(8)
Os(1)–C(1121)–C(112)	121(1)	Os(2)–Os(1)–C(12)	111.6(7)

The course of these reactions is of interest. In one case, the first-formed product (**14a**) of the reaction between $Ru_3(CO)_{12}$ and $PPh_2(C_6H_4CHO\text{-}2)$ appears to contain a terminal hydride ligand ($\delta = -6.0$), but changes readily on attempted purification to an isomeric complex (**14b**) containing a μ-H ligand ($\delta = -13.3$). This observation suggests that initial oxidative addition of the functional group to a single Ru centre occurs to give an intermediate of type (C), which readily transforms to the more commonly observed product (B) (Scheme 1). It is noteworthy that the possibility of forming μ- and μ_3-acyl groups apparently prevents the decarbonylation reactions of the type often found with mononuclear rhodium complexes and aldehydes or acid chlorides, for example [19].

The ^1H NMR spectrum of **6** contains two NH resonances at $\delta = 4.95$ and $\delta = 5.34$, whereas in **4** only one resonance is present. By analogy with the *exo* and *endo* isomers of the amido cluster $Os_3(\mu\text{-}NHPh)(\mu\text{-}Cl)(CO)_{10}$, which have been separated and individually characterised by single-crystal X-ray structure determinations [13], we might assign these two resonances similarly to *exo* and *endo* isomers of **6**. We note, however, that in the case of **4**, which has the *exo* configuration, the NH resonance is found considerably down-field (at $\delta = 6.08$) from both these systems, suggesting that the NMR criterion may not be a reliable guide to the assignment of stereochemistry of these systems.

Further, we note that considerable rearrangement of the coordination sphere about Ru(2) and Ru(3) would be necessary to accommodate the *endo* geometry in **6**. The plane of the C_6H_4 group in *endo* isomer would be approximately perpendicular to the Ru_3 plane, resulting in an even larger movement of P(3) out of the Ru_3 plane. Some of the resulting steric congestion can be alleviated if the dppm ligand occupies axial coordination sites (as found in **17**). At this stage, we believe that the *endo* isomer would be considerably less stable than the structurally characterised *exo* isomer; however, an alternative explanation for the observation of the two NH resonances must await further studies.

While the reactions of the phosphine complexes proceed quite well on heating, we have also observed that oxidative decarbonylation of these complexes (with Me_3NO) offers a convenient route to the hydrido clusters under mild conditions and in high yield. Evidently the generation of a vacant coordination site facilitates the intramolecular migration of hydride. Complex **18** is relatively stable towards thermally promoted hydrogen migration, requiring heating in refluxing xylene to form **19**. However, treatment of **18** with Me_3NO at room temperature resulted in conversion to **19** in 62% yield.

The mechanisms of these reactions are similiar to those of other trinuclear complexes with phosphine ligands [2c,20]. However, the influence of both the dppm ligand and the phosphine $PPh_2(C_6H_4CHO\text{-}2)$ have to be considered. The lability of **2** towards decarbonylation promotes the initial substitution. The acidity of the aldehydic hydrogen, in addition to the size of the resulting cyclic system, enables hydrogen migration to occur at low temperatures.

The hydrido cluster $Ru_3(\mu\text{-}H)(\mu\text{-}dppm)\{\mu\text{-}PPh_2\text{-}(C_6H_4NC(Ph)O\text{-}2)\}(CO)_7$ (**9**), obtained by thermolysis of **8**, has a structure which differs from that of **6** in that the coordination of the deprotonated amide function is *via* the O and N atoms. In accord with this, the IR spectrum of **9** has the acyl $\nu(CO)$ absorption at 1742 cm^{-1} as a result of coordination and delocalisation of the NCO group. It was expected that the NH group in **8** would react faster than that in **5**; this feature overcomes the statistical advantage provided by there being two H atoms in **5**. However, the actual reactivity was reversed to the extent that hydrogen migration in **8** occurred only at much higher temperatures than in **5**. The formation of a $\mu\text{-}\eta^2(N,O)$–RNC(R')O system appears to have only the one precedent, mentioned above; related ligands formed by addition of amines to cluster-bound CO ligands are found attached *via* μ-C–O groups [8]. In the present example, this novel behaviour probably results from the relief of steric strain that would be experienced by an NC(O)Ph group bridging *via* the N atom alone as found in parent amino derivative **6**.

The formation of the μ_3-imino and -acyl clusters **13** and **17** respectively, offers a route towards further activation of these ligands. The μ_3-ligand is formed by involvement of the C=N or C=O π-systems respectively, and while many previous μ_3-imino systems have been described [21], relatively few examples of μ_3-acyls are known. Previous reports have described the complexes $Fe_3(\mu_3\text{-}O{=}CR)(CO)_9$ [22] and the heterometallic system $Os_3W\{\mu_3\text{-}O{=}CCH_2(tol)\}(CO)_{11}(\eta\text{-}C_5H_5)$, obtained from $W\{C(tol)\}(CO)_2(\eta\text{-}C_5H_5)$ and $Os_3(\mu\text{-}H)_2(CO)_{10}$ [23].

4.1. Further reactions of $PPh_2\{CH_2C(O)Ph\}$

Our initial studies of the reactions of $Ru_3(CO)_{12}$ with $PPh_2\{CH_2C(O)Ph\}$ showed the ready formation of the hydrido cluster **22**, containing a μ-phosphino-enolate ligand [5]. This orange-red complex is formed nearly quantitatively on heating $Ru_3(CO)_{11}\{PPh_2[CH_2\text{-}C(O)Ph]\}$ (**21**) in refluxing THF. Alternatively, it is formed readily in the presence of [PPN][OAc], which can successively labilise two CO ligands in $Ru_3(CO)_{12}$, allowing consecutive CO-substitution and H-migration reactions to give **22** in 48% yield. Reversion of **22** to

the precursor **21** was accomplished by its reaction with CO.

Protonation of the enolate complex gave the cationic hydrido complex **23**, formed by conversion of the enolate into the keto complex with retention of the hydrido ligand ($\delta = -15.20$). Addition of NaOH rapidly produces **22**. The corresponding disubstituted cationic complex **24** has also been obtained. In these complexes, the inequivalence of the CH_2 protons was evident in the ^1H NMR spectra, which were analysed on the basis of an ABX (H^1H^2P) spin system.

It is notable that the pyrolysis of $Ru_3(CO)_{12-n}\{PPh_2[CH_2C(O)Ph]\}_n$ ($n = 2, 3$) resulted in loss of $PPh_2\{CH_2C(O)Ph\}$ and formation of clusters containing one less tertiary phosphine ligand, namely **22** and $Ru_3(CO)_{10}\{PPh_2[CH_2C(O)Ph]\}_2$ respectively.

Reactions of **22** with 4-MeC_6H_4NCO, RC≡CR′ (R = H, R′ = ^{t}Bu; R = R′ = CO_2Me) or $CNC_6H_3Me_2$-2,6 were attempted, in order to achieve C–C bond formation with the enolato carbon [24] or insertion into the Ru–H bond. Although the ^1H NMR resonance of the hydrido ligand disappeared, no products could be isolated.

Reactions between the keto-phosphine and $Ru_3(\mu\text{-}H)(\mu_3\text{-}C_2{}^t\text{Bu})(CO)_9$ afforded only the CO-substitution products $Ru_3(\mu\text{-}H)(\mu_3\text{-}C_2{}^t\text{Bu})(CO)_{9-n}\{PPh_2[CH_2C(O)Ph]\}_n$ [$n = 1$ (**25**) and 2 (**26**)]; no further H migration was observed. Deprotonation of **25** with NaOH in ethanol, followed by reaction with $AuCl(PPh_3)$ gave $AuRu_3(\mu_3\text{-}C_2{}^t\text{Bu})(CO)_8\{PPh_2[CH_2C(O)Ph]\}(PPh_3)$ (**27**). Interestingly, this contrasts with the conversion of **23** to **22**, mentioned above. However, in the absence of further experiments, we cannot state whether the site of deprotonation is the cluster or the ligand, because the kinetic product may not correspond to the thermodynamic product [25].

5. Conclusions

This study has provided several further examples of cluster-induced dehydrogenation of functional groups attached to tertiary phosphine ligands. The reactions proceed by initial coordination of the tertiary phosphine followed by hydrogen atom migration, possibly by initial oxidative addition to one metal centre. The resulting hydrido complexes contain bridging ligands, which may be induced in two cases, at least, to interact further with the cluster with concomitant decarbonylation and formation of μ_3-ligands. The reactions differ considerably from those involving related tertiary phosphines containing as the functional group an alkene or alkyne, for which the predominant reactions involve P–C bond cleavage. The latter reactions are a useful source of phosphido-bridged clusters containing hydrocarbon ligands. In the reaction of $PPh_2(CH{=}CH_2)$ with $Ru_3(CO)_{12}$, however, oxidative addition of the vinyl group to the Ru_3 cluster occurs to give $Ru_3(\mu\text{-}H)(\mu_3\text{-}\sigma,\eta^2,P\text{-}CH{=}CHPPh_2)(CO)_8\{PPh_2(CH{=}CH_2)\}$ [26], which has some analogy with the syntheses of **13** and **17**.

Clearly, the extended coordination of these functional groups by multi-site attachment to metal clusters is likely to lead to increased reactivity ("activation"), which may be achieved without P–C bond cleavage.

6. Experimental details

Reactions were performed under dinitrogen. Solvents were distilled prior to use using standard drying agents. Preparative thin layer chromatography (TLC) was carried out on 20 × 20 cm glass plates coated with silica gel containing gypsum binder (13%) (Merck 60 GF_{254}, 0.5 mm thick). The standard solvent combination for TLC was 3 : 1 light petroleum (b.p. 60–80°C)/acetone. Elemental analyses were carried out by the Canadian Microanalytical Service, Delta, B.C., Canada V4G 1G7, or the Service Central de Microanalyses du CNRS.

6.1. Reagents

$PPh_2(C_6H_4NH_2$-2) [27], $PPh_2(C_6H_4N{=}CHPh$-2) and $PPh_2(C_6H_4CHO$-2) [28], $PPh_2\{C_6H_4NHC(O)Ph$-2$\}$ [29] (in the preparation of the later aqueous HCl was used instead of water to remove excess pyridine), $PPh_2\{CH_2C(O)Ph\}$ [30], $Ru_3(CO)_{12}$ [31] and $Ru_3(\mu\text{-dppm})(CO)_{10}$ [32] were prepared as described in the literature. $Me_3NO \cdot 2H_2O$ (Aldrich) was dehydrated by sublimation (100°C/0.1 torr). 2,4-Dinitrophenylhydrazine was a commercial product.

6.2. Instrumentation

Adelaide: IR: Perkin-Elmer 1700X FTIR; 683 double beam, NaCl optics. NMR: Bruker CXP 300 or ACP 300 (^1H NMR at 300.13 MHz, ^{13}C NMR at 75.47 MHz, ^{31}P NMR at 121.49 MHz). FAB mass spectra: VG ZAB 2HF (FAB MS, using 3-nitrobenzyl alcohol as matrix, exciting gas Ar, FAB gun voltage 7.5 kV, current 1 mA, accelerating potential 7 kV). Strasbourg: IR: Perkin-Elmer 398 or Bruker IFS. NMR: Bruker WP 200 SY (^1H NMR at 200.13 MHz, ^{31}P NMR at 81.02 MHz).

6.3. Preparation of $PPh_2\{C_6H_4$-2-$CH{=}NNHC_6H_3$-2,4-$(NO_2)_2\}$

$PPh_2(C_6H_4CHO$-2) (58 mg, 0.2 mmol) and 2,4-dinitrophenylhydrazine (40 mg, 0.2 mmol) were dissolved in ethanol (50 ml) and heated to reflux for 90 min. An orange precipitate (54 mg, 55%), m.p. 212°C, was

formed. Anal. Found: C, 63.08; H, 4.17; N, 11.64; *M*, 470. $C_{25}H_{19}N_4O_4P$ calc.: C, 63.83; H, 4.07; N, 11.91%; *M*, 470. ^1H NMR ($CDCl_3$): δ 8.03–6.99 (m, 14H, Ph); 8.22 (dd, 1H, $J(PH) = 9.6$, 2.0 Hz, C_6H_3); 8.75 (d, 1H, $J(PH) = 4.5$ Hz); 9.12 (d, 1H, $J(PH) = 2.2$ Hz); 11.28 (s, 1H, CH=N). EI mass spectrum: 424 $[M-NO_2]^+$; 378 $[M-2NO_2]^+$; 303 $[M-C_6H_3(NO_2)_2]^+$; 288 $[M-NHC_6H_3(NO_2)_2]^+$; 182 $[NHC_6H_3(NO_2)_2]^+$; 167 $[C_6H_3(NO_2)_2]^+$; no M^+ found.

6.4. General method for $Ru_3(CO)_9(\mu$-dppm)(L)

$Ru_3(\mu$-dppm)$(CO)_{10}$ (97 mg, 0.1 mmol) and the ligand (0.1 mmol) were stirred in CH_2Cl_2 (25 ml) overnight (*ca.* 12–16 h) at room temperature. The solvent was evaporated to dryness and the complex purified by preparative TLC.

6.5. General method for $Os_3(CO)_{11}(L)$

$Os_3(CO)_{11}$(NCMe) was made by suspending $Os_3(CO)_{12}$ (200 mg, 0.22 mmol) in a mixture of CH_2Cl_2 (50 ml) and acetonitrile (5 ml) and stirring at room temperature. Me_3NO (2×8.3 mg in 5 ml CH_2Cl_2) was added to the slurry. All the $Os_3(CO)_{12}$ dissolved after addition of the first half of the Me_3NO. After completion of the reaction (monitored by TLC) the solution was filtered through silica to remove excess Me_3NO, the solvent was partially removed, 15 ml MeOH was added, and the remaining CH_2Cl_2 was removed. Filtration afforded $Os_3(CO)_{11}$(NCMe) (168 mg, 83%) as a yellow powder.

$Os_3(CO)_{11}$(NCMe) (2 mg, 0.1 mmol) was stirred in CH_2Cl_2 (25 ml) together with the ligand (0.1 mmol) for 2–3 h at room temperature. The solvent was evaporated to dryness and the product was purified by preparative TLC.

6.6. Reactions of 2-diphenylphosphino-aniline

6.6.1. With $Ru_3(CO)_{12}$

$Ru_3(CO)_{12}$ (100 mg, 0.156 mmol) and 2-diphenylphosphino-aniline (44 mg, 0.159 mmol) were dissolved in tetrahydrofuran (20 ml) and sodium benzophenone ketyl (THF solution) added dropwise until a colour change was observed (4–5 drops). The solution was heated to 65–70° for 30 min. The solvent was removed and the residue purified by preparative TLC (light petroleum : acetone 4 : 1) to produce one major band. The orange band ($R_f = 0.4$) was recrystallised (CH_2Cl_2/MeOH) to yield red crystals of $Ru_3(\mu$-H)$\{\mu$-$Ph_2P(C_6H_4NH$-2)$\}(CO)_9$ (**4**) (82 mg, 63%), m.p. 187–189°C (dec.). Anal. Found: C, 38.69; H, 1.93; N, 1.70%; *M*, 834. $C_{27}H_{16}NO_9PRu_3$ calc.: C, 38.95; H, 1.94; N, 1.52%; *M*, 834. IR (cyclohexane): ν(CO) 2082m, 2045vs, 2015s, 2010s, 1999m, 1992m, 1982w, 1974m cm^{-1}. ^1H NMR ($CDCl_3$): δ −13.54 (d, 1H, $J(PH) = 8.7$ Hz, Ru–H); 6.08 (s, 1H, NH); 7.06–7.72 (m, 14H, Ph). ^{13}C NMR ($CDCl_3$): δ 121.43 [d, $J(CP) = 44.2$ Hz, C(1)]; 123.85 [d, $J(CP) = 10.9$ Hz, C(5)]; 124.32 [d, $J(CP) = 5.7$ Hz, C(3)]; 9, 128.78–129.08 (m, C(3′, 5′)]; 130.25 [d, $J(CP) = 2.3$ Hz, C(4′)]; 130.96 [d, $J(CP) = 2.3$ Hz, C(4)]; 131.18 [d, $J(CP) = 11.3$ Hz, C(12)]; 132.35 [d, $J(CP) = 2.1$ Hz, C(4′)]; 132.38 [d, $J(CP) = 59.3$ Hz, C(1′)]; 132.93–133.10 [m, C(2′, 6′)]; 135.11 [d, $J(CP) = 50.1$ Hz, C(1′)]; 171.65 [d, $J(CP) = 28.1$ Hz, C(2)]; 183.41 (s); 194.40 [d, $J(CP) = 9.7$ Hz]; 196.50 (s); 196.77 [d, $J(CP) = 5.1$ Hz]; 200.59 (s); 205.99 [d, $J(CP) = 6.5$ Hz]; 206.75 (s); 213.03 (s, Ru–CO). FAB MS (*m/z*): 834 M^+; 806–582 $[M-nCO]^+$ ($n = 1$–9).

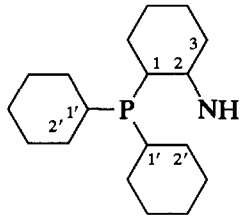

6.6.2. With $Ru_3(\mu$-dppm)$(CO)_{10}$

From $PPh_2(C_6H_4NH_2$-2) (28 mg). The orange band ($R_f = 0.35$) afforded $Ru_3(\mu$-dppm)$(CO)_9\{PPh_2(C_6H_4$-NH_2-2)$\}$ (**5**) (111 mg, 91%) from a reaction carried out at 15°C. At higher temperatures the yield of **5** decreased, red $Ru_3(\mu$-H)$(\mu$-dppm)$\{\mu$-$PPh_2(C_6H_4NH$-2)$\}(CO)_7$ (**6**) ($R_f = 0.44$) also being obtained. At 30°C the yield of **5** was 35% whereas that of **6** was 37%. Recrystallisation of **5** (CH_2Cl_2/MeOH) afforded a bright orange powder. Anal. Found: C, 50.63; H, 3.32; N, 1.21%; *M*, 1218. $C_{52}H_{38}NO_9P_3Ru_3$ calc.: C, 51.25; H, 3.31; N, 1.15%; *M*, 1218. IR (cyclohexane): ν(CO) 2058w, 2032w, 1997vs, 1984vs, 1964(sh), 1943m cm^{-1}. ^1H NMR ($CDCl_3$): δ 3.77 (br s, 2H, NH_2); 4.17 (m, 2H, CH_2); 7.56–6.57 (m, 34H, Ph). ^{13}C NMR ($CDCl_3$): δ 212.21 (s, Ru–CO); 147.66 (d, Ph *ipso* to NH); 136.87–128.26 (m, Ph); 118.05–116.17 (m, Ph); 54.42 (t, CH_2). FAB MS: 1218 M^+; 1190–966 $[M-nCO]^+$ ($n = 1$–9); 874 $[M-9CO-C_6H_4NH_2]^+$.

6.6.3. Formation of 6

$Ru_3(\mu$-dppm)$(CO)_{10}$ (97 mg, 0.1 mmol) and $PPh_2(C_6H_4NH_2$-2) (28 mg, 0.1 mmol) were heated in refluxing THF (25 ml) for 45 min. Purification by TLC gave a red band ($R_f = 0.44$) containing $Ru_3(\mu$-H)$\{\mu$-$PPh_2(C_6H_4NH$-2)$\}(\mu$-dppm)$(CO)_7$ (**6**) (67 mg, 56%). Recrystallisation (CH_2CH_2/MeOH) afforded dark red crystals. Anal. Found: C, 50.03; H, 3.39; N, 1.19%; *M*, 1162. $C_{51}H_{38}NO_8P_3Ru_3.0.5CH_2Cl_2$ calc.: C, 50.23; H, 3.19; N, 1.14%; *M*, 1162. IR (cyclohexane): ν(CO) 2032vs, 1997vs, 1984m, 1963vs, 1953w, 1939m, 1930w,

1903w cm^{-1}. ^1H NMR ($CDCl_3$): δ −13.27 (d of d, 1H, $J(PH)$ = 10.8, 56.4 Hz, Ru–H); 4.43 (m, 2H, CH_2); 4.95 and 5.34 (approx. ratio 2:3, s, 1H, NH); 7.66–6.67 (m, 34H, PhH). ^{13}C NMR ($CDCl_3$): δ 58.84 [t, $J(PC)$ = 24.2 Hz, CH_2]; 120.52–137.85 (m, Ph); 173.28 [d, $J(PC)$ = 28.7 Hz, Ph *ipso* to NH]; 189.18, 199.05, 204.29, 207.87, 208.09, 208.31, 213.80, 223.36 (8 s, Ru–CO). FAB MS (m/z): 1162 M^+; 1134–966 $[M-nCO]^+$ (n = 1–7); 890 $[M-7CO-C_6H_4]^+$; 812 $[M-7CO-2Ph]^+$.

6.6.4. With $Os_3(CO)_{12}$

From $PPh_2(C_6H_4NH_2$-2) (28 mg). The yellow-orange band (R_f = 0.58) afforded $Os_3(CO)_{11}\{PPh_2(C_6H_4NH_2$-2)} (99 mg, 89%) (**7**) as light orange crystals (CH_2Cl_2/MeOH). Anal. Found: C, 30.16; H, 1.40; N, 1.24%; M, 1157. $C_{29}H_{16}NO_{11}Os_3P$ calc.: C, 30.13; H, 1.40; N, 1.21%; M, 1157. IR (CH_2Cl_2): ν(CO) 2108s, 2055vs, 2034vs, 2018vs, 1999s, 1987s, 1977s, 1953m cm^{-1}. ^1H NMR ($CDCl_3$): δ 3.77 (s, 2H, NH_2), 7.54–6.67 (m, 14H, Ph). ^{13}C NMR ($CDCl_3$): δ 137.43–117.18 (m, Ph); 147.33 (s, Ph *ipso* to NH_2); 183.46 (s, Os–CO). ^{31}P NMR ($CDCl_3$): δ −9.39 (s). FAB MS (m/z): 1157 M^+; 1129–849 $[M-nCO]^+$ (n = 1–11); 772 $[M-11CO-Ph]^+$.

An unidentified minor product (yellow, R_f = 0.37; 1.4 mg) was also isolated.

6.7. Reactions of $PPh_2\{C_6H_4NHC(O)Ph$-2)}

6.7.1. With $Ru_3(\mu$-dppm)$(CO)_{10}$

From $PPh_2\{C_6H_4NHC(O)Ph$-2} (38 mg). The orange-red band (R_f = 0.28) afforded $Ru_3(\mu$-dppm)$(CO)_9\{PPh_2[C_6H_4NHC(O)Ph$-2]} (**8**) (78 mg, 59%). Recrystallization (CH_2Cl_2/MeOH) afforded dark red crystals. Anal. Found: C, 52.76; H, 3.15; N, 1.12%; M, 1322. $C_{59}H_{42}NO_{10}P_3Ru_3$ calc.: C, 53.64; H, 3.20; N, 1.06%; M, 1322. IR (cyclohexane): ν(CO) 2056w, 2018w, 2000vs, 1991vs, 1982vs, 1968(sh), 1950m, 1943m cm^{-1}. ^1H NMR ($CDCl_3$): δ 4.10 (t, 2H, $J(PH)$ = 10.3 Hz, CH_2); 6.89–7.56 (m, 34H, Ph); 8.02–8.01 (m, 1H, H *ortho* to NHR). ^{13}C NMR ($CDCl_3$): δ 54.12 [t, $J(PC)$ = 24.2 Hz, CH_2]; 138.18–124.96 (m, Ph); 165.22 (s, NCOPh); 211.49 (s, Ru–CO). FAB MS (m/z): 1322 M^+; 1294–1070 $[M-nCO]^+$ (n = 1–9); 993 $[M-9CO-Ph]^+$.

6.7.2. Pyrolysis of 8

Complex **8** (100 mg, 0.076 mmol) was heated in refluxing cyclohexane for 1 h. The dark red product (R_f = 0.38) was crystallised (CH_2Cl_2/MeOH) and characterised as $Ru_3(\mu$-H)$\{\mu$-$PPh_2[C_6H_4NC(O)Ph$-2]}$(\mu$-dppm)$(CO)_7$ (**9**) (65 mg, 66%). IR (cyclohexane): ν(CO) 2035s, 1992s, 1986m, 1968vs, 1948m, 1922w, 1742w (sh), 1721m cm^{-1}. ^1H NMR ($CDCl_3$): δ −11.30 (m, 1H, Ru–H); 4.45 (m, H, CH_2); 5.06 (m, H, CH_2); 7.58–6.12 (m, 38H, Ph); 8.07 (m, 1H, H *ortho* to N). FAB MS (m/z): 1266 M^+; 1238–1070 $[M-nCO]^+$ (n = 1–7); 993 $[M-7CO-Ph]^+$.

6.7.3. With $Os_3(CO)_{12}$

From $PPh_2\{C_6H_4NHC(O)Ph$-2} (38 mg). The yellow band (R_f = 0.39) afforded $Os_3(CO)_{11}\{PPh_2[C_6H_4NHC(O)Ph$-2]} (**10**) (83 mg, 67%). Recrystallization (CH_2Cl_2/MeOH) afforded yellow needles. Anal. Found: C, 34.45; H, 1.60; N, 1.14%; M, 1261. $C_{36}H_{20}NO_{12}Os_3P$ calc.: C, 34.31; H, 1.60; N, 1.11%; M, 1261. IR (cyclohexane): ν(CO) 2109m, 2068w, 2058s, 2035w, 2021vs, 2003w, 1992m, 1981m, 1966w, 1958w cm^{-1}. FAB MS (m/z): 1261 M^+; 1233–953, $[M-nCO]^+$ (n = 1–11); 848 $[M-12CO-Ph]^+$.

Minor products were present in two yellow bands (R_f = 0.41 and R_f = 0.21) and an orange band (R_f = 0.11).

6.8. Reactions of $PPh_2(C_6H_4N$=CHPh-2)

6.8.1. With $Ru_3(CO)_{12}$

$Ru_3(CO)_{12}$ (56 mg, 0.088 mmol) and the phosphine (34 mg, 0.092 mmol) were dissolved in THF (10 ml) and sodium benzophenone ketyl (THF solution) was added dropwise until a colour change was observed (5–6 drops). The solution was heated to 70–80°C for 15 min. The solvent was removed and the residue purified by preparative TLC (light petroleum:acetone 4:1) to produce one major orange band (R_f = 0.5) which was recrystallised (1,2-dichloroethane/EtOH) to yield red crystals of $Ru_3(\mu$-H)$\{\mu$-$PPh_2(C_6H_4N$=CPh-2)}$(CO)_9$ (**11**) (73 mg, 90%), m.p. 160–162°C (dec.). Found: C, 44.08; H, 2.19; N, 1.52%; M^+, 922. $C_{34}H_{20}NO_9PRu_3$ requires C, 44.35; H, 2.19; N, 1.52%; M, 922. IR: ν(CO) (cyclohexane) 2081s, 2044vs, 2015vs, 2008(sh), 1988m, 1986s, 1978m, 1967vw, 1958w cm^{-1}. ^1H NMR ($CDCl_3$): δ −13.95 [d, 1H, $J(PH)$ = 4.8 Hz, Ru–H]; 6.35–7.76 (m, 19H, Ph). ^{13}C NMR ($CDCl_3$): δ 121.22 [d, $J(CP)$ = 6.1 Hz]; 121.57 (s, br); 125.84 [d, $J(CP)$ = 6.0 Hz]; 126.84 (s); 128.21 (s); 128.78 [d, $J(CP)$ = 10.4 Hz]; 129.11 [d, $J(CP)$ = 10.6 Hz]; 130.26 (s, Ph); 130.96 [d, $J(CP)$ = 51.3 Hz, C(1) or (1′)]; 131.02 (s); 131.14 [d, $J(CP)$ = 1.9 Hz] (Ph); 131.83 [d, $J(CP)$ = 46.8 Hz, C(1) or C(1′)]; 132.33 [d, $J(CP)$ = 12.0 Hz, Ph]; 132.86 [d, $J(CP)$ = 37.8 Hz, C(1) or C(1′)]; 133.76 [d, $J(CP)$ = 12.9 Hz, Ph]; 148.36 [s, C(1″)]; 158.79 [d, $J(CP)$ = 23.3 Hz, C(2)]; 189.43 (s); 192.14 [d, $J(CP)$ = 8.2 Hz]; 193.87 (s); 197.98 [d, $J(CP)$ = 5.6 Hz]; 202.29 (s); 207.48 [d, $J(CP)$ = 7.1 Hz]; 210.75 (s); 212.22 (s), (Ru–CO); 221.60 [d, $J(CP)$ = 2.5 Hz, C=N]. FAB MS (m/z): 922 M^+; 894–670 $[M-nCO]^+$ (n = 1–9); 592 $[M-9CO-C_6H_6]^+$; 566 $[Ru_3(C_6H_4PPh_2)]^+$; 490 $[Ru_3(PPh_2)]^+$.

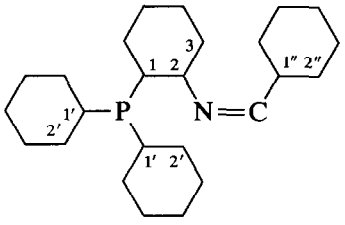

6.8.2. With $Ru_3(\mu\text{-dppm})(CO)_{10}$

From $PPh_2(C_6H_4N{=}CHPh\text{-}2)$ (37 mg). The orange band ($R_f = 0.32$) afforded $Ru_3(\mu\text{-dppm})(CO)_9\{PPh_2(C_6H_4N{=}CHPh\text{-}2)\}$ (**12**) (79 mg, 60%) as orange-red rectangular crystals (from CH_2Cl_2/hexane). Anal. Found: C, 54.12; H, 3.45; N, 1.13%; *M*, 1306. $C_{59}H_{42}NO_9P_3Ru_3$ calc.: C, 54.30; H, 3.24; N, 1.07%; *M*, 1306. IR (cyclohexane): ν(CO) 2055m, 2035w, 2020m, 1997vs, 1992(sh), 1980vs, 1963m, 1943m cm^{-1}. ^1H NMR ($CDCl_3$): δ 4.16 [t, 2H, J(PH) = 10.2 Hz, CH_2)]; 6.99–7.46 (m, 36H, Ph); 7.62–7.69 (m, 3H, H *ortho* to N=C); 8.10 (s, 1H, CH). ^{13}C NMR ($CDCl_3$): δ 54.22 (t, CH_2); 118.54–137.04 (m, Ph); 152.65 [d, J(PC) = 2.8 Hz, C *ipso* to N]; 159.13 (s, CH); 212.35 (s, Ru–CO). FAB MS (*m/z*): 1306 M^+; 1278–1054 [M–*n*CO]$^+$ (n = 1–9); 977 [M–9CO–Ph]$^+$.

6.8.3. Pyrolysis of 12

Complex **12** (123 mg, 0.094 mmol) was heated in refluxing cyclohexane (20 ml, 1 h). An orange band ($R_f = 0.21$) separated by TLC afforded $Ru_3(\mu\text{-H})\{\mu_3\text{-}PPh_2(C_6H_4N{=}CPh\text{-}2)\}(\mu\text{-dppm})(CO)_6$ (**13**) (35 mg, 29%) as an orange powder. IR (cyclohexane): ν(CO) 2016w, 2003s, 1992w, 1959vs, 1934w, 1898w cm^{-1}. Anal. Found: C, 53.12; H, 3.52; N, 1.20%; *M* (unsolvated), 1221. $C_{56}H_{41}NO_6P_3Ru_3 \cdot 0.5CH_2Cl_2$ calc.: C, 53.25; H, 3.28; N, 1.06%; *M*, 1262. ^1H NMR ($CDCl_3$): δ 4.03 (m, 2H, CH_2); 6.57–7.47 (m, 39H, Ph). FAB MS (*m/z*): 1221 M^+; 1193–1053 [M–*n*CO]$^+$ (n = 1–6); 976 [M–6CO–Ph]$^+$; 899 [M–6CO–2Ph]$^+$.

6.9. Reactions of $PPh_2(C_6H_4CHO\text{-}2)$

6.9.1. With $Ru_3(CO)_{12}$

$Ru_3(CO)_{12}$ (128 mg, 0.2 mmol) was dissolved in a mixture of CH_2Cl_2 (100 ml) and MeCN (10 ml). A solution of Me_3NO (16.5 mg, 0.22 mmol) in CH_2Cl_2 (40 ml) was added dropwise to the stirred solution at room temperature. Stirring was continued for 2 h after addition of Me_3NO was complete and the solution filtered through silica to remove excess Me_3NO. The solvent was evaporated to dryness and the residue dissolved in CH_2Cl_2 (40 ml). The phosphino-aldehyde (58 mg, 0.2 mmol) in CH_2Cl_2 (10 ml) was added and the solution stirred for 30 min. The orange band (R_f = 0.50) afforded a mixture of isomers of $Ru_3(\mu\text{-H})\{\mu\text{-}PPh_2(C_6H_4CO\text{-}2)\}(CO)_9$ (**14**) (68 mg, 39%). Repeated purification by TLC afforded pure **14b**. IR (cyclohexane): ν(CO) 2088s, 2052vs, 2018vs, 2002s, 1982m, 1960w cm^{-1}. ^1H NMR (C_6D_6): δ −13.30 [d, 1H, J(PH) = 5.5 Hz, Ru–H in **14b**]; −6.00 [d, 1H, J(PH) = 17.3 Hz, Ru–H in **14a**], 6.7–8.0 (m, 14H, Ph). ^{13}C NMR ($CDCl_3$): δ 119.6–140.71 (m, Ph); 192.03 [d, J(CP) = 6.7 Hz]; 194.65 (s); 199.26 [d, J(CP) = 3.7 Hz]; 201.99 (s); 208.45 [d, J(CP) = 3.7 Hz]; 209.29 (s); 210.55 [d, J(CP) = 2.3 Hz] (Ru–CO); 249 (s, acyl CO). ^{31}P NMR ($CDCl_3$): δ 66.40 (**14a**); 62.92 (**14b**). FAB MS (*m/z*): 819–567 [M–*n*CO]$^+$ (n = 1–10).

6.9.2. With $Ru_3(\mu\text{-dppm})(CO)_{10}$

From $PPh_2(C_6H_4CHO\text{-}2)$ (29 mg). Dark red $Ru_3(\mu\text{-dppm})(CO)_9\{PPh_2(C_6H_4CHO\text{-}2)\}$ (**15**) (53 mg, 43%) (from CH_2Cl_2/MeOH) and red $Ru_3(\mu\text{-H})(\mu\text{-dppm})\{\mu\text{-}PPh_2(C_6H_4CO\text{-}2)\}(CO)_7$ (**16**) (23 mg, 19%) were obtained from bands at $R_f = 0.28$ and $R_f = 0.41$ respectively. For **15**: Anal. Found: C, 51.10; H, 3.28%; *M*, 1231. $C_{53}H_{37}O_{10}P_3Ru_3$ calc.: C, 51.75; H, 3.03%; *M*, 1231. IR (cyclohexane): ν(CO) 2057w, 2021w, 2001vs, 1982vs, 1951m cm^{-1}. ^1H NMR ($CDCl_3$): δ 4.11 (m, 1H, CH_2); 4.20 (m, 1H, CH_2); 7.03–7.57 (m, 33H, Ph); 7.98 (m, 1H, H *ortho* to CHO); 10.02 (s, 1H, CHO). ^{13}C NMR ($CDCl_3$): δ 54.35 [t, J(PC) = 21.1 Hz, CH_2]; 128.63–138.87 (m, Ph); 189.85 (s, CHO); 211.63 (s, Ru–CO). FAB MS (*m/z*): 1231 M^+; 1203–951 [M–*n*CO]$^+$ (n = 1–10); 874 [M–10CO–Ph]$^+$.

6.9.3. Conversion of 15 to 16

Complex **15** (178 mg, 0.145 mmol) was heated for 45 min in refluxing cyclohexane (25 ml). Purification by TLC gave a red band ($R_f = 0.41$) containing $Ru_3(\mu\text{-H})\{\mu\text{-}PPh_2(C_6H_4CO\text{-}2)\}(\mu\text{-dppm})(CO)_7$ (**16**) (118 mg, 66%). When the reaction was carried out in refluxing THF (25 ml) for 1 h the yield of **16** was 45%. The ^1H NMR of a $CDCl_3$ solution indicated the presence of two isomers in 1:1 ratio, but in C_6D_6 only one isomer was observed. IR (cyclohexane): ν(CO) 2059w, 2035m, 1996s, 1974vs, 1953m, 1927w cm^{-1}. ^1H NMR ($CDCl_3$): δ −13.11 [d of d, 1H, J(PH) = 2.8 and 5.4 Hz, Ru–H, isomer B]; −12.93 [d of d, 1H, J(PH) = 2.8 and 5.3 Hz, Ru–H, isomer A]; 4.25 (m, 1H, CH_2, isomer B); 4.78 (m, 2H, CH_2, isomer A); 6.99–7.61 (m, 34H, Ph). ^{13}C NMR ($CDCl_3$): δ 55.01–54.36 (m, CH_2, both isomers); 141.54–119.20 (m, Ph); 159.93 [d, J(CP) = 17 Hz, C *ipso* to CO]; 190.12 [d, J(CP) = 2.6 Hz]; 200.33 [d, J(CP) = 1.0 Hz]; 201.04 [d, J(CP) = 3.3 Hz]; 201.25 [d, J(CP) = 3.3 Hz]; 211.11 [d, J(CP) = 1.3 Hz]; 211.98 [d, J(CP) = 6.3 Hz]; 217.0 [d, J(CP) = 1.3 Hz]; 218.21 [d, J(CP) = 2.0 Hz] (Ru–CO); 286.44 (s, Ru–COR). ^{31}P NMR (C_6D_6): δ 9.55 [d, J(PP) = 45.3 Hz, dppm]; 14.18 [d, J(PP) = 48.3 Hz, dppm)]; 61.48 [s, $PPh_2(C_6H_4CO$-

2)]. FAB MS (m/z): M^+ not observed, 1147–923 [M–nCO]$^+$ (n = 1–9); 874 [M–9CO–C_6H_4]$^+$.

6.9.4. Formation of $Ru_3(\mu\text{-}H)\{\mu_3\text{-}PPh_2(C_6H_4CO\text{-}2)\}(\mu\text{-}dppm)(CO)_6$ (17)

Complex **16** (97 mg, 0.081 mmol) was dissolved in toluene (30 ml) and heated to 100°C for 10 min. Purification by TLC gave an orange band (R_f = 0.28) which contained $Ru_3(\mu\text{-}H)\{\mu_3\text{-}PPh_2(C_6H_4CO\text{-}2)\}(\mu\text{-}dppm)(CO)_6$ (**17**) (47 mg, 50%), obtained as orange crystals from CH_2Cl_2/MeOH. IR (cyclohexane): ν(CO) 2022s, 2007m, 1996w, 1972vs, 1957m, 1919w cm^{-1}. ^{1}H NMR ($CDCl_3$): δ −14.95 (t, 1H, Ru–H); 3.68 (m, 1H, CH_2); 4.34 (m, 1H, CH_2); 6.61–7.53 (m, 34H, Ph). ^{13}C NMR ($CDCl_3$): δ 44.24 [t, J(PC) = 18.1 Hz, CH_2]; 128.10–133.39 (m, Ph); 207.18 (s); 208.98 (s), (Ru–CO). FAB MS (m/z): 1147 M^+; further fragmentation was similar to that of **16**.

6.9.5. With $Os_3(CO)_{12}$

From $PPh_2(C_6H_4CHO\text{-}2)$ (29 mg). The yellow band (R_f = 0.53) afforded $Os_3(CO)_{11}\{PPh_2(C_6H_4CHO\text{-}2)\}$ (**18**) (107 mg, 91%) as yellow crystals (CH_2Cl_2/MeOH). As the reaction is almost quantitative the product was isolated by adding MeOH followed by removal of CH_2Cl_2. Anal. Found: C, 30.79; H, 1.31%; M, 1170. $C_{30}H_{15}O_{12}Os_3P$ calc.: C, 30.85; H, 1.29%; M, 1170. IR (cyclohexane): ν(CO) 2109s, 2090w, 2057vs, 2033vs, 2019vs, 1990s, 1980s, 1954m cm^{-1}. ^{1}H NMR ($CDCl_3$): δ 7.56–7.05 (m, 13H, Ph); 8.16–8.12 (m, 1H, H *ortho* to CHO); 10.13 (s, 1H, CHO). ^{13}C NMR ($CDCl_3$): δ 128.65–136.99 (m, Ph); 171.05 (s); 174.70 (s); 182.67 (s), (Os–CO); 189.46 [d, J(PC) = 5.7 Hz, CHO]. ^{31}P NMR ($CDCl_3$): δ −3.54 (s). FAB MS (m/z): 1170 M^+; 1142–834 [M–nCO]$^+$ (n = 1–12); 757 [M–12CO–Ph]$^+$.

6.9.6. Synthesis of $Os_3(\mu\text{-}H)\{\mu\text{-}PPh_2(C_6H_4CO\text{-}2)\}(CO)_9$ (19)

6.9.6.1. By thermolysis of 18 Complex **18** (90 mg) was heated in refluxing xylene (20 ml) for 7 h. The orange band (R_f = 0.41) afforded $Os_3(\mu\text{-}H)\{\mu\text{-}PPh_2(C_6H_4CO\text{-}2)\}(CO)_9$ (**19**) (76 mg, 84%). IR (cyclohexane): ν(CO) 2093s, 2055vs, 2015vs, 1999s, 1982m, 1977m, 1960w cm^{-1}. ^{1}H NMR ($CDCl_3$): δ −13.39 [d, 1H, J(PH) = 5.7 Hz, Os–H]; 7.62–7.30 (m, 14H, Ph). ^{13}C NMR ($CDCl_3$): δ 162.42 (s); 162.80 (s); 174.99 [d, J(PC) = 2.6 Hz]; 176.12 (s); 176.97 (s); 177.62 [d, J(PC) = 6.1 Hz]; 178.71 [d, J(PC) = 6.6 Hz]; 184.77 (s); 186.93 (s); 191.65 [d, J(PC) = 5.4 Hz][Os–CO]; 271.68 [d, J(PC) = 3.1 Hz, acyl CO]. ^{31}P NMR ($CDCl_3$): δ 35.65 (s). FAB MS (m/z): 1114–834 [M–nCO]$^+$ (n = 1–10).

6.9.6.2. By reaction with Me_3NO Complex **18** (207 mg, 0.177 mmol) was stirred in a mixture of CH_2Cl_2 (40 ml) and MeCN (5 ml). Me_3NO (16 mg, 0.213 mmol) in CH_2Cl_2 (10 ml) was added and the mixture stirred for 2 h at room temperature. The solvent was evaporated after filtration through silica to remove excess Me_3NO. The residue was dissolved in CH_2Cl_2 (30 ml) and stirred for 3 h under gentle reflux. Separation of the mixture by TLC afforded **19** (129 mg, 62%) and recovered **18** (46 mg, 22%).

6.10. Preparation of $Os_3(CO)_{11}\{PPh_2[C_6H_4\{CH{=}NNHC_6H_3(NO_2)_2\text{-}2,4\}]\text{-}2\}$ (20)

From $PPh_2\{C_6H_4[CH{=}NNHC_6H_3(NO_2)_2\text{-}2,4]\text{-}2\}$ (47 mg). The yellow band (R_f = 0.49) afforded $Os_3(CO)_{11}\{PPh_2[C_6H_4\{CH{=}NNHC_6H_3(NO_2)_2\text{-}2,4\}\text{-}2]\}$ (**20**) (112 mg, 81%). Recrystallisation (CH_2Cl_2/MeOH) afforded orange crystals. IR (cyclohexane): ν(CO) 2109w, 2068vw, 2058s, 2035m, 2022vs, 2004vw, 1993w, 1981w, 1966vw, 1958vw cm^{-1}. Anal. Found: C, 32.00; H, 1.46; N, 4.23%; M, 1350. $C_{36}H_{19}N_4O_{15}Os_3P$ calc.: C, 32.05; H, 1.42; N, 4.15%; M, 1350.

Minor products were not identified and included two bands, yellow (R_f = 0.26) and orange (R_f = 0.43).

Complex **20** (19 mg, 14.1 mmol) was heated in refluxing EtOH for 1 h. The yellow band (R_f = 0.36) afforded **18** as the major product (16 mg, 84%).

6.11. Preparation of $Ru_3(\mu\text{-}H)(CO)_9\{PPh_2CH{=}C(=O)Ph\}$ (22)

6.11.1.

A solution of $Ru_3(CO)_{11}\{PPh_2[CH_2C(O)Ph]\}$ (**21**) (78 mg, 0.085 mmol) in THF (15 ml) was refluxed for 3 h. The solvent was evaporated under reduced pressure and the residue was extracted with pentane (4 × 10 ml). This orange solution was concentrated to *ca.* 3 ml and cooled (−20°C) overnight to give orange-red crystals of $Ru_3(\mu\text{-}H)\{\mu\text{-}PPh_2CH{=}C(=O)Ph\}(CO)_9$ (**22**) (68 mg, 93%). Anal. Found: C, 40.23; H, 2.09%; M, 860. $C_{29}H_{17}O_{10}PRu_3$ calc.: C, 40.50; H, 1.97%; M, 861. IR ($CHCl_3$): ν(CO) 2093m, 2053s, 2009(sh) cm^{-1}. IR (KBr): ν(C=O) + ν(C=C) 1553m cm^{-1}. ^{1}H NMR ($CDCl_3$): δ −11.77 [d, 1H, ^2J(PH) 7.43, Ru–H]; 5.38 (s, 1H, CH); 7.38–7.76 (15H, Ph). ^{31}P{^{1}H} NMR ($CDCl_3$): δ 44.45 (s).

6.11.2.

To a stirred solution of $Ru_3(CO)_{12}$ (600 mg, 0.938 mmol) and $PPh_2\{CH_2C(O)Ph\}$ (150 mg, 0.493 mmol) in THF (100 ml) was added [PPN][OAc] (39 mg, 0.065 mmol). After being stirred for 15 min, the solvent was evaporated under reduced pressure. The residue was extracted with toluene (60 ml), and this solution was

TABLE 7. Crystal data and refinement details

Compound	4	6	7	8	9
Formula	$C_{27}H_{16}NO_9PRu_3$	$C_{50}H_{38}NO_7P_3Ru_3 \cdot 0.553CH_2Cl_2$	$C_{29}H_{16}NO_{11}Os_3P$	$C_{59}H_{42}NO_{10}P_3Ru_3 \cdot 1.36CH_2Cl_2$	$C_{57}H_{42}NO_8P_3Ru_3 \cdot CH_2Cl_2$
MW	832.6	1207.7	1156.0	1436.6	1350.0
Crystal system	Monoclinic	Monoclinic	Monoclinic	Monoclinic	Monoclinic
Space group	$P2_1/n$ (No. 14)	Cc (No. 9)	$P2_1/c$ (No. 14)	$P2_1/c$ (No. 14)	$P2_1/c$ (No. 14)
a, Å	13.824(4)	59.439(11)	15.848(7)	15.373(7)	15.490(2)
b, Å	19.361(5)	10.761(4)	9.454(9)	24.343(4)	19.099(18)
c, Å	12.261(4)	23.122(14)	23.779(10)	17.743(1)	23.350(5)
α, deg.					
β, deg.	115.68(2)	100.20(4)	118.56(3)	114.86(2)	125.36(1)
γ, deg.					
U, Å^3	2957	14555	3129	6024	5634
Z	4	12	4	4	4
D_c, g cm^{-3}	1.870	1.65	2.45	1.58	1.59
$F(000)$	1616	7213.4	2112	2868.5	2696
Crystal size, mm	0.03 × 0.15 × 0.18	0.08 × 0.33 × 0.16	0.134 × 0.70 × 0.60	0.42 × 0.32 × 0.26	0.30 × 0.30 × 0.25
A^* (min, max)	1.10, 1.85 (analytical)	1.09, 1.19 (Gaussian)	14.1, 95.8 (analytical)	1.25, 1.33 (Gaussian)	1.25, 1.30 (Gaussian)
μ, cm^{-1}	15.57	11.1	135.7	9.8	10.3
$2\theta_{max}$, deg.	45	45	50	50	55
N	4231	8891	5506	9598	12888
N_0	3288	5268	4386	6718	6879
R	0.054	0.062	0.041	0.044	0.046
R_w	0.068	0.059	0.046	0.046	0.043

Abnormal features / variations in procedure. **4, 11**: Phenyl C_6 ring skeletons were modelled in the refinement as rigid bodies. Cluster hydrogen atoms were not located. **6**: Three molecules comprise the asymmetric unit of this structure which does not appear to have a higher symmetry space group; residuals quoted are for the preferred hand. Data were weak and did not support meaningful anisotropic thermal parameter refinement for all non-hydrogen atoms; accordingly, only Ru, P, Cl (solvent) were refined thus, C, N, O having the isotropic form. The core hydrogen atom was not observed in difference maps and is inferred from the chemistry; difference map artefacts were modelled as CH_2Cl_2 solvent, one moiety refining to a site occupancy of 1 and constrained at that, the other refining to a population of *ca.* 2/3. **8**: Difference map artefacts were modelled as CH_2Cl_2 solvent molecules, populations refining respectively as 0.855(4) and 0.5 (constrained at that value); for the

heated to 85°C for 3 h. The solvent was evaporated and the residue chromatographed on silica gel. Elution with toluene:pentane (1:6) gave $Ru_3(CO)_{12}$. Elution with toluene:pentane (1:3) yielded **22** which was recrystallized from pentane (385 mg, 48%).

6.12. Preparation of $[Ru_3(\mu\text{-}H)\{\mu\text{-}PPh_2CH_2C(O)Ph\}(CO)_{10}][BF_4]$ (23)

An excess of $HBF_4 \cdot OEt_2$ (0.03 ml) was added to a solution of $Ru_3(\mu\text{-}H)\{\mu\text{-}PPh_2CH{=}C({=}O)Ph\}(CO)_9$ (**22**) (29 mg, 0.033 mmol) in CH_2Cl_2 (10 ml). An immediate darkening occurred, followed by a gradual lightening to orange. After being stirred for 1 h, the solution was saturated with CO and the colour changed immediately from orange to yellow. The solvent was removed under reduced pressure, the residue washed with diethyl ether (3 × 5 ml) and extracted in CH_2Cl_2. Concentration, followed by addition of hexane, led to precipitation of a yellow powder of $[Ru_3(\mu\text{-}H)\{\mu\text{-}PPh_2[CH_2C(O)Ph]\}(CO)_{10}][BF_4]$ (**23**) (23 mg, 70%). Anal. Found: C, 36.80; H, 2.19%; *M*, 889. $C_{30}H_{18}BF_4O_{11}PRu_3$ calc.: C, 36.93; H, 1.84%; *M*, 890. IR ($CHCl_3$): ν(CO) 2070s, 2054s, 2009s. IR (KBr): ν(CO) 1558m, ν(BF) 1084s (br) cm^{-1}. ^{1}H NMR ($CDCl_3$): δ −15.20 [d, 1H, ^2J(PH) = 11.89 Hz]; δ_B 4.89 and δ_A 5.27 [2H, AB part of an ABX spin system; J(AB) = 19.1 Hz, J(AX) = 11.1 Hz, J(BX) = 11.4 Hz]; 7.26–8.29 (15H, Ph). ^{31}P{^{1}H}NMR ($CDCl_3$): δ 50.73 (s).

6.13. Reaction of $[Ru_3(\mu\text{-}H)\{\mu\text{-}PPh_2[CH_2C(O)Ph]\}(CO)_{10}][BF_4]$ (23) with NaOH

An ethanolic solution of NaOH (0.017 M; 1.73 ml) was added to a solution of **23** (0.020 g, 0.020 mmol) in CH_2Cl_2 (10 ml). The colour changed immediately from orange-yellow to orange. The IR spectrum of the solution showed only the presence of **22**.

10	11	15	18	18a	19	20
$C_{36}H_{20}NO_{12}Os_3P$	$C_{34}H_{20}NO_9PRu_3$	$C_{53}H_{38}O_{10}P_3Ru_3 \cdot 0.5CH_2Cl_2$	$C_{30}H_{15}O_{12}Os_3P$	$C_{30}H_{15}O_{12}Os_3P \cdot 0.5CH_2Cl_2$	$C_{28}H_{15}O_{10}Os_3P$	$C_{36}H_{19}N_4O_{15}Os_3P$
1260.1	920.7	1273.5	1169.0	1211.5	1113.0	1349.1
Monoclinic	Triclinic	Monoclinic	Monoclinic	Triclinic	Monoclinic	Triclinic
$P2_1/c$ (No. 14)	$P\bar{1}$ (No. 2)	$C2/c$ (No. 15)	$P2_1/c$ (No. 14)	$P\bar{1}$ (No. 2)	$P2_1/c$ (No. 14)	$P\bar{1}$ (No 2)
18.430(11)	11.198(2)	34.321(7)	14.788(6)	15.59(1)	8.214(2)	15.909(6)
11.223(6)	17.822(4)	13.593(4)	10.538(3)	11.108(8)	24.527(10)	15.511(5)
19.369(15)	9.477(1)	22.216(6)	20.827(8)	10.658(3)	16.256(5)	9.187(3)
	104.94(1)			73.14(4)		87.89(3)
113.31(6)	99.99(1)	98.72(2)	95.83(3)	71.10(5)	114.44(2)	83.57(3)
	101.38(2)			78.70(6)		62.70(3)
3679	1740	10245	3229	1660	2981	2001
4	2	8	4	2	4	2
2.28	1.757	1.65	2.40	2.42	2.48	2.24
2328	900	5072	2136	1110	2024	1252
$0.32 \times 0.75 \times 0.71$	$0.16 \times 0.19 \times 0.09$	$0.18 \times 0.65 \times 0.40$	$0.24 \times 0.48 \times 0.64$	$0.30 \times 0.12 \times 0.20$	$0.52 \times 0.18 \times 0.16$	$0.04 \times 0.03 \times 0.25$
12.9, 96.2	1.236, 1.46	1.20, 1.39	8.2, 53.5	2.92, 10.5	5.26, 10.1	1.82, 2.31
(analytical)	(analytical)	(Gaussian)	(analytical)	(analytical)	(analytical)	(analytical)
115.6	13.27	10.6	131.6	128.0	136.7	106.4
60	45	50	60	55	50	45
8866	5056	8824	9404	7599	5227	7015
5680	3959	6376	6683	5346	4047	4759
0.044	0.035	0.043	0.051	0.083	0.059	0.042
0.045	0.048	0.045	0.056	0.093	0.065	0.043

second, anisotropic thermal parameter refinement for the carbon [C(20)] was not meaningful and the isotropic form was used. **9**: Core hydrogen H(23) was located and refined; solvent population (modelled as CH_2Cl_2) was held constant at 1 after initial refinement. **15**: Difference map artefacts were modelled as solvent CH_2Cl_2 located about a two-fold axis and with population constrained at 1 (≡hemi-solvate) after initial refinement. **18a**: The crystal decomposed badly during data collection (about 30%) and data were scaled accordingly. Difference map artefacts were modelled as an occupied CH_2Cl_2 solvent after initial refinement; material was limited and crystal shape awkward, so that proper absorption correction was difficult. Only Os, P, Cl atoms were refined with anisotropic thermal parameters, C, N, O having the isotropic form. **19**: A fibrous crystal contributed to a rather inferior data set; the core hydride atom is inferred from the chemistry.

6.14. Preparation of $[Ru_3(\mu\text{-}H)\{\mu\text{-}PPh_2[CH_2C(O)Ph]\}_2(CO)_8][BF_4]$ (24)

To a stirred solution of **22** (100 mg, 0.116 mmol) in THF (50 ml) was added $PPh_2\{CH_2C(O)Ph\}$ (38 mg, 0.126 mmol) and the reaction flask was placed at −78°C. A solution of Me_3NO (8 mg, 0.117 mmol) in THF (40 ml) was added over a period of 10 min. After all the amine oxide had been added, the reaction mixture was slowly brought to ambient temperature. After evaporation of solvent to approximately 10 ml under reduced pressure, an excess of $HBF_4 \cdot OEt_2$ (0.04 ml) was added. The solvent was removed, the residue washed with diethyl ether (3 × 5 ml), and crystallized from CH_2Cl_2/hexane (−20°C) to give $[Ru_3(\mu\text{-}H)\{\mu\text{-}PPh_2[CH_2C(O)Ph]\}_2(CO)_8][BF_4]$ (**24**) as red crystals (120 mg, 84%). Anal. Found: C, 46.96; H, 3.18%; *M*, 1138. $C_{48}H_{35}BF_4O_{10}P_2Ru_3$ calc.: C, 47.10; H, 2.86%; *M*, 1138. IR (CH_2Cl_2): ν(CO) 2065s, 2029s, 2015s, 1999s (br). IR (KBr): ν(CO) 1606m, 1588m cm^{-1}. ^1H NMR ($CDCl_3$): δ −11.75 [t, 1H, $^2J(PH) = 13.83$ Hz]; δ_A 4.74 and δ_B 3.01 [4H, AB part of an ABX spin system, $J(AB) = 18.7$ Hz, $J(AX) = 11.5$ Hz, $J(BX) = 9.4$ Hz]; 6.98–8.36 (m, 30H, Ph). $^{31}P\{^1H\}$ NMR ($CDCl_3$): δ 42.19 (s).

6.15. Reaction of $Ru_3(\mu\text{-}H)\{\mu\text{-}PPh_2[CH{=}C(=O)Ph]\}(CO)_9$ with $PPh_2\{CH_2C(O)Ph\}$

To a solution of **22** (60 mg, 0.069 mmol) in THF (30 ml) was added $PPh_2\{CH_2C(O)Ph\}$ (21 mg, 0.069 mmol) and the reaction flask was placed at −78°C. A solution of Me_3NO (5 mg, 0.066 mmol) in THF (30 ml) was added over a period of 10 min. After all the amine oxide had been added, the reaction mixture was allowed to reach ambient temperature. The solvent was removed under reduced pressure. The residue was extracted with CH_2Cl_2 (20 ml) and the solution was concentrated to *ca.* 5 ml. Addition of pentane induced the precipitation of a brown powder, which was dried *in vacuo* (63 mg). ^1H NMR ($CDCl_3$): δ −9.96 [t, 1H, $J(PH) = 9.7$ Hz]; 5.40 [d, 4H, $J(PH) = 3.6$ Hz]; 6.86–7.98 (m, 30H, Ph). $^{31}P\{^1H\}$ NMR ($CDCl_3$): δ 41.46 (s), 47.80 (s).

6.16. Pyrolysis of $Ru_3(CO)_{10}\{PPh_2[CH_2C(O)Ph]\}_2$

A solution of $Ru_3(CO)_{10}\{PPh_2[CH_2C(O)Ph]\}_2$ (56 mg, 0.047 mmol) in THF (20 ml) was refluxed for 4 h. The solvent was evaporated under reduced pressure and the residue was extracted with toluene (10 ml). After evaporation of the solvent, orange solid $Ru_3(\mu\text{-}H)\{\mu\text{-}PPh_2[CH{=}C({=}O)Ph]\}(CO)_9$ was obtained (23 mg, 57%). This complex was identified by comparison of its IR and ^1H NMR spectra with those of an authentic sample.

6.17. Pyrolysis of $Ru_3(CO)_9\{PPh_2[CH_2C(O)Ph]\}_3$

A solution of $Ru_3(CO)_9\{PPh_2[CH_2C(O)Ph]\}_3$ (42 mg, 0.028 mmol) in toluene (10 ml) was heated to 60°C for

TABLE 8. Non-hydrogen positional factors ($\times 10^4$) for **4**

Atom	x	y	z
Ru(1)	2338(1)	−750(1)	−3252(1)
Ru(2)	1981(1)	−1877(1)	−4858(1)
Ru(3)	1515(1)	−1972(1)	−2833(1)
P(3)	1387(1)	−1805(1)	−1035(2)
C(11)	1488(7)	−189(5)	−4588(8)
O(11)	1008(7)	167(5)	−5386(8)
C(12)	3598(7)	−538(4)	−3459(8)
O(12)	4328(5)	−410(4)	−3616(7)
C(13)	2390(7)	−44(4)	−2076(8)
O(13)	2410(7)	383(3)	−1432(7)
C(21)	546(9)	−1488(6)	−5691(8)
O(21)	−281(6)	−1275(5)	−6244(8)
C(22)	2473(8)	−1456(6)	−5932(8)
O(22)	2784(8)	−1204(6)	−6545(8)
C(23)	3370(7)	−2216(5)	−3744(7)
O(23)	4208(6)	−2403(4)	−3106(7)
C(24)	1510(7)	−2803(6)	−5504(8)
O(24)	1243(7)	−3326(4)	−5908(8)
C(31)	87(8)	−2200(4)	−3829(8)
O(31)	−796(6)	−2307(4)	−4442(8)
C(32)	1888(7)	−2913(4)	−2511(8)
O(32)	2145(6)	−3477(3)	−2302(8)
C(311)	2596(5)	−1310(3)	−170(6)
C(312)	3329(5)	−1283(3)	−665(6)
N(312)	3038(4)	−1512(3)	−1857(5)
C(313)	4341(6)	−965(4)	10(6)
C(314)	4552(7)	−696(4)	1129(8)
C(315)	3828(7)	−700(4)	1607(7)
C(316)	2839(6)	−1016(3)	976(6)
C(321)	1452(4)	−2576(3)	−148(4)
C(322)	682(4)	−3089(3)	−687(4)
C(323)	673(4)	−3673(3)	−27(4)
C(324)	1433(4)	−3745(3)	1172(4)
C(325)	2203(4)	−3232(3)	1711(4)
C(326)	2213(4)	−2648(3)	1051(4)
C(331)	308(4)	−1311(2)	−919(4)
C(332)	−178(4)	−771(2)	−1725(4)
C(333)	−991(4)	−386(2)	−1632(4)
C(334)	−1319(4)	−540(2)	−732(4)
C(335)	−834(4)	−1080(2)	75(4)
C(336)	−21(4)	−1466(2)	−19(4)

TABLE 9. Non-hydrogen positional and isotropic displacement parameters, **6**

Atom	x	y	z	U_{eq} (Å^2)
Ru(11)	0.00000	0.6611(2)	0.00000	0.0346(9)
Ru(12)	0.00793(5)	0.7711(2)	0.1137(1)	0.038(1)
Ru(13)	0.02267(5)	0.8861(2)	0.0177(1)	0.040(1)
C(111)	0.0173(5)	0.521(3)	0.033(1)	0.05(1)
O(111)	0.0285(4)	0.436(2)	0.048(1)	0.080(8)
C(112)	−0.0035(5)	0.614(3)	−0.078(1)	0.051(9)
O(112)	−0.0023(4)	0.574(2)	−0.1241(9)	0.070(7)
C(121)	0.0337(5)	0.700(3)	0.123(1)	0.06(1)
O(121)	0.0532(3)	0.631(2)	0.1295(8)	0.056(6)
C(122)	0.0163(4)	0.872(2)	0.178(1)	0.027(7)
O(122)	0.0243(4)	0.930(2)	0.220(1)	0.089(8)
C(123)	−0.0160(8)	0.840(5)	0.095(2)	0.12(2)
O(123)	−0.0298(4)	0.943(2)	0.078(1)	0.080(8)
C(131)	0.0519(4)	0.897(2)	0.061(1)	0.025(7)
O(131)	0.0706(4)	0.903(2)	0.0842(9)	0.069(7)
C(132)	0.0164(7)	1.059(4)	0.037(2)	0.10(1)
O(132)	0.0174(5)	1.157(3)	0.051(1)	0.13(1)
P(11)	−0.0338(1)	0.5773(8)	0.0167(4)	0.041(3)
C(1111)	−0.0412(5)	0.410(3)	−0.008(1)	0.032(8)
C(1112)	−0.0609(6)	0.362(4)	0.008(2)	0.08(1)
G(1113)	−0.0663(6)	0.243(3)	−0.015(1)	0.06(1)
C(1114)	−0.0509(6)	0.173(3)	−0.034(1)	0.07(1)
C(1115)	−0.0311(6)	0.215(3)	−0.044(1)	0.07(1)
C(1116)	−0.0253(5)	0.341(3)	−0.029(1)	0.043(9)
C(1121)	−0.0579(5)	0.646(3)	−0.022(1)	0.041(8)
C(1122)	−0.0697(6)	0.755(3)	−0.003(1)	0.06(1)
C(1123)	−0.0889(6)	0.815(3)	−0.033(1)	0.07(1)
C(1124)	−0.0973(6)	0.776(3)	−0.084(1)	0.07(1)
C(1125)	−0.0875(6)	0.680(3)	−0.111(1)	0.08(1)
C(1126)	−0.0685(5)	0.624(3)	−0.079(1)	0.049(9)
C(10)	−0.0385(5)	0.576(3)	0.094(1)	0.035(8)
P(12)	−0.0130(1)	0.6155(8)	0.1471(4)	0.043(3)
C(1211)	0.0028(5)	0.466(3)	0.171(1)	0.040(8)
C(1212)	0.0218(6)	0.470(3)	0.212(1)	0.07(1)
C(1213)	0.0329(7)	0.361(4)	0.231(2)	0.10(1)
C(1214)	0.0237(7)	0.260(4)	0.205(2)	0.09(1)
C(1215)	0.0040(6)	0.246(3)	0.167(1)	0.07(1)
C(1216)	−0.0052(5)	0.352(3)	0.148(1)	0.06(1)
C(1221)	−0.0269(5)	0.645(3)	0.210(1)	0.041(8)
C(1222)	−0.0320(6)	0.756(3)	0.226(1)	0.07(1)
C(1223)	−0.0436(6)	0.777(3)	0.276(1)	0.07(1)
C(1224)	−0.0500(7)	0.689(4)	0.301(2)	0.11(2)
C(1225)	−0.0460(7)	0.570(4)	0.287(2)	0.09(1)
C(1226)	−0.0335(7)	0.542(4)	0.242(2)	0.10(1)
P(13)	0.0297(1)	0.9331(7)	−0.0741(3)	0.037(3)
C(1311)	0.0020(5)	0.894(3)	−0.124(1)	0.035(8)
C(1312)	−0.0146(4)	0.869(2)	−0.092(1)	0.032(8)
N(1312)	−0.0101(4)	0.850(2)	−0.0311(9)	0.038(6)
C(1313)	−0.0362(5)	0.862(3)	−0.121(1)	0.051(9)
C(1314)	−0.0402(6)	0.867(3)	−0.185(1)	0.08(1)
C(1315)	−0.0215(5)	0.890(3)	−0.213(1)	0.051(9)
C(1316)	−0.0005(5)	0.895(3)	−0.183(1)	0.06(1)
C(1321)	0.0363(5)	1.095(3)	−0.087(1)	0.048(9)
C(1322)	0.0548(6)	1.153(4)	−0.052(2)	0.08(1)
C(1323)	0.0560(6)	1.294(3)	−0.059(1)	0.06(1)
C(1324)	0.0389(5)	1.345(3)	−0.097(1)	0.046(9)
C(1325)	0.0217(7)	1.296(4)	−0.126(2)	0.10(1)
C(1326)	0.0186(7)	1.163(4)	−0.124(2)	0.09(1)
C(1331)	0.0520(4)	0.857(2)	−0.106(1)	0.024(7)

TABLE 9 (continued)

Atom	x	y	z	U_{eq} (Å^2)
C(1332)	0.0576(5)	0.732(3)	−0.095(1)	0.06(1)
C(1333)	0.0733(5)	0.683(3)	−0.122(1)	0.047(9)
C(1334)	0.0836(5)	0.745(3)	−0.163(1)	0.06(1)
C(1335)	0.0766(6)	0.855(3)	−0.178(1)	0.07(1)
C(1336)	0.0604(5)	0.910(3)	−0.149(1)	0.035(8)
Ru(21)	−0.34890(4)	−0.3500(2)	0.6155(1)	0.0331(9)
Ru(22)	−0.35640(5)	−0.2351(2)	0.5022(1)	0.040(1)
Ru(23)	−0.37078(5)	−0.1211(2)	0.5983(1)	0.043(1)
C(211)	−0.3658(4)	−0.488(2)	0.584(1)	0.023(7)
O(211)	−0.3774(3)	−0.567(2)	0.5665(8)	0.058(6)
C(212)	−0.3473(5)	−0.401(3)	0.690(1)	0.040(8)
O(212)	−0.3459(4)	−0.432(2)	0.7396(9)	0.069(7)
C(221)	−0.3852(4)	−0.328(2)	0.492(1)	0.022(7)
O(221)	−0.4016(3)	−0.379(2)	0.4803(9)	0.061(7)
C(222)	−0.3676(7)	−0.149(4)	0.438(2)	0.11(2)
O(222)	−0.3704(4)	−0.076(2)	0.397(1)	0.092(9)
C(223)	−0.3320(4)	−0.125(2)	0.529(1)	0.026(7)
O(223)	−0.3160(4)	−0.062(2)	0.5428(9)	0.067(7)
C(231)	−0.3974(5)	−0.122(3)	0.566(1)	0.045(9)
O(231)	−0.4178(4)	−0.109(2)	0.5318(9)	0.072(7)
C(232)	−0.3676(5)	0.042(3)	0.577(1)	0.06(1)
O(232)	−0.3626(4)	0.143(2)	0.5665(9)	0.079(8)
P(21)	−0.3154(1)	−0.4378(7)	0.5988(3)	0.034(3)
C(2111)	−0.3094(5)	−0.605(3)	0.617(1)	0.042(8)
C(2112)	−0.2882(5)	−0.656(3)	0.608(1)	0.052(9)
C(2113)	−0.2853(5)	−0.781(3)	0.620(1)	0.05(1)
C(2114)	−0.2979(6)	−0.850(3)	0.652(1)	0.07(1)
C(2115)	−0.3186(5)	−0.787(3)	0.662(1)	0.06(1)
C(2116)	−0.3218(5)	−0.673(3)	0.646(1)	0.054(9)
C(2121)	−0.2888(5)	−0.364(3)	0.640(1)	0.049(9)
C(2122)	−0.2801(6)	−0.406(3)	0.695(2)	0.08(1)
C(2123)	−0.2626(6)	−0.358(4)	0.731(2)	0.09(1)
C(2124)	−0.2518(6)	−0.261(3)	0.712(2)	0.08(1)
C(2125)	−0.2603(6)	−0.211(4)	0.655(1)	0.08(1)
C(2126)	−0.2804(6)	−0.258(3)	0.618(1)	0.07(1)
C(20)	−0.3096(5)	−0.430(3)	0.519(1)	0.046(9)
P(22)	−0.3352(1)	−0.3899(8)	0.4677(3)	0.042(3)
C(2211)	−0.3493(6)	−0.534(3)	0.449(1)	0.07(1)
C(2212)	−0.3678(6)	−0.526(4)	0.402(2)	0.09(1)
C(2213)	−0.3801(6)	−0.635(3)	0.382(2)	0.08(1)
C(2214)	−0.3752(6)	−0.752(3)	0.407(1)	0.07(1)
C(2215)	−0.3566(5)	−0.756(3)	0.449(1)	0.038(8)
C(2216)	−0.3411(5)	−0.652(3)	0.473(1)	0.051(9)
C(2221)	−0.3213(5)	−0.364(3)	0.404(1)	0.06(1)
C(2222)	−0.3154(5)	−0.242(3)	0.394(1)	0.051(9)
C(2223)	−0.3027(7)	−0.210(4)	0.350(2)	0.10(1)
C(2224)	−0.2965(7)	−0.317(4)	0.316(2)	0.09(1)
C(2225)	−0.3031(7)	−0.434(4)	0.326(2)	0.11(2)
C(2226)	−0.3135(5)	−0.450(3)	0.374(1)	0.042(9)
P(23)	−0.3776(2)	−0.0725(8)	0.6900(4)	0.048(4)
C(2311)	−0.3504(4)	−0.103(3)	0.736(1)	0.035(8)
C(2312)	−0.3319(5)	−0.145(3)	0.709(1)	0.036(8)
N(2312)	−0.3377(3)	−0.159(2)	0.6456(8)	0.026(6)
C(2313)	−0.3108(5)	−0.154(3)	0.739(1)	0.042(8)
C(2314)	−0.3069(5)	−0.148(3)	0.796(1)	0.048(9)
C(2315)	−0.3243(5)	−0.126(3)	0.828(1)	0.06(1)
C(2316)	−0.3461(5)	−0.094(3)	0.796(1)	0.041(9)
C(2321)	−0.3818(5)	0.109(3)	0.703(1)	0.037(8)
C(2322)	−0.4021(6)	0.139(3)	0.668(1)	0.07(1)

TABLE 9 (continued)

Atom	x	y	z	U_{eq} (Å^2)
C(2323)	−0.4107(7)	0.273(4)	0.660(2)	0.12(2)
C(2324)	−0.3934(6)	0.329(4)	0.696(2)	0.09(1)
C(2325)	−0.3745(6)	0.303(4)	0.737(2)	0.08(1)
C(2326)	−0.3661(6)	0.171(3)	0.741(1)	0.06(1)
C(2331)	−0.3972(5)	−0.143(3)	0.726(1)	0.047(9)
C(2332)	−0.4060(5)	−0.265(3)	0.711(1)	0.048(9)
C(2333)	−0.4233(6)	−0.321(3)	0.733(1)	0.06(1)
C(2334)	−0.4326(5)	−0.262(3)	0.775(1)	0.06(1)
C(2335)	−0.4268(6)	−0.141(3)	0.791(1)	0.06(1)
C(2336)	−0.4096(6)	−0.090(3)	0.767(1)	0.06(1)
Ru(31)	−0.18038(5)	0.7935(2)	0.0567(1)	0.039(1)
Ru(32)	−0.18790(5)	1.0012(2)	−0.0208(1)	0.0399(9)
Ru(33)	−0.15133(5)	0.9958(2)	0.0743(1)	0.041(1)
C(311)	−0.2070(5)	0.816(3)	0.067(1)	0.037(8)
O(311)	−0.2265(4)	0.838(2)	0.0844(9)	0.067(7)
C(312)	−0.1727(6)	0.665(3)	0.114(1)	0.07(1)
O(312)	−0.1701(5)	0.587(3)	0.153(1)	0.13(1)
C(321)	−0.2040(6)	1.065(3)	0.036(1)	0.07(1)
O(321)	−0.2136(4)	1.116(2)	0.071(1)	0.093(9)
C(322)	−0.1903(6)	1.152(3)	−0.067(1)	0.07(1)
O(322)	−0.1913(4)	1.229(2)	−0.101(1)	0.096(9)
C(323)	−0.1652(5)	0.940(3)	−0.052(1)	0.045(9)
O(323)	−0.1511(3)	0.903(2)	−0.0806(8)	0.054(6)
C(331)	−0.1614(6)	1.143(4)	0.103(1)	0.08(1)
O(331)	−0.1650(4)	1.241(2)	0.121(1)	0.086(8)
C(332)	−0.1307(5)	1.067(3)	0.036(1)	0.049(9)
O(332)	−0.1186(4)	1.105(2)	0.007(1)	0.084(8)
P(31)	−0.1934(2)	0.6583(7)	−0.0202(4)	0.048(4)
C(3111)	−0.2141(5)	0.542(3)	−0.011(1)	0.05(1)
C(3112)	−0.2234(6)	0.458(3)	−0.058(1)	0.08(1)
C(3113)	−0.2406(5)	0.376(3)	−0.051(1)	0.05(1)
C(3114)	−0.2479(6)	0.371(3)	0.001(1)	0.08(1)
C(3115)	−0.2397(5)	0.430(3)	0.046(1)	0.06(1)
C(3116)	−0.2227(6)	0.527(3)	0.039(1)	0.07(1)
C(3121)	−0.1706(5)	0.561(3)	−0.040(1)	0.048(9)
C(3122)	−0.1576(6)	0.587(3)	−0.082(1)	0.06(1)
C(3123)	−0.1398(6)	0.517(3)	−0.088(1)	0.08(1)
C(3124)	−0.1342(8)	0.415(4)	−0.061(2)	0.12(2)
C(3125)	−0.1468(6)	0.377(3)	−0.014(2)	0.08(1)
C(3126)	−0.1654(5)	0.453(3)	−0.004(1)	0.05(1)
C(30)	−0.2055(5)	0.733(3)	−0.090(1)	0.045(9)
P(32)	−0.2161(1)	0.8918(8)	−0.0805(4)	0.045(3)
C(3211)	−0.2437(5)	0.867(3)	−0.062(1)	0.036(8)
C(3212)	−0.2528(5)	0.973(3)	−0.037(1)	0.046(9)
C(3213)	−0.2742(6)	0.962(3)	−0.022(1)	0.07(1)
C(3214)	−0.2868(7)	0.860(4)	−0.029(2)	0.12(2)
C(3215)	−0.2781(5)	0.757(3)	−0.050(1)	0.06(1)
C(3216)	−0.2569(5)	0.757(3)	−0.068(1)	0.047(9)
C(3221)	−0.2230(6)	0.953(3)	−0.154(1)	0.06(1)
C(3222)	−0.2058(6)	0.953(3)	−0.190(1)	0.07(1)
C(3223)	−0.2101(6)	0.993(3)	−0.249(2)	0.08(1)
C(3224)	−0.2310(7)	1.052(4)	−0.267(2)	0.09(1)
C(3225)	−0.2473(7)	1.054(4)	−0.231(2)	0.10(1)
C(3226)	−0.2440(6)	1.001(3)	−0.176(1)	0.07(1)
P(33)	−0.1241(2)	0.9470(8)	0.1554(4)	0.048(4)
C(3311)	−0.1155(5)	0.794(3)	0.138(1)	0.047(9)
C(3312)	−0.1263(4)	0.750(2)	0.085(1)	0.031(8)
N(3312)	−0.1445(4)	0.815(2)	0.051(1)	0.045(7)
C(3313)	−0.1200(5)	0.632(3)	0.065(1)	0.043(9)

TABLE 9 (continued)

Atom	x	y	z	U_{eq} (Å^2)
C(3314)	−0.1023(6)	0.563(3)	0.100(1)	0.06(1)
C(3315)	−0.0925(6)	0.615(3)	0.152(1)	0.06(1)
C(3316)	−0.0981(6)	0.728(4)	0.168(2)	0.08(1)
C(3321)	−0.0999(5)	1.052(3)	0.162(1)	0.050(9)
C(3322)	−0.1020(6)	1.170(3)	0.189(2)	0.08(1)
C(3323)	−0.0852(7)	1.252(4)	0.189(2)	0.12(2)
C(3324)	−0.0667(7)	1.229(4)	0.169(2)	0.09(1)
C(3325)	−0.0639(5)	1.125(3)	0.140(1)	0.06(1)
C(3326)	−0.0804(6)	1.026(3)	0.141(1)	0.07(1)
C(3331)	−0.1287(5)	0.923(3)	0.229(1)	0.044(9)
C(3332)	−0.1490(6)	0.887(3)	0.239(1)	0.07(1)
C(3333)	−0.1534(6)	0.860(4)	0.298(2)	0.08(1)
C(3334)	−0.1361(6)	0.874(4)	0.343(2)	0.09(1)
C(3335)	−0.1149(6)	0.909(4)	0.333(2)	0.09(1)
C(3336)	−0.1116(6)	0.935(3)	0.278(1)	0.07(1)
Cl(11) [a]	−0.1507(4)	0.257(2)	0.2799(8)	0.16(1)
Cl(12) [a]	−0.1281(5)	0.480(3)	0.251(1)	0.27(2)
C(1) [a]	−0.150(1)	0.389(8)	0.253(4)	0.17(3)
Cl(21)	−0.1962(5)	0.455(6)	0.275(1)	0.66(5)
Cl(22)	−0.228(1)	0.631(3)	0.237(4)	1.09(8)
C(2)	−0.213(2)	0.54(1)	0.216(5)	0.46(7)

[a] Site occupancy factor = 0.66(1).

2 h. The IR spectrum of the solution showed only the presence of $Ru_3(CO)_{10}\{PPh_2[CH_2C(O)Ph]\}_2$.

6.18. *Reaction of $Ru_3(\mu\text{-}H)\{\mu\text{-}PPh_2[CH{=}C(=O)\text{-}Ph]\}(CO)_9$ (22) with CO*

CO was bubbled through a solution of **22** (18 mg, 0.021 mmol) in pentane (20 ml) for 2 h. After evaporation of the solvent, a yellow solid was obtained. Its ^{1}H NMR spectrum showed a mixture containing $Ru_3(CO)_{11}\{PPh_2[CH_2C(O)Ph]\}$ (**21**).

6.19. *Preparation of $Ru_3(\mu\text{-}H)(\mu_3\text{-}C_2{}^tBu)(CO)_8\{PPh_2[CH_2C(O)Ph]\}$ (25)*

$PPh_2\{CH_2C(O)Ph\}$ (47 mg, 0.157 mmol) was added to a stirred solution of $Ru_3(\mu\text{-}H)(\mu_3\text{-}C_2{}^tBu)(CO)_9$ (100 mg, 0.157 mmol) in THF (30 ml) and the reaction flask was placed at −78°C. A solution of Me_3NO (11 mg, 0.145 mmol) in THF (20 ml) was added over a period of 15 min with stirring. After all the amine oxide has been added, the reaction mixture was slowly allowed to reach ambient temperature. The solvent was evaporated under reduced pressure and the residue was extracted with pentane (80 ml). The yellow solution was concentrated to *ca.* 10 ml, and cooling (−20°C) over night gave yellow crystals of $Ru_3(\mu\text{-}H)(\mu_3\text{-}C_2{}^tBu)(CO)_8\{PPh_2[CH_2C(O)Ph]\}$ (**25**) (124 mg, 87%). Anal. Found: C, 44.94; H, 3.11%; *M*, 916. $C_{34}H_{27}O_9PRu_3$ calc.: C, 44.67; H, 2.95%; *M*, 915. IR ($CHCl_3$): ν(CO) 2096w, 2077m, 2069s, 2052s, 2014s (br). IR (KBr): ν(CO) 1668m cm^{-1}. ^{1}H NMR (C_6D_6): δ −21.09 [d, 1H, ^3J(PH) = 1.5 Hz]; 1.24 (s, 9H, ^{t}Bu); 4.01 [d, 2H, PCH_2, ^2J(PH) = 8.5]; 6.94–7.76 (15H, Ph). $^{31}P\{^1H\}$ NMR ($CDCl_3$): δ 43.0 (s).

6.20. *Preparation of $Ru_3(\mu\text{-}H)(\mu_3\text{-}C_2{}^tBu)(CO)_7\{PPh_2[CH_2C(O)Ph]\}_2$ (26)*

$PPh_2\{CH_2C(O)Ph\}$ (157 mg, 0.516 mmol) was added to a stirred solution of **25** (157 mg, 0.246 mmol) in THF (50 ml), and the reaction flask was placed at −78°C. A solution of Me_3NO (37 mg, 0.493 mmol) in THF (50 ml) was added over a period of 10 min with stirring.

TABLE 10. Non-hydrogen positional and isotropic displacement parameters, 7

Atom	x	y	z	U_{eq} (Å^2)
Os(1)	0.28772(3)	0.73691(5)	0.25173(2)	0.0291(2)
Os(2)	0.10473(4)	0.59287(6)	0.20319(3)	0.0401(2)
Os(3)	0.12808(4)	0.82057(6)	0.13154(2)	0.0420(2)
C(11)	0.3244(9)	0.587(2)	0.2115(6)	0.043(6)
O(11)	0.3534(8)	0.509(1)	0.1900(5)	0.066(6)
C(12)	0.2521(9)	0.893(1)	0.2869(6)	0.039(6)
O(12)	0.2362(8)	0.992(1)	0.3099(5)	0.063(6)
C(13)	0.380(1)	0.854(1)	0.2472(6)	0.044(6)
O(13)	0.4299(7)	0.929(1)	0.2399(5)	0.058(5)
C(21)	0.138(1)	0.466(2)	0.1544(8)	0.057(8)
O(21)	0.153(1)	0.381(1)	0.1254(7)	0.104(9)
C(22)	0.089(1)	0.721(1)	0.2601(6)	0.044(6)
O(22)	0.0752(7)	0.790(1)	0.2939(5)	0.067(6)
C(23)	0.1240(9)	0.444(2)	0.2616(7)	0.055(7)
O(23)	0.1331(8)	0.351(1)	0.2944(5)	0.074(6)
C(24)	−0.031(1)	0.579(2)	0.1473(8)	0.066(9)
O(24)	−0.1097(8)	0.567(2)	0.1125(6)	0.096(7)
C(31)	0.181(1)	0.693(2)	0.0918(7)	0.071(9)
O(31)	0.206(1)	0.621(1)	0.0655(6)	0.089(8)
C(32)	0.072(1)	0.941(2)	0.1719(8)	0.074(8)
O(32)	0.038(1)	1.018(1)	0.1924(6)	0.099(8)
C(33)	0.010(1)	0.820(2)	0.0544(8)	0.067(8)
O(33)	−0.0617(9)	0.822(2)	0.0093(6)	0.109(7)
C(34)	0.194(1)	0.976(2)	0.1202(8)	0.067(9)
O(34)	0.2348(9)	1.071(1)	0.1161(6)	0.093(7)
P(1)	0.3813(2)	0.6324(3)	0.3541(1)	0.029(1)
C(111)	0.4899(9)	0.732(1)	0.4058(6)	0.033(5)
C(112)	0.5634(9)	0.754(1)	0.3896(6)	0.041(6)
N(112)	0.5551(8)	0.692(1)	0.3338(5)	0.046(5)
C(113)	0.6409(9)	0.836(1)	0.4270(7)	0.047(7)
C(114)	0.649(1)	0.894(1)	0.4827(7)	0.058(7)
C(115)	0.583(1)	0.870(2)	0.5023(6)	0.051(7)
C(116)	0.5041(9)	0.786(1)	0.4645(6)	0.038(6)
C(121)	0.4256(9)	0.455(1)	0.3547(5)	0.032(5)
C(122)	0.3679(9)	0.353(1)	0.3109(6)	0.038(6)
C(123)	0.400(1)	0.218(1)	0.3106(7)	0.052(7)
C(124)	0.492(1)	0.182(1)	0.3560(7)	0.056(8)
C(125)	0.550(1)	0.277(2)	0.4002(7)	0.058(7)
C(126)	0.519(1)	0.413(2)	0.4010(6)	0.048(6)
C(131)	0.3169(8)	0.609(1)	0.4011(5)	0.031(5)
C(132)	0.272(1)	0.722(1)	0.4114(6)	0.044(6)
C(133)	0.218(1)	0.706(2)	0.4430(7)	0.055(7)
C(134)	0.208(1)	0.578(2)	0.4615(7)	0.062(8)
C(135)	0.252(1)	0.465(2)	0.4527(8)	0.063(9)
C(136)	0.3073(9)	0.480(1)	0.4224(6)	0.042(6)

TABLE 11. Non-hydrogen positional and isotropic displacement parameters, **8**

Atom	x	y	z	U_{eq} (Å^2)
Ru(1)	0.24828(4)	0.34735(2)	0.63635(3).	0.0388(2)
Ru(2)	0.41699(4)	0.37652(2)	0.77821(3)	0.0340(2)
Ru(3)	0.42490(4)	0.34310(2)	0.62273(3)	0.0357(2)
C(11)	0.1601(5)	0.3328(4)	0.5279(5)	0.065(4)
O(11)	0.1059(4)	0.3256(4)	0.4607(3)	0.124(4)
C(12)	0.2413(5)	0.4244(3)	0.6191(4)	0.046(3)
O(12)	0.2305(3)	0.4707(2)	0.6039(3)	0.061(3)
C(13)	0.2737(5)	0.2707(3)	0.6588(4)	0.052(3)
O(13)	0.2842(4)	0.2240(2)	0.6698(4)	0.074(3)
C(21)	0.5328(5)	0.3873(3)	0.8713(4)	0.046(3)
O(21)	0.6011(4)	0.3931(2)	0.9308(3)	0.074(3)
C(22)	0.4390(5)	0.4410(3)	0.7269(4)	0.041(3)
O(22)	0.4582(4)	0.4830(2)	0.7084(3)	0.060(3)
C(23)	0.4030(5)	0.3058(3)	0.8184(4)	0.049(3)
O(23)	0.3993(4)	0.2650(2)	0.8486(3)	0.074(3)
C(31)	0.3640(5)	0.2934(3)	0.5360(4)	0.047(3)
O(31)	0.3247(4)	0.2616(2)	0.4852(3)	0.073(3)
C(32)	0.3767(5)	0.4080(3)	0.5564(4)	0.048(3)
O(32)	0.3525(4)	0.4449(2)	0.5117(3)	0.075(3)
C(33)	0.4807(5)	0.2864(3)	0.7027(4)	0.047(3)
O(33)	0.5181(4)	0.2480(2)	0.7406(3)	0.064(3)
P(1)	0.1469(1)	0.34904(8)	0.7027(1)	0.0386(7)
C(111)	0.1003(5)	0.2817(3)	0.7086(4)	0.043(3)
C(112)	0.1293(8)	0.2504(4)	0.7782(5)	0.101(6)
C(113)	0.0962(9)	0.1961(4)	0.7735(6)	0.129(7)
C(114)	0.0315(7)	0.1747(4)	0.7005(6)	0.094(6)
C(115)	0.0053(6)	0.2051(4)	0.6319(5)	0.074(4)
C(116)	0.0376(5)	0.2585(3)	0.6351(4)	0.061(4)
C(121)	0.0382(5)	0.3908(3)	0.6594(4)	0.044(3)
C(122)	0.0119(5)	0.4181(3)	0.5845(4)	0.056(4)
C(123)	−0.0670(5)	0.4523(3)	0.5542(5)	0.069(4)
C(124)	−0.1198(5)	0.4606(3)	0.5993(6)	0.072(4)
C(125)	−0.0972(5)	0.4333(3)	0.6723(5)	0.068(4)
C(126)	−0.0193(5)	0.3977(3)	0.7018(4)	0.052(3)
C(0)	0.2088(5)	0.3726(3)	0.8104(4)	0.041(3)
P(2)	0.3155(1)	0.41513(7)	0.8316(1)	0.0359(7)
C(211)	0.2721(5)	0.4841(3)	0.7980(4)	0.040(3)
C(212)	0.3384(6)	0.5247(3)	0.8082(5)	0.058(4)
C(213)	0.3099(7)	0.5783(3)	0.7828(6)	0.083(6)
C(214)	0.2136(7)	0.5906(3)	0.7451(5)	0.085(5)
C(215)	0.1475(7)	0.5515(4)	0.7360(6)	0.091(S)
C(216)	0.1769(5)	0.4978(3)	0.7634(5)	0.066(4)
C(221)	0.3599(5)	0.4195(3)	0.9460(4)	0.041(3)
C(222)	0.3447(6)	0.4655(3)	0.9836(4)	0.058(4)
C(223)	0.3684(6)	0.4646(3)	1.0687(5)	0.072(4)
C(224)	0.4047(6)	0.4188(3)	1.1135(4)	0.066(4)
C(225)	0.4220(6)	0.3735(3)	1.0769(4)	0.066(4)
C(226)	0.3994(5)	0.3735(3)	0.9930(4)	0.056(4)
P(3)	0.5677(1)	0.35983(7)	0.6096(1)	0.0347(7)
C(311)	0.6340(4)	0.4179(3)	0.6717(4)	0.036(3)
C(312)	0.6952(5)	0.4143(3)	0.7563(4)	0.039(3)
N(3121)	0.7102(4)	0.3629(2)	0.7993(3)	0.044(2)
C(3121)	0.7979(5)	0.3416(3)	0.8440(4)	0.050(3)
O(3121)	0.8715(3)	03649(2)	0.8504(3)	0.073(3)
C(313)	0.7389(5)	0.4610(3)	0.8011(4)	0.055(3)
C(314)	0.7233(6)	0.5115(3)	0.7622(5)	0.062(4)
C(315)	0.6624(6)	0.5164(3)	0.6806(5)	0.058(4)
C(316)	0.6180(5)	0.4702(3)	0.6358(4)	0.048(3)
C(321)	0.6518(4)	0.3026(3)	0.6292(4)	0.035(3)
C(322)	0.6144(5)	0.2504(3)	0.6048(4)	0.049(3)
C(323)	0.6739(6)	0.2072(3)	0.6100(5)	0.065(4)
C(324)	0.7717(6)	0.2151(3)	0.6401(5)	0.067(4)
C(325)	0.8085(5)	0.2664(3)	0.6643(5)	0.059(4)
C(326)	0.7494(5)	0.3104(3)	0.6580(4)	0.047(3)
C(331)	0.5571(4)	0.3767(3)	0.5049(4)	0.035(3)
C(332)	0.4811(5)	0.3556(3)	0.4353(4)	0.045(3)
C(333)	0.4797(6)	0.3606(3)	0.3573(4)	0.058(4)
C(334)	0.5516(6)	0.3886(3)	0.3484(4)	0.063(4)
C(335)	0.6253(5)	0.4101(3)	0.4151(4)	0.056(4)
C(336)	0.6300(5)	0.4033(3)	0.4939(4)	0.049(3)
C(341)	0.7989(5)	0.2874(3)	0.8816(4)	0.046(3)
C(342)	0.7302(6)	0.2721(3)	0.9101(5)	0.061(4)
C(343)	0.7354(6)	0.2210(3)	0.9449(5)	0.069(4)
C(344)	0.8071(6)	0.1855(3)	0.9539(5)	0.070(4)
C(345)	0.8742(6)	0.1997(3)	0.9261(5)	0.069(4)
C(346)	0.8714(5)	0.2508(3)	0.8909(5)	0.063(4)
Cl(11) [a]	1.0162(3)	0.4781(2)	1.1296(3)	0.187(3)
Cl(12) [a]	0.8397(2)	0.4215(1)	1.0400(2)	0.114(2)
C(10) [a]	0.915(1)	0.4731(9)	1.049(1)	0.23(1)
Cl(21) [b]	0.0709(7)	0.1120(5)	0.4289(6)	0.262(9)
Cl(22) [b]	0.1331(8)	0.1556(5)	0.4970(7)	0.42(1)
C(20) [b]	0.092(2)	0.1548(7)	0.443(1)	0.21(1)

[a] Site occupation = 0.855(4); [b] Site occupation = 0.5.

After all the amine oxide had been added, the cold bath was removed and the reaction mixture was further stirred for 3 h. The solvent was evaporated under reduced pressure and the residue was chromatographed on silica gel. Elution with ether:pentane (1:8) gave a minor fraction of the monosubstituted product **25**. Elution with ether:pentane (1:5) gave $Ru_3(\mu\text{-}H)(\mu_3\text{-}C_2{}^tBu)(CO)_7\{PPh_2[CH_2C(O)Ph]\}_2$ (**26**). Recrystallization from pentane (−20°C) afforded yellow microcrystals (187 mg, 64%). Anal. Found: C, 54.12; H, 3.95%; *M*, 1189. $C_{53}H_{44}O_9P_2Ru_3$ calc.: C, 53.48; H, 3.70%; *M*, 1191. IR (CH_2Cl_2): ν(CO) 2061s, 2009s, 1990s (br), 1948m. IR (KBr): ν(CO) 1675m cm^{-1}. ^{1}H NMR (CD_2Cl_2): δ −20.42 [d, 1H, ^2J(PH) = 11 Hz)]; 1.24 (s, 9H, ^{t}Bu); 4.30 (m, 4H, PCH_2); 7.26–7.74 (m, 30H, Ph). ^{1}H NMR (CD_2Cl_2, 210 K): δ −20.54 (d, J = 10.84 Hz) and −20.74 (d, J = ~ 10 Hz). ^{31}P{^{1}H} NMR ($CDCl_3$, 250 K): δ 45.97 (s); 38.57 (s); 32.77 (s); 23.39 (s).

6.21. Preparation of $AuRu_3(\mu_3\text{-}C_2{}^tBu)(CO)_8\{PPh_2[CH_2C(O)Ph]\}(PPh_2)$ (27)

To a solution of **25** (53 mg, 0.058 mmol) in CH_2Cl_2 (15 ml) was added an ethanolic solution of NaOH (0.017 M; 3.40 ml). After stirring for 15 min, solid $AuCl(PPh_3)$ (28 mg, 0.056 mmol) was added and the reaction mixture was stirred for 1 h. The solvent was evaporated under reduced pressure and the residue was extracted with pentane (20 ml). The solution was

TABLE 12. Non-hydrogen positional and isotropic displacement parameters, **9**

Atom	x	y	z	U_{eq} (Å^2)
Ru(1)	0.68995(4)	0.20782(3)	0.70567(3)	0.0337(3)
Ru(2)	0.71364(4)	0.31563(3)	0.63112(3)	0.0330(3)
Ru(3)	0.57049(4)	0.33432(3)	0.67200(3)	0.0342(3)
C(11)	0.5605(5)	0.1707(4)	0.6259(4)	0.050(4)
O(11)	0.4843(4)	0.1434(3)	0.5824(3)	0.072(3)
C(12)	0.8081(5)	0.2584(3)	0.7800(3)	0.040(4)
O(12)	0.8812(4)	0.2837(2)	0.8286(2)	0.058(3)
C(13)	0.6701(6)	0.1577(4)	0.7664(4)	0.051(4)
O(13)	0.6595(5)	0.1281(3)	0.8038(3)	0.085(4)
C(21)	0.6246(5)	0.2576(4)	0.5581(3)	0.044(4)
O(21)	0.5676(4)	0.2239(3)	0.5087(2)	0.061(3)
C(22)	0.7134(5)	0.3843(4)	0.5725(3)	0.046(4)
O(22)	0.7071(4)	0.4222(3)	0.5326(3)	0.079(4)
C(31)	0.5402(5)	0.2925(4)	0.7320(3)	0.046(4)
O(31)	0.5223(4)	0.2696(3)	0.7686(3)	0.075(4)
C(32)	0.4485(5)	0.3022(3)	0.5903(3)	0.049(4)
O(32)	0.3712(4)	0.2882(3)	0.5370(3)	0.080(3)
P(1)	0.7896(1)	0.12561(9)	0.69458(9)	0.0362(9)
C(111)	0.9110(5)	0.0906(3)	0.7735(3)	0.040(4)
C(112)	0.9420(6)	0.1110(4)	0.8397(3)	0.053(4)
C(113)	1.0372(7)	0.0878(4)	0.8979(4)	0.075(5)
C(114)	1.1017(6)	0.0439(4)	0.8923(4)	0.074(5)
C(115)	1.0689(6)	0.0209(4)	0.8264(4)	0.067(5)
C(116)	0.9749(5)	0.0439(4)	0.7675(3)	0.050(4)
C(121)	0.7215(5)	0.0442(3)	0.6504(3)	0.039(4)
C(122)	0.6968(7)	−0.0006(4)	0.6841(4)	0.068(6)
C(123)	0.6412(7)	−0.0622(4)	0.6536(5)	0.073(6)
C(124)	0.6066(6)	−0.0784(4)	0.5870(4)	0.069(5)
C(125)	0.6313(9)	−0.0341(5)	0.5537(4)	0.110(8)
C(126)	0.6859(8)	0.0269(4)	0.5837(4)	0.092(6)
C(0)	0.8342(5)	0.1585(3)	0.6414(3)	0.041(4)
P(2)	0.8570(1)	0.25337(9)	0.64926(9)	0.0370(9)
C(211)	0.8811(6)	0.2649(3)	0.5820(3)	0.046(4)
C(212)	0.7999(6)	0.2553(5)	0.5125(4)	0.069(5)
C(213)	0.8125(7)	0.2613(5)	0.4589(4)	0.085(6)
C(214)	0.9090(9)	0.2782(5)	0.4754(5)	0.107(8)
C(215)	0.9916(9)	0.2887(6)	0.5439(5)	0.126(9)
C(216)	0.9784(7)	0.2812(5)	0.5974(4)	0.079(6)
C(221)	0.9873(5)	0.2667(3)	0.7298(3)	0.042(4)
C(222)	1.0209(5)	0.3327(4)	0.7550(4)	0.066(5)
C(223)	1.1215(6)	0.3453(5)	0.8166(5)	0.093(6)
C(224)	1.1861(7)	0.2901(6)	0.8515(5)	0.100(6)
C(225)	1.1566(7)	0.2249(5)	0.8275(6)	0.137(8)
C(226)	1.0570(6)	0.2137(4)	0.7672(5)	0.092(6)
P(3)	0.5012(1)	0.44263(9)	0.67193(9)	0.0380(9)
C(311)	0.5789(5)	0.4551(3)	0.7665(3)	0.039(4)
C(312)	0.6787(5)	0.4259(3)	0.8000(3)	0.040(4)
C(3121)	0.7860(5)	0.4119(3)	0.7578(3)	0.035(3)
O(3121)	0.8095(3)	0.3857(2)	0.7185(2)	0.038(2)
N(3121)	0.7032(4)	0.3935(3)	0.7555(2)	0.035(3)
C(313)	0.7446(5)	0.4232(4)	0.8731(3)	0.053(4)
C(314)	0.7103(6)	0.4510(5)	0.9109(4)	0.066(5)
C(315)	0.6125(6)	0.4806(5)	0.8779(4)	0.075(5)
C(316)	0.5454(6)	0.4842(4)	0.8045(4)	0.056(5)
C(321)	0.3649(5)	0.4503(3)	0.6432(3)	0.043(4)
C(322)	0.2970(6)	0.4999(4)	0.5950(4)	0.059(4)
C(323)	0.1935(6)	0.5036(5)	0.5750(4)	0.076(5)
C(324)	0.1569(6)	0.4600(5)	0.6011(5)	0.079(6)
C(325)	0.2235(7)	0.4106(5)	0.6488(5)	0.083(6)
C(326)	0.3267(6)	0.4047(4)	0.6687(4)	0.064(5)
C(331)	0.5291(5)	0.5210(3)	0.6411(3)	0.042(4)
C(332)	0.5604(6)	0.5166(4)	0.5969(4)	0.054(5)
C(333)	0.5860(7)	0.5762(4)	0.5755(4)	0.069(6)
C(334)	0.5779(6)	0.6412(4)	0.5972(4)	0.065(5)
C(335)	0.5475(7)	0.6465(4)	0.6419(5)	0.072(6)
C(336)	0.5239(6)	0.5870(4)	0.6633(4)	0.063(5)
C(341)	0.8598(5)	0.4687(3)	0.8069(3)	0.044(4)
C(342)	0.9603(6)	0.4515(4)	0.8614(4)	0.074(5)
C(343)	1.0281(7)	0.5025(5)	0.9087(4)	0.089(6)
C(344)	0.9957(7)	0.5693(4)	0.9003(4)	0.078(6)
C(345)	0.8973(7)	0.5876(4)	0.8452(5)	0.075(6)
C(346)	0.8287(6)	0.5369(4)	0.7976(4)	0.056(4)
Cl(1)	0.2966(4)	0.1970(3)	0.6463(2)	0.256(4)
Cl(2)	0.1529(5)	0.1732(4)	0.5046(3)	0.322(6)
C(01)	0.243(1)	0.1449(8)	0.572(1)	0.22(2)
H(23)	0.611(5)	0.366(3)	0.619(3)	0.06(2)

concentrated to *ca.* 10 ml and cooling (−20°C) over night gave yellow microcrystals of $AuRu_3(\mu_3\text{-}C_2{}^tBu)(CO)_8\{PPh_2[CH_2C(O)Ph]\}(PPh_3)$ (**27**) (38 mg, 48%). IR (CH_2Cl_2): ν(CO) 2043w, 2017s, 1988s, 1970s. IR (KBr): ν(CO) 1673w cm^{-1}. ^{1}H NMR ($CDCl_3$): δ 1.37 (s, 9H, ^{t}Bu); 4.25 [d, 2H, PCH_2, $^2J(PH) = 8.1$ Hz]; 7.21–7.81 (m, 30H, aromatic). $^{31}P\{^1H\}$ NMR ($CDCl_3$): δ 44.3 [s, $PPh_2\{CH_2C(O)Ph\}$]; 60.15 (s, PPh_3). Anal. Found: C, 45.69; H, 3.18%; *M*, 1374. $C_{52}H_{41}AuO_9P_2Ru_3$ calc.: C, 45.52; H, 2.99%; *M*, 1373.

7. Crystallography

Unique diffractometer data sets were measured at *ca.* 295 K ($2\theta/\theta$ scan mode; monochromatic Mo–Kα radiation, $\lambda = 0.71073$ Å) yielding *N* independent reflections; N_0 of these with $I > 3\sigma(I)$ were considered "observed" and used in large block/full matrix least-squares refinements after absorption correction. Anisotropic thermal parameters were refined for the non-hydrogen atoms; $(x, y, z, U_{iso})_H$ were included constrained at estimated values. Conventional residuals *R*, R_w on $|F|$ are quoted at convergence. Statistical weights derivative of $\sigma^2(I) = \sigma^2(I_{diff}) + 0.0004\sigma^4(I_{diff})$ were used; for **4** and **11**, a weighting scheme of the form $w = [\sigma^2(F) + g|F|^2]^{-1}$ [$g = 0.0039$ (**4**), 0.0033 (**11**)] was used. Neutral atom complex scattering factors were employed; for **4** and **11**, those for Ru were from Ref. 33. Computation used the XTAL2.6 program system [34] implemented by Hall, or the SHELX76 [35] and SHELXS86 [36] programmes. For **4** and **11** *P*-bound phenyl groups were refined as hexagonal rigid groups, and the remaining non-H atoms were refined with

anisotropic thermal parameters. H atoms were included in each model at their calculated positions; cluster bound H atoms were not located. Diagrams showing the crystallographic numbering schemes were drawn with the ORTEP program [37] with 25% probability ellipsoids. Relevant crystal data and refinement details are collected in Table 7, and pertinent results are given in the figures and tables 8–19.

TABLE 13. Non-hydrogen positional and isotropic displacement parameters, **10**

Atom	x	y	z	U_{eq} (Å^2)
Os(1)	0.28284(2)	0.27489(3)	0.22933(2)	0.0402(2)
Os(2)	0.34827(3)	0.36170(4)	0.38294(2)	0.0522(2)
Os(3)	0.37112(3)	0.49366(4)	0.26589(3)	0.0611(2)
C(11)	0.1888(6)	0.3611(9)	0.2152(5)	0.050(4)
O(11)	0.1298(4)	0.4085(7)	0.2031(4)	0.066(4)
C(12)	0.3767(8)	0.195(1)	0.2383(7)	0.071(6)
O(12)	0.4311(6)	0.1430(9)	0.2385(6)	0.113(6)
C(13)	0.2554(9)	0.280(1)	0.1258(6)	0.080(7)
O(13)	0.2354(8)	0.285(1)	0.0612(5)	0.129(7)
C(21)	0.2531(7)	0.443(1)	0.3647(6)	0.060(5)
O(21)	0.1967(5)	0.4945(9)	0.3588(4)	0.084(4)
C(22)	0.4428(8)	0.277(1)	0.3948(7)	0.080(6)
O(22)	0.4997(6)	0.224(1)	0.4066(6)	0.122(6)
C(23)	0.3180(9)	0.235(1)	0.4318(7)	0.085(7)
O(23)	0.3009(9)	0.161(1)	0.4604(6)	0.153(9)
C(24)	0.3978(7)	0.467(1)	0.4649(7)	0.094(7)
O(24)	0.4249(6)	0.531(1)	0.5142(6)	0.151(7)
C(31)	0.2764(7)	0.576(1)	0.2470(6)	0.068(6)
O(31)	0.2209(6)	0.6351(8)	0.2349(6)	0.097(5)
C(32)	0.4642(8)	0.408(1)	0.2801(9)	0.093(8)
O(32)	0.5237(6)	0.367(1)	0.2878(7)	0.129(7)
C(33)	0.4343(9)	0.618(1)	0.3268(9)	0.104(9)
O(33)	0.4732(7)	0.691(1)	0.3610(7)	0.150(8)
C(34)	0.368(1)	0.530(1)	0.1710(9)	0.11(1)
O(34)	0.3583(9)	0.556(1)	0.1106(6)	0.151(9)
P(1)	0.2230(1)	0.0916(2)	0.2339(1)	0.0348(9)
C(111)	0.2057(6)	0.0066(9)	0.1483(5)	0.043(4)
C(112)	0.1482(6)	0.0379(8)	0.0761(5)	0.042(4)
N(112)	0.0951(5)	0.1279(7)	0.0701(4)	0.048(3)
C(1121)	0.0401(6)	0.180(1)	0.0070(5)	0.051(4)
O(1121)	0.0360(6)	0.1537(8)	−0.0556(4)	0.084(4)
C(113)	0.1464(7)	−0.026(1)	0.0152(5)	0.060(5)
C(114)	0.2010(8)	−0.112(1)	0.0218(6)	0.074(6)
C(115)	0.2569(8)	−0.146(1)	0.0909(6)	0.068(6)
C(116)	0.2594(7)	−0.0832(9)	0.1541(6)	0.056(5)
C(121)	0.2756(7)	−0.0148(9)	0.3112(5)	0.050(4)
C(122)	0.3534(8)	−0.006(1)	0.3530(7)	0.083(6)
C(123)	0.3914(9)	−0.086(1)	0.4099(8)	0.112(7)
C(124)	0.344(1)	−0.168(1)	0.4275(6)	0.101(8)
C(125)	0.268(1)	−0.183(2)	0.3840(8)	0.108(8)
C(126)	0.2338(8)	−0.102(1)	0.3268(7)	0.081(6)
C(131)	0.1286(5)	0.0966(8)	0.2416(4)	0.036(3)
C(132)	0.1155(6)	0.1766(9)	0.2909(5)	0.043(4)
C(133)	0.0461(7)	0.179(1)	0.3004(6)	0.059(5)
C(134)	−0.0140(7)	0.103(1)	0.2601(6)	0.063(6)
C(135)	−0.0026(7)	0.021(1)	0.2119(5)	0.056(5)
C(136)	0.0666(6)	0.0177(8)	0.2033(4)	0.040(4)
C(141)	−0.0119(7)	0.270(1)	0.0179(5)	0.055(5)
C(142)	−0.0226(7)	0.287(1)	0.0843(5)	0.064(5)
C(143)	−0.0717(8)	0.370(1)	0.0915(6)	0.081(6)
C(144)	−0.1146(8)	0.441(1)	0.0293(7)	0.089(7)
C(145)	−0.1072(9)	0.425(1)	−0.0354(7)	0.098(8)
C(146)	−0.0562(9)	0.343(1)	−0.0420(6)	0.082(7)

TABLE 14. Non-hydrogen positional factors ($\times 10^5$ for Ru, $\times 10^4$ for other atoms) for **11**

Atom	x	y	z
Ru(1)	21527(4)	65531(2)	24394(4)
Ru(2)	29747(3)	77925(2)	53536(4)
Ru(3)	34377(4)	62581(3)	50316(5)
P(1)	2146(1)	8894(1)	5341(1)
N(12)	1013(4)	7297(2)	4680(4)
C(1)	1329(6)	6842(4)	769(7)
O(1)	889(5)	6997(3)	−232(6)
C(2)	3607(6)	6535(4)	1574(7)
O(2)	4400(5)	6552(4)	982(6)
C(3)	1422(5)	5419(4)	1685(7)
O(3)	974(5)	4752(3)	1224(6)
C(4)	3081(5)	7877(3)	7393(7)
O(4)	3186(5)	7921(3)	8632(5)
C(5)	4679(6)	8295(3)	5755(7)
O(5)	5719(4)	8637(3)	6054(7)
C(6)	1820(7)	6043(4)	5571(8)
O(6)	945(5)	5910(3)	5966(6)
C(7)	3387(7)	5137(5)	4205(9)
O(7)	3334(7)	4478(3)	3757(9)
C(8)	4943(7)	6672(4)	4411(7)
O(8)	5853(5)	6888(4)	4144(6)
C(9)	4410(6)	6463(4)	7019(8)
O(9)	5035(5)	6597(4)	8158(6)
C(11)	2848(4)	9899(2)	6649(4)
C(12)	2728(4)	10582(2)	6234(4)
C(13)	3216(4)	11342(2)	7284(4)
C(14)	3825(4)	11419(2)	8748(4)
C(15)	3945(4)	10736(2)	9163(4)
C(16)	3457(4)	9976(2)	8113(4)
C(21)	1765(3)	9044(3)	3512(4)
C(22)	2751(3)	9232(3)	2839(4)
C(23)	2503(3)	9307(3)	1394(4)
C(24)	1270(3)	9193(3)	623(4)
C(25)	284(3)	9005(3)	1296(4)
C(26)	532(3)	8930(3)	2741(4)
C(31)	649(5)	8560(3)	5801(5)
C(32)	238(4)	7728(3)	5432(5)
C(33)	−844(5)	7381(4)	5802(7)
C(34)	−1477(5)	7889(4)	6571(7)
C(35)	−1088(5)	8715(4)	6905(6)
C(36)	−12(5)	9049(3)	6531(6)
C(40)	652(4)	6740(3)	3401(6)
C(41)	−684(3)	6383(2)	2619(5)
C(42)	−1269(3)	5612(2)	2598(5)
C(43)	−2512(3)	5259(2)	1806(5)
C(44)	−3171(3)	5677(2)	1036(5)
C(45)	−2587(3)	6449(2)	1057(5)
C(46)	−1343(3)	6802(2)	1848(5)

TABLE 15. Non-hydrogen positional and isotropic displacement parameters, **15**

Atom	x	y	z	U_{eq} (Å^2)
Ru(1)	0.61006(1)	0.64459(3)	0.67666(2)	0.0361(2)
Ru(2)	0.60867(2)	0.82678(3)	0.61432(2)	0.0438(2)
Ru(3)	0.63731(2)	0.81664(3)	0.74380(2)	0.0422(2)
C(11)	0.6209(2)	0.5467(4)	0.7363(3)	0.047(2)
O(11)	0.6266(1)	0.4896(3)	0.7741(2)	0.075(2)
C(12)	0.6567(2)	0.6234(4)	0.6392(3)	0.046(2)
O(12)	0.6838(1)	0.6033(3)	0.6179(2)	0.065(2)
C(13)	0.5652(2)	0.6793(4)	0.7145(3)	0.046(2)
O(13)	0.5385(1)	0.6888(3)	0.7389(2)	0.067(2)
C(21)	0.6045(2)	0.9554(5)	0.5818(3)	0.067(3)
O(21)	0.6009(2)	1.0317(3)	0.5615(3)	0.106(3)
C(22)	0.6643(2)	0.8312(5)	0.6148(3)	0.058(3)
O(22)	0.6972(1)	0.8407(4)	0.6091(2)	0.083(2)
C(23)	0.5555(2)	0.8307(5)	0.6292(3)	0.060(3)
O(23)	0.5224(1)	0.8369(4)	0.6329(2)	0.078(2)
C(31)	0.6405(2)	0.7513(5)	0.8180(3)	0.060(3)
O(31)	0.6409(2)	0.7074(4)	0.8620(2)	0.099(3)
C(32)	0.6854(2)	0.7582(4)	0.7290(3)	0.050(2)
O(32)	0.7161(1)	0.7257(3)	0.7247(2)	0.064(2)
C(33)	0.5870(2)	0.8712(5)	0.7520(3)	0.061(3)
O(33)	0.5581(1)	0.9051(4)	0.7628(3)	0.091(2)
P(1)	0.57156(5)	0.5595(1)	0.59910(7)	0.0401(5)
C(111)	0.5248(2)	0.5137(4)	0.6182(3)	0.047(2)
C(112)	0.4936(2)	0.5751(5)	0.6234(3)	0.057(3)
C(113)	0.4593(2)	0.5400(6)	0.6418(3)	0.075(3)
C(114)	0.4566(2)	0.4416(6)	0.6555(3)	0.079(3)
C(115)	0.4873(2)	0.3802(6)	0.6519(4)	0.084(4)
C(116)	0.5209(2)	0.4146(5)	0.6332(3)	0.064(3)
C(121)	0.5906(2)	0.4470(4)	0.5687(3)	0.044(2)
C(122)	0.6241(2)	0.4026(5)	0.5975(3)	0.060(3)
C(123)	0.6371(2)	0.3152(6)	0.5759(4)	0.088(4)
C(124)	0.6165(3)	0.2746(6)	0.5239(4)	0.098(4)
C(125)	0.5825(3)	0.3161(5)	0.4954(4)	0.089(4)
C(126)	0.5699(2)	0.4024(5)	0.5178(3)	0.060(3)
C(0)	0.5563(2)	0.6380(4)	0.5319(3)	0.046(2)
P(2)	0.59045(5)	0.7403(1)	0.52402(7)	0.0410(6)
C(211)	0.6299(2)	0.6889(4)	0.4871(2)	0.042(2)
C(212)	0.6298(2)	0.5926(4)	0.4650(3)	0.055(3)
C(213)	0.6599(2)	0.5591(5)	0.4371(3)	0.068(3)
C(214)	0.6913(2)	0.6179(5)	0.4303(3)	0.069(3)
C(215)	0.6919(2)	0.7131(5)	0.4514(3)	0.065(3)
C(216)	0.6612(2)	0.7486(5)	0.4793(3)	0.050(2)
C(221)	0.5620(2)	0.8119(4)	0.4628(3)	0.048(2)
C(222)	0.5746(2)	0.8317(5)	0.4090(3)	0.062(3)
C(223)	0.5533(2)	0.8898(6)	0.3646(3)	0.078(3)
C(224)	0.5189(2)	0.9282(6)	0.3736(3)	0.083(3)
C(225)	0.5045(2)	0.9079(7)	0.4261(4)	0.101(4)
C(226)	0.5260(2)	0.8499(6)	0.4707(3)	0.089(4)
P(3)	0.66749(5)	0.9679(1)	0.77514(7)	0.0429(6)
C(311)	0.7108(2)	0.9954(5)	0.7394(3)	0.051(2)
C(312)	0.7475(2)	0.9469(5)	0.7538(3)	0.067(3)
C(3121)	0.7543(2)	0.8709(6)	0.8036(4)	0.084(3)
O(3121)	0.7871(2)	0.8410(5)	0.8197(3)	0.134(3)
C(313)	0.7776(2)	0.9696(6)	0.7215(4)	0.093(4)
C(314)	0.7732(3)	1.0390(6)	0.6765(4)	0.114(5)
C(315)	0.7377(3)	1.0881(6)	0.6623(4)	0.103(4)
C(316)	0.7070(2)	1.0649(5)	0.6932(3)	0.071(3)
C(321)	0.6386(2)	1.0821(4)	0.7614(3)	0.045(2)
C(322)	0.6074(2)	1.0892(5)	0.7151(3)	0.062(3)
C(323)	0.5861(2)	1.1756(5)	0.7039(3)	0.074(3)
C(324)	0.5974(2)	1.2562(5)	0.7390(3)	0.077(3)
C(325)	0.6288(2)	1.2520(5)	0.7842(3)	0.071(3)
C(326)	0.6492(2)	1.1653(5)	0.7954(3)	0.060(3)
C(331)	0.6843(2)	0.9820(4)	0.8574(3)	0.047(2)
C(332)	0.7201(2)	1.0220(5)	0.8810(3)	0.058(3)
C(333)	0.7308(2)	1.0335(6)	0.9431(3)	0.086(4)
C(334)	0.7055(3)	1.0052(6)	0.9810(3)	0.091(4)
C(335)	0.6694(3)	0.9685(5)	0.9584(3)	0.081(3)
C(336)	0.6585(2)	0.9549(5)	0.8965(3)	0.062(3)
Cl(1)	0.7190(2)	0.2887(5)	0.4664(3)	0.314(4)
C(1) [a]	0.7313(8)	0.276(2)	0.5331(9)	0.17(1)

[a] Site occupation factor = 0.5

TABLE 16. Non-hydrogen positional and isotropic displacement parameters, **18**

Atom	x	y	z	U_{eq} (Å^2)
Os(1)	0.25337(3)	0.65995(4)	0.36148(2)	0.0232(1)
Os(2)	0.42937(3)	0.75499(4)	0.41876(2)	0.0284(1)
Os(3)	0.41960(3)	0.55732(4)	0.32259(2)	0.0307(1)
C(11)	0.2640(8)	0.789(1)	0.2957(7)	0.040(4)
O(11)	0.2668(6)	0.864(1)	0.2575(5)	0.053(4)
C(12)	0.2458(8)	0.533(1)	0.4282(6)	0.033(4)
O(12)	0.2356(7)	0.4566(9)	0.4649(5)	0.052(4)
C(13)	0.1775(9)	0.565(1)	0.3040(6)	0.036(4)
O(13)	0.1314(8)	0.5060(9)	0.2666(5)	0.061(4)
C(21)	0.429(1)	0.890(1)	0.3555(7)	0.048(5)
O(21)	0.437(1)	0.977(1)	0.3218(6)	0.095(6)
C(22)	0.4170(8)	0.622(1)	0.4809(7)	0.036(4)
O(22)	0.4119(6)	0.5495(9)	0.5211(5)	0.048(3)
C(23)	0.404(1)	0.880(1)	0.4814(7)	0.050(5)
O(23)	0.3950(9)	0.954(1)	0.5197(7)	0.087(6)
C(24)	0.559(1)	0.756(1)	0.4309(6)	0.043(5)
O(24)	0.6347(7)	0.756(1)	0.4388(6)	0.063(4)
C(31)	0.429(1)	0.686(1)	0.2579(8)	0.048(5)
O(31)	0.4360(8)	0.755(1)	0.2169(6)	0.073(5)
C(32)	0.4059(9)	0.424(1)	0.3839(7)	0.044(5)
O(32)	0.3979(8)	0.3382(9)	0.4174(5)	0.063(4)
C(33)	0.5473(9)	0.534(1)	0.3291(6)	0.039(4)
O(33)	0.6225(7)	0.521(1)	0.3327(5)	0.063(4)
C(34)	0.376(1)	0.444(1)	0.2560(8)	0.049(5)
O(34)	0.350(1)	0.373(1)	0.2160(7)	0.099(6)
P(1)	0.1384(2)	0.7778(3)	0.4047(1)	0.0249(8)
C(111)	0.138(1)	0.947(1)	0.3807(6)	0.041(4)
C(112)	0.1060(9)	0.992(1)	0.3179(7)	0.042(4)
C(1121)	0.070(1)	0.912(2)	0.2653(7)	0.055(6)
O(1121)	0.0635(7)	0.798(1)	0.2650(5)	0.053(4)
C(113)	0.116(1)	1.121(2)	0.3035(8)	0.068(7)
C(114)	0.161(2)	1.203(2)	0.352(1)	0.09(1)
C(115)	0.187(1)	1.158(1)	0.408(1)	0.09(1)
C(116)	0.177(1)	1.033(1)	0.4245(8)	0.057(6)
C(121)	0.1448(9)	0.790(1)	0.4936(6)	0.033(4)
C(122)	0.071(1)	0.837(2)	0.5221(7)	0.061(6)
C(123)	0.075(1)	0.844(2)	0.5889(8)	0.069(7)
C(124)	0.150(1)	0.808(1)	0.6267(7)	0.056(6)
C(125)	0.223(1)	0.761(1)	0.6004(6)	0.051(5)
C(126)	0.2188(9)	0.751(1)	0.5327(6)	0.037(4)
C(131)	0.0233(8)	0.718(1)	0.3916(6)	0.036(4)
C(132)	−0.053(1)	0.790(2)	0.3753(8)	0.055(5)
C(133)	−0.138(1)	0.742(2)	0.375(1)	0.075(7)
C(134)	−0.150(1)	0.617(2)	0.3903(9)	0.074(7)
C(135)	−0.079(1)	0.542(2)	0.4061(9)	0.062(6)
C(136)	0.009(1)	0.592(1)	0.4076(8)	0.052(5)

TABLE 17. Non-hydrogen positional and isotropic displacement parameters, **18a**

Atom	x	y	z	U_{eq} (Å^2)
Os(1)	0.20093(6)	0.31633(8)	0.9684(1)	0.0325(4)
Os(2)	0.24182(7)	0.04326(8)	1.0221(1)	0.0395(4)
Os(3)	0.07653(6)	0.15594(8)	1.1823(1)	0.0390(4)
C(11)	0.136(1)	0.320(2)	0.834(2)	0.043(6)
O(11)	0.091(1)	0.331(2)	0.766(2)	0.053(4)
C(12)	0.260(2)	0.312(2)	1.107(3)	0.049(6)
O(12)	0.297(1)	0.325(2)	1.179(2)	0.077(6)
C(13)	0.135(2)	0.473(2)	0.993(3)	0.047(6)
O(13)	0.092(1)	0.566(2)	1.019(2)	0.079(6)
C(21)	0.186(2)	0.054(2)	0.876(3)	0.053(7)
O(21)	0.153(1)	0.052(2)	0.798(2)	0.062(5)
C(22)	0.305(2)	0.046(3)	1.156(3)	0.073(9)
O(22)	0.347(1)	0.046(2)	1.224(2)	0.092(7)
C(23)	0.349(2)	0.013(2)	0.906(3)	0.053(7)
O(23)	0.420(1)	−0.015(2)	0.824(2)	0.078(6)
C(24)	0.208(2)	−0.119(3)	1.108(3)	0.073(9)
O(24)	0.187(1)	−0.227(2)	1.172(2)	0.081(6)
C(31)	0.015(2)	0.153(2)	1.046(3)	0.049(6)
O(31)	−0.026(1)	0.147(2)	0.981(2)	0.062(5)
C(32)	0.130(2)	0.152(3)	1.323(3)	0.079(9)
O(32)	0.170(1)	0.147(2)	1.397(2)	0.095(7)
C(33)	0.025(2)	0.011(3)	1.304(3)	0.077(9)
O(33)	−0.010(2)	−0.078(2)	1.382(3)	0.110(8)
C(34)	−0.008(2)	0.290(2)	1.236(3)	0.060(7)
O(34)	−0.058(1)	0.369(2)	1.274(2)	0.075(6)
P(1)	0.3259(4)	0.3871(5)	0.7803(6)	0.033(2)
C(111)	0.295(1)	0.546(2)	0.677(2)	0.039(5)
C(112)	0.278(2)	0.657(2)	0.723(3)	0.047(6)
C(1121)	0.286(2)	0.653(3)	0.862(3)	0.074(9)
O(1121)	0.295(2)	0.752(2)	0.878(3)	0.116(9)
C(113)	0.247(2)	0.775(2)	0.648(3)	0.057(7)
C(114)	0.241(2)	0.782(3)	0.523(3)	0.067(8)
C(115)	0.263(2)	0.676(3)	0.471(3)	0.079(9)
C(116)	0.293(2)	0.559(3)	0.546(3)	0.062(8)
C(121)	0.429(1)	0.407(2)	0.813(2)	0.037(5)
C(122)	0.466(2)	0.305(2)	0.910(3)	0.049(6)
C(123)	0.545(2)	0.309(2)	0.933(3)	0.060(7)
C(124)	0.592(2)	0.412(2)	0.870(3)	0.057(7)
C(125)	0.560(2)	0.519(2)	0.774(3)	0.051(7)
C(126)	0.477(1)	0.506(2)	0.747(2)	0.042(6)
C(131)	0.372(1)	0.293(2)	0.654(2)	0.035(5)
C(132)	0.315(2)	0.245(2)	0.610(3)	0.049(6)
C(133)	0.349(2)	0.177(2)	0.512(3)	0.057(7)
C(134)	0.439(2)	0.151(2)	0.457(3)	0.059(7)
C(135)	0.496(2)	0.197(2)	0.501(3)	0.058(7)
C(136)	0.466(2)	0.267(2)	0.598(3)	0.049(6)
Cl(1) [a]	0.128(2)	0.455(2)	0.400(3)	0.19(2)
Cl(2) [a]	−0.054(2)	0.487(4)	0.562(3)	0.20(2)
C(0) [a]	0.03(2)	0.44(2)	0.48(3)	0.4(1)

[a] Site occupancy factor = 0.5

Acknowledgments

We are grateful to the Australian Research Council and the CNRS for support of this work; part was done by O.K. for his Diplom-Arbeit (Universität Tübingen). S.C.C. thanks the Universidad de Valladolid for leave of absence and the MRT/MEC for a grant. M.I.B. thanks CNRS and NSERC for a Visiting Scientist position (Strasbourg) and an International Exchange Fellowship (Vancouver) respectively, and Johnson Matthey Technology Centre for generous loans of $RuCl_3 \cdot nH_2O$ and OsO_4.

TABLE 18. Non-hydrogen positional and isotropic displacement parameters, **19**

Atom	x	y	z	U_{eq} (Å^2)
Os(1)	0.25487(9)	0.38006(3)	0.72163(5)	0.0364(3)
Os(2)	0.4130(1)	0.47299(3)	0.66940(5)	0.0421(3)
Os(3)	0.2875(1)	0.48389(3)	0.80674(6)	0.0536(4)
C(12)	−0.009(3)	0.3802(9)	0.658(1)	0.07(1)
O(12)	−0.155(2)	0.3781(7)	0.623(1)	0.093(9)
C(13) [a]	0.263(3)	0.3461(8)	0.823(1)	0.052(5)
O(13)	0.271(2)	0.3272(7)	0.892(1)	0.080(8)
C(22)	0.241(3)	0.5218(8)	0.594(1)	0.07(1)
O(22)	0.135(2)	0.5520(7)	0.550(1)	0.090(9)
C(23)	0.478(3)	0.4509(7)	0.572(1)	0.047(8)
O(23)	0.514(2)	0.4400(6)	0.514(1)	0.071(8)
C(24)	0.576(3)	0.5314(8)	0.719(2)	0.07(1)
O(24)	0.678(3)	0.5665(7)	0.747(1)	0.10(1)
C(31)	0.503(5)	0.4576(9)	0.887(2)	0.09(2)
O(31)	0.653(3)	0.4414(8)	0.940(1)	0.12(1)
C(32)	0.058(4)	0.4985(9)	0.708(2)	0.07(1)
O(32)	−0.082(2)	0.5077(8)	0.654(1)	0.10(1)
C(33)	0.358(3)	0.5565(9)	0.837(2)	0.07(1)
O(33)	0.399(3)	0.6023(6)	0.848(1)	0.12(1)
C(34) [a]	0.148(4)	0.472(1)	0.863(2)	0.11(1)
O(34)	0.117(4)	0.4598(8)	0.932(1)	0.13(1)
P(1)	0.3029(6)	0.2998(2)	0.6597(3)	0.035(2)
C(111)	0.522(2)	0.2788(7)	0.741(1)	0.033(6)
C(112)	0.622(2)	0.3240(7)	0.788(1)	0.045(8)
C(1121)	0.526(2)	0.3758(7)	0.763(2)	0.06(1)
O(1121)	0.612(2)	0.4167(5)	0.7503(8)	0.050(6)
C(113)	0.801(3)	0.3159(8)	0.852(1)	0.054(8)
C(114)	0.870(3)	0.2654(8)	0.869(1)	0.059(9)
C(115)	0.770(3)	0.2209(8)	0.828(1)	0.055(9)
C(116)	0.595(2)	0.2265(7)	0.761(1)	0.053(9)
C(121)	0.332(2)	0.3077(7)	0.555(1)	0.039(7)
C(122)	0.481(3)	0.2880(8)	0.544(1)	0.06(1)
C(123)	0.490(3)	0.296(1)	0.461(2)	0.08(1)
C(124)	0.361(3)	0.3235(9)	0.392(1)	0.07(1)
C(125)	0.217(3)	0.3424(9)	0.405(1)	0.06(1)
C(126)	0.200(2)	0.3363(7)	0.484(1)	0.044(7)
C(131)	0.160(2)	0.2404(6)	0.637(1)	0.031(6)
C(132)	0.194(2)	0.1952(7)	0.594(1)	0.045(8)
C(133)	0.089(3)	0.1484(8)	0.579(1)	0.054(9)
C(134)	−0.042(3)	0.1454(9)	0.606(1)	0.06(1)
C(135)	−0.075(3)	0.1898(9)	0.648(2)	0.07(1)
C(136)	0.023(2)	0.2378(8)	0.667(1)	0.052(9)

[a] Isotropic thermal parameters

TABLE 19. Non-hydrogen positional and isotropic displacement parameters, **20**

Atom	x	y	z	U_{eq} (Å^2)
Os(1)	0.24825(4)	0.97455(4)	0.03161(6)	0.0316(2)
Os(2)	0.18364(4)	1.12870(4)	0.24979(6)	0.0406(3)
Os(3)	0.11415(4)	1.16922(4)	−0.03368(6)	0.0406(3)
C(11)	0.137(1)	0.9598(9)	0.092(1)	0.039(6)
O(11)	0.0711(7)	0.9459(7)	0.117(1)	0.053(5)
C(12)	0.356(1)	0.9956(9)	−0.034(2)	0.039(6)
O(12)	0.4212(7)	1.0040(7)	−0.079(1)	0.060(6)
C(13)	0.263(1)	0.910(1)	−0.149(2)	0.048(7)
O(13)	0.2704(9)	0.8709(9)	−0.254(1)	0.086(7)
C(21)	0.0971(9)	1.080(1)	0.328(1)	0.043(7)
O(21)	0.0493(8)	1.0489(8)	0.388(1)	0.063(6)
C(22)	0.283(1)	1.156(1)	0.168(2)	0.07(1)
O(22)	0.346(1)	1.173(1)	0.131(2)	0.099(9)
C(23)	0.245(1)	1.083(1)	0.420(2)	0.064(8)
O(23)	0.2822(8)	1.065(1)	0.526(1)	0.084(7)
C(24)	0.097(1)	1.259(1)	0.304(2)	0.063(8)
O(24)	0.0424(9)	1.3359(9)	0.337(2)	0.098(7)
C(31)	0.007(1)	1.164(1)	0.073(1)	0.047(7)
O(31)	−0.0615(7)	1.1670(8)	0.136(1)	0.062(6)
C(32)	0.220(1)	1.179(1)	−0.121(2)	0.064(8)
O(32)	0.2839(8)	1.1945(9)	−0.178(1)	0.083(7)
C(33)	0.044(1)	1.303(1)	−0.046(2)	0.073(9)
O(33)	0.003(1)	1.3864(9)	−0.054(2)	0.114(8)
C(34)	0.093(1)	1.128(1)	−0.218(2)	0.07(1)
O(34)	0.0821(9)	1.103(1)	−0.323(1)	0.109(9)
P(1)	0.3383(2)	0.8381(3)	0.1668(4)	0.033(2)
C(111)	0.2628(9)	0.7900(9)	0.261(1)	0.039(6)
C(112)	0.2288(9)	0.733(1)	0.194(2)	0.040(6)
C(1121)	0.2564(9)	0.7086(9)	0.034(1)	0.039(6)
N(1121)	0.2349(8)	0.6489(8)	−0.025(1)	0.042(5)
N(1122)	0.2665(8)	0.6315(8)	−0.172(1)	0.046(6)
C(113)	0.168(1)	0.704(1)	0.275(2)	0.052(7)
C(114)	0.137(1)	0.730(1)	0.418(2)	0.07(1)
C(115)	0.165(1)	0.790(1)	0.484(2)	0.059(8)
C(116)	0.227(1)	0.819(1)	0.408(2)	0.046(7)
C(121)	0.4095(9)	0.8448(9)	0.306(1)	0.035(6)
C(122)	0.4474(9)	0.909(1)	0.288(1)	0.044(7)
C(123)	0.512(1)	0.905(1)	0.383(2)	0.048(7)
C(124)	0.534(1)	0.840(1)	0.496(2)	0.063(9)
C(125)	0.496(1)	0.778(1)	0.514(2)	0.07(1)
C(126)	0.435(1)	0.777(1)	0.419(2)	0.057(8)
C(131)	0.4354(9)	0.7337(9)	0.066(1)	0.034(6)
C(132)	0.467(1)	0.642(1)	0.123(2)	0.052(7)
C(133)	0.547(1)	0.565(1)	0.056(2)	0.061(8)
C(134)	0.599(1)	0.577(1)	−0.064(2)	0.060(8)
C(135)	0.569(1)	0.668(1)	−0.117(2)	0.054(8)
C(136)	0.487(1)	0.746(1)	−0.054(2)	0.045(7)
C(141)	0.254(1)	0.564(1)	−0.243(1)	0.042(7)
C(142)	0.296(1)	0.532(1)	−0.386(1)	0.046(7)
N(142)	0.360(1)	0.564(1)	−0.463(2)	0.064(8)
O(1421)	0.3801(9)	0.6191(9)	−0.401(1)	0.078(7)
O(1422)	0.393(1)	0.535(1)	−0.587(1)	0.095(8)
C(143)	0.280(1)	0.464(1)	−0.456(2)	0.054(8)
C(144)	0.223(1)	0.430(1)	−0.387(2)	0.051(8)
N(144)	0.207(1)	0.356(1)	−0.462(2)	0.08(1)
O(1441)	0.246(1)	0.334(1)	−0.588(2)	0.104(9)
O(1442)	0.154(1)	0.328(1)	−0.398(2)	0.11(1)
C(145)	0.180(1)	0.460(1)	−0.246(2)	0.07(1)
C(146)	0.197(1)	0.525(1)	−0.176(2)	0.054(8)

References

1 G. Lavigne, in D.F. Shriver, H.D. Kaesz and R.D. Adams (eds.), *The Chemistry of Metal Cluster Complexes*, VCH, New York, 1990, p. 204.

2 (a) E.G. Brian, B.F.G. Johnson, J.W. Kelland, J. Lewis and M. McPartlin, *J. Chem. Soc., Chem. Commun.*, (1976) 254;
(b) B.F.G. Johnson, J. Lewis and D.A. Pippard, *J. Organomet. Chem., 145* (1978) C4; *J. Chem. Soc., Dalton Trans.*, (1981) 407;
(c) M.I. Bruce, D.C. Kehoe, J.G. Matisons, B.K. Nicholson, P.H. Rieger and M.L. Williams, *J. Chem. Soc., Chem. Commun.*, (1982) 442; M.I. Bruce, J.G. Matisons and B.K. Nicholson, *J. Organomet. Chem., 247* (1983) 321;
(d) G. Lavigne and H.D. Kaesz, *J. Am. Chem. Soc., 106* (1984) 4647;
(e) K. Burgess, *Polyhedron, 3* (1984) 1175;
(f) A.J. Deeming, *Adv. Organomet. Chem., 26* (1986) 1;
(g) G. Lavigne and H.D. Kaesz, in B.C. Gates, L. Guzci and H. Knözinger, (eds.), *Metal Clusters in Catalysis*, Elsevier, Amsterdam, 1986, p. 43;
(h) P.C. Ford and A. Rokicki, *Adv. Organomet. Chem., 28* (1988) 139.

3 P. Braunstein and J. Rosé, Heterometallic Clusters in Catalysis, in I. Bernal (ed.), *Stereochemistry of Organometallic and Inorganic Compounds*, Elsevier, Amsterdam, 1989, vol. 3, pp 3–138, and references therein.

4 D.F. Foster, J. Harrison, B.S. Nicholls and A.K. Smith, *J. Organomet. Chem., 295* (1985) 99.

5 P. Braunstein, S. Coco Cea, M.I. Bruce, B.W. Skelton and A.H. White, *J. Organomet. Chem., 423* (1992) C38.

6 P. Braunstein, S. Coco Cea, M.I. Bruce, B.W. Skelton and A.H. White, *J. Chem. Soc., Dalton Trans.*, (1992) 2539.

7 P. Braunstein, S. Coco Cea, A. De Cian and J. Fischer, *Inorg. Chem., 31* (1992) 4203.

8 (a) R. Szostak, C.E. Strouse and H.D. Kaesz, *J. Organomet. Chem., 191* (1980) 243;
(b) H.D. Kaesz, C.B. Knobler, M.A. Andrews, G. van Buskirk, R. Szostak, C.E. Strouse, Y.C. Lin and A. Mayr, *Pure Appl. Chem., 54* (1982) 151;
(c) H.D. Kaesz, *J. Organomet. Chem., 383* (1990) 413.

9 (a) A. Mayr, Y.C. Lin, N.M. Boag and H.D. Kaesz, *Inorg. Chem., 21* (1982) 1704;
(b) C.M. Jensen and H.D. Kaesz, *J. Am. Chem. Soc., 105* (1983) 6969;
(c) C.M. Jensen and H.D. Kaesz, *J. Organomet. Chem., 330* (1987) 133;

10 (a) K.A. Azam, A.J. Deeming and I.P. Rothwell, *J. Chem. Soc., Dalton Trans.*, (1981) 91;
(b) A.J. Arce, Y. de Sanctis and A.J. Deeming, *J. Organomet. Chem., 311* (1986) 371.

11 B.F.G. Johnson, J. Lewis and T.I. Odiaka, *J. Organomet. Chem., 307* (1986) 61.

12 D.S. Böhle, V.F. Breidt, A.K. Powell and H. Vahrenkamp, *Chem. Ber., 125* (1992) 1111.

13 D.L. Ramage, G.L. Geoffroy, A.L. Rheingold and B.S. Haggerty, *Organometallics, 11* (1992) 1242.

14 R.D. Adams, N.M. Golembeski and J.P. Selegue, *Inorg. Chem., 20* (1981) 1242.

15 M.I. Bruce, O. Kühl, B.W. Skelton and A.H. White, *J. Organomet. Chem., 445* (1993) C6.

16 (a) M.I. Bruce, M.J. Liddell, C.A. Hughes, B.W. Skelton and A.H. White, *J. Organomet. Chem., 347* (1988) 157;
(b) M.I. Bruce, M.J. Liddell, C.A. Hughes, J.M. Patrick, B.W. Skelton and A.H. White, *J. Organomet. Chem., 347* (1988) 181;

(c) M.I. Bruce, M.J. Liddell, O. bin Shawkataly, C.A. Hughes, B.W. Skelton and A.H. White, *J. Organomet. Chem., 347* (1988) 207;
(d) M.I. Bruce, M.J. Liddell, O. bin Shawkataly, I.R. Bytheway, B.W. Skelton and A.H. White, *J. Organomet. Chem., 369* (1989) 217.

17 A.W. Coleman, D.F. Jones, P.H. Dixneuf, C. Brisson, J.-J. Bonnet and G. Lavigne, *Inorg. Chem., 23* (1984) 952.

18 (a) C.W. Bradford and R.S. Nyholm, *J. Chem. Soc., Dalton Trans.*, (1973) 529;
(b) S.C. Brown, J. Evans and L. Smart, *J. Chem. Soc. Chem. Commun.*, (1980) 1021;
(c) A.J. Deeming, S.E. Kabir, N.I. Powell, P.A. Bates and M.B. Hursthouse, *J. Chem. Soc., Dalton Trans.*, (1987) 1529.

19 (a) J.P. Collman, L.S. Hegedus, J.R. Norton and R.G. Finke, *Principles and Applications of Organotransition Metal Chemistry*, University Science Books, Mill Valley, CA, 1987, pp. 768–775;
(b) H.M. Colquhoun, D.J. Thompson and M.V. Twigg, *Carbonylation*, Plenum, New York, 1991, p. 205.

20 (a) M.I. Bruce, P.A. Humphrey, O. bin Shawkataly, M.R. Snow, E.R.T. Tiekink and W.R. Cullen, *Organometallics, 9* (1990) 2910;
(b) S.A.R. Knox, B.R. Lloyd, D.A.V. Morton, S.M. Nicholls, A.G. Orpen, J.M. Viñas, M. Weber and G.K. Williams, *J. Organomet. Chem., 394* (1990) 385.

21 See, for example (a) M.A. Andrews and H.D. Kaesz, *J. Am. Chem. Soc., 101* (1979) 7255;
(b) E. Singleton and H.E. Oosthuizen, *Adv. Organomet. Chem., 22* (1983) 269;.
(c) M.W. Day, S. Hajela, S.E. Kabir, M. Irving, T. McPhillips, E. Wolf, K.I. Hardcastle, E. Rosenberg, L. Milone, R. Gobetto and D. Osella, *Organometallics, 10* (1991) 2743;
(d) G. Süss-Fink, T. Jenke, H. Heitz, M.A. Pellinghelli and A. Tiripicchio, *J. Organomet. Chem., 379* (1989) 311.

22 W.K. Wong, K.W. Chiu, G. Wilkinson, A.M.R. Galas, M. Thornton-Pett and M.B. Hursthouse, *J. Chem. Soc., Dalton Trans.*, (1983) 1557.

23 (a) J.T. Park, J.R. Shapley, M.R. Churchill and C. Bueno, *Inorg. Chem., 22* (1983) 1577;
(b) J.R. Shapley, J.T. Park, M.R. Churchill, J.W. Ziller and L.R. Beanan, *J. Am. Chem. Soc., 106* (1984) 1144.

24 (a) P. Braunstein and D. Nobel, *Chem. Rev., 89* (1989) 1927, and references therein;
(b) P. Braunstein, T.M. Gomes Carneiro, D. Matt, F. Balegroune and D. Grandjean, *Organometallics, 8* (1989) 1737.

25 G. Predieri, A. Tiripicchio, C. Vignali, E. Sappa and P. Braunstein, *J. Chem. Soc., Dalton Trans.*, (1986) 1135.

26 R. Gobetto, E. Sappa, A. Tiripicchio, M. Tiripicchio-Camellini and M.J. Mays, *J. Chem. Soc., Dalton Trans.*, (1990) 807.

27 M.K. Cooper, J.M. Downes and P.A. Duckworth, *Inorg. Synth., 25* (1989) 129.

28 T.B. Rauchfuss, J.E. Hoots and D.A. Wroblewski, *Inorg. Synth., 21* (1982) 175.

29 D. Hedden and D.M. Roundhill, *Inorg. Synth., 27* (1990) 323.

30 S.-E. Bouaoud, P. Braunstein, D. Grandjean, D. Matt and D. Nobel, *Inorg. Chem., 25* (1986) 3765.

31 M.I. Bruce, C.M. Jensen and N.L. Jones, *Inorg. Synth., 28* (1990) 216.

32 M.I. Bruce, B.K. Nicholson and M.L. Williams, *Inorg. Synth., 28* (1990) 225.

33 J.A. Ibers and W.C. Hamilton, (eds.) *International Tables for X-Ray Crystallography*, Kynoch Press, Birmingham, 1974, vol. 4, p. 99.

34 S.R. Hall and J.M. Stewart, (eds.), *The XTAL Users' Manual - Version 2.6*, Universities of Western Australia and Maryland, 1988.

35 G.M. Sheldrick, *SHELX76, Programme for crystal structure determination*, University of Cambridge, UK, 1976.

36 G.M. Sheldrick, *SHELXS86, Program for the solution of crystal structure*, University of Göttingen, Germany, 1986.

37 C.K. Johnson, *ORTEP-II, Report ORNL-5138*, Oak Ridge National Laboratory, Tennessee, USA, 1976.

38 Part LXXXIX: C.J. Adams, M.I. Bruce, B.W. Skelton and A.H. White, *J. Organomet. Chem., 456* (1993) 113.